ALKYLATION OF ACETONITRILE WITH METHANOL USING ALKALI CATION EXCHANGED ZEOLITE X AS CATALYST

PRACHYA THUENSUKON

A THESIS SUBMITTED IN PARTIAL FULFILLMENT
OF THE REQUIRMENTS FOR THE DEGREE OF
MASTER OF SCIENCE IN PETROCHEMICALS AND
HYDROCARBON CHEMISTRY
SCHOOL OF GRADUATE STUDIES
KING MONGKUT'S INSTITUTE OF TECHNOLOGY LADKRABANG
2006

ISBN 974-15-2377-7

หัวข้อวิทยานิพนธ์	ปฏิกิริยาอัลคิลเลชันของอะซิโตไนไตรล์ด้วยเมทานอลโดยใช้ตัวเร่งปฏิกิริยาซีโอไลต์ X ที่แลกเปลี่ยนไอออนด้วยโลหะอัลคาไลน์
นักศึกษา	นายปรัชญา เถื่อนสุคนธ์
รหัสประจำตัว	44065710
ปริญญา	วิทยาศาสตรมหาบัณฑิต
สาขา	ปิโตรเคมีและเคมีของไฮโดรคาร์บอน
อาจารย์ผู้ควบคุมวิทยานิพนธ์	ผศ. ดร. ตะวัน สุขน้อย

บทคัดย่อ

วิทยานิพนธ์เล่มนี้เป็นการศึกษาปฏิกิริยาอัลคิลเลชันของอะซิโตไนไตรล์ด้วยเมทานอลโดยใช้ตัวเร่งปฏิกิริยาซีโอไลต์ X ที่ปรับปรุงความเป็นเบสโดยการแลกเปลี่ยนไอออนกับโลหะอัลคาไลน์โพแทสเซียมและซีเซียม โดยทดสอบสมบัติความเป็นกรด-เบสของตัวเร่งปฏิกิริยาด้วยปฏิกิริยาไซไคล-เซชันของอะซิโตนิลอะซิโตนและเทคนิคการดูดซับก๊าซคาร์บอนไดออกไซด์ การทดสอบความสามารถในการเร่งปฏิกิริยาสามารถทำได้โดยผสมเมทานอลกับอะซิโตไนไตรล์ที่อัตราส่วน 10:1 โดยโมล แล้วป้อนเข้าสู่ชุดทดสอบปฏิกิริยาชนิดเบดนิ่งอย่างต่อเนื่อง ที่อุณหภูมิ 350-425 องศาเซลเซียสทดสอบในระยะเวลา 8 ชั่วโมง ผลิตภัณฑ์ที่เกิดขึ้นถูกควบแน่นเป็นของเหลวที่สามารถเก็บเป็นช่วง และนำไปวิเคราะห์ด้วยเทคนิคก๊าซโครมาโทกราฟี จากการศึกษาพบว่าการเลือกสรรผลิตภัณฑ์ขึ้นกับอุณหภูมิในการทำปฏิกิริยาและความเป็นเบสของตัวเร่งปฏิกิริยา โดยความเป็นเบสของตัวเร่งปฏิกิริยาเพิ่มขึ้นตามขนาดของแคทไอออน $Cs^+ > K^+ > Na^+$ อุณหภูมิที่เหมาะสมในการทำปฏิกิริยาคือ 400 องศาเซลเซียส อุณหภูมิในการทำปฏิกิริยาสามารถสลายเมทานอลเป็นฟอร์มาลดีไฮด์และไฮโดรเจนโดยฟอร์มาลดีไฮด์ทำปฏิกิริยากับอะซิโตรไนไตรล์ได้อะคริโลไนไตรล์เป็นผลิตภัณฑ์เริ่มต้น จากนั้นอะคริโลไนไตรล์เกิดปฏิกิริยาไฮโดรจีเนชันได้โพรพิโอไนไตรล์ ความเป็นเบสของซีโอไลต์ที่เพิ่มขึ้นส่งผลให้ปฏิกิริยาอัลคิลเลชัน ไฮโดรจีเนชัน และไฮโดรจีโนไลซิสเกิดได้ดีขึ้น แสดงถึงปฏิกิริยาเกิดผ่านคาร์แบนไอออนอินเตอร์มีเดียต นอกจากนั้นพบว่าซีเซียมที่มากเกินและตกค้างบนโครงสร้างซีโอไลต์ทำให้ปฏิกิริยาไฮโดรจีเนชันเกิดเพิ่มขึ้น อย่างไรก็ตามซีเซียมที่มากเกินและตกค้างบนโครงสร้างซีโอไลต์ไม่มีผลในการเร่งปฏิกิริยาอัลคิลเลชัน

Thesis Title	Alkylation of acetonitrile with methanol using alkali cation exchanged zeolite X as catalysts
Student	Mr. Prachya Thuensukon
Student ID.	44065710
Degree	Master of Science
Programme	Petrochemicals and Hydrocarbon Chemistry
Thesis Advisor	Asst. Prof. Dr. Tawan Sooknoi

ABSTRACT

In this thesis, the catalytic alkylation of methanol with acetonitrile was investigated over basic zeolite catalysts. The incorporation of highly polarisable cations namely, potassium and cesium, were used to modify basicity of zeolite X. Acidity and basicity of catalysts were described by cyclisation of acetonylacetone and carbon dioxide adsorption. Feed mixture containing methanol and acetonitrile at 10:1 by mole was fed continuously into the reactor. The catalytic reactions were carried out at 350-425 °C in a fixed bed flow reactor and were tested for 8 hours on stream. Products can be condensed to liquid and then collected periodically. Liquid products were then analyzed by Gas chromatography. The result showed that the product selectivity was found to depend on basicity of the catalyst and reaction temperature. The basicity of the catalysts increased with the cation size, in the order of $Cs^+ > K^+ > Na^+$. The optimum reaction temperature was found to be 400 °C. As reaction temperature, methanol also decomposed to formaldehyde and hydrogen. Acrylonitrile was the primary product formed by the reaction between acetonitrile and formaldehyde. Then, acrylonitrile can undergo hydrogenation to give propionitrile. The alkylation, hydrogenation and hydrogenolysis activities were found to increase with increasing catalyst basicity, indicately that the reaction proceed via carbanion intermediate. Moreover, the excess cesium "cluster" present in the zeolite framework increases the hydrogenation activity. However, such species do not affect the alkylation activity.

ACKNOWLEDGEMENTS

The author wishes to express his profound gratitude to his advisor, Asst. Prof. Dr. Tawan Sooknoi for his supervisions, helpful suggestions and encouragements throughout this thesis. He is also grateful to Asst. Prof. Dr. Vanchat Chuenchom, Asst. Prof. Dr. Punnama Siriphannon and Asst. Prof. Dr. Sirirat Jitkarnka for serving as the chairperson and the committee, and their valuable comments.

The author would like to extend his sincere appreciation to all of his teachers, his friends and his research group for their constant guidance advice, support and encouragement.

Sincere thanks to the Department of Chemistry, Faculty of Science, King Mongkut's Institute of Technology Ladkrabang for the equipment, chemicals and facilitates.

Finally, the author dedicates his thesis to parents and his family for the constant love and encouragement.

Prachya Thuensukon

CONTENTS

CONTENTS (Continued)

CONTENTS (Continued)

CONTENTS (Continued)

LIST OF TABLES

LIST OF TABLES (Continued)

LIST OF FIGURES

LIST OF FIGURES (Continued)

Figure Page

LIST OF FIGURES (Continued)

Figure Page

LIST OF FIGURES (Continued)

Figure Page

CHAPTER 1

INTRODUCTION

1.1 Motivation

Zeolites exchanged with alkaline cations have been known since the beginning of zeolite history. Considered from the viewpoint of basic solids [1], it appears that the properties of these zeolites are adjustable to specific applications, and that the solids may therefore be seen as new materials. Until now, no systematic way of improvement has been applied. The present attempts to rationalize the concepts of basicity in zeolites open up new route for the scientific search for adsorbents or catalysts with specified properties.

The advantages associated with the use of zeolites as catalysts would make it desirable to expand their application to base-catalyzed reactions. The constitution of zeolites leads to acidic rather than basic properties, i.e. the negatively charged zeolite frameworks create Brønsted acidic sites. Zeolites with a positively charged framework which would provide Brønsted-basic OH groups are not known. Two principal methods to create and enhance basicity in zeolites have been proposed and investigated [2]. (i) The more or less insignificant use of the zeolite as a support for basic species, i.e. the occlusion of metal (alkali) clusters, or small metal hydroxide and/or oxide particles, and (ii) modification of the intrinsic basicity of the zeolite, i.e. the Lewis basicity of the framework oxygens, by either using different framework cations (isomorphous substitution), or by exchange of the cations that balance the charge of the framework. Specifically, as charge balancing cations, low electronegativity cations such as alkali metal cations appear suitable; and in zeolites of the faujasite-type alkali metal cations can be introduced into the supercages by means of ion-exchange in an aqueous solution of a salt of the desired cation (referred to hereafter as conventional ion exchange) [3].

In this work, cation exchanged zeolite X is used as catalysts. Alkali metal cations used is focused on cesium, which is expected to pursue the strongest effect on the basicity. The basicity of the cations exchanged zeolite X can be described by the product selectivity observed from the cyclisation of acetonylacetone. Then, the role of exchangeable cations and the excess cationic "clusters" present in the zeolite framework are demonstrated by considering activity and selectivity of the alkylated products obtained from the alkylation of acetonitrile with methanol.

Since the reaction proceeded via bimolecular intermediate, competitive sorption activity of the substrate over the catalyst is suggested to be significant. Therefore, the reaction pathway will be further described by the hydrogenation of acrylonitrile and hydrogenolysis of propionitrile over basic zeolite catalysts.

1.2 Objectives

The objective of this thesis is to study alkylation of acetonitrile with methanol in a fixed bed flow reactor over basic zeolites catalysts. The specific objectives are as follows:

1.2.1 To understand the effect of parameters on the alkylation of acetonitrile with methanol over basic zeolites catalysts.

1.2.2 To understand a catalytic behavior of excess cesium "clusters" present in the zeolite framework.

1.2.3 To understand the alkylation mechanism of acetonitrile with methanol over basic zeolites catalysts.

1.3 Scope of the study

The scopes of the study on alkylation of acetonitrile with methanol in a fixed bed flow reactor over basic zeolites catalysts are as follow:

1.3.1 Modification and characterization of solid base faujasite-type zeolites

1.3.2 Study on basicity in alkali cation exchanged faujasite zeolites by using catalytic cyclisation of acetonylacetone.

1.3.3 Study on mechanism of alkylation of methanol with acetonitrile.

1.3.4 Study on catalytic activity of hydrogenation of acrylonitrile.

1.3.5 Study on catalytic activity of hydrogenolysis of propionitrile.

1.3.6 Analysis of products from the reactions by gas chromatography.

1.4 Expected results

1.4.1 To apply zeolite as base catalyst for other alkylation, hydrogenation and isomerisation

1.4.2 To comprehend the reaction pathway for the alkylation of acetonitrile with methanol over basic zeolite catalysts.

CHAPTER 2

THEORY AND LITERTURE REVIEWS

2.1 Zeolites

Zeolites are crystalline aluminosilicate minerals. They have three-dimensional structures arise from a framework of $(SiO_4)^{4-}$ and $(AlO_4)^{5-}$ coordination polyhedral (Figure 2.1) linked by all their corners. The frameworks are generally very open and contain channels and cavities in which are located cations and water molecules (Figure2.2). The cations often have a high degree of mobility giving rise to facile ion exchange and the water molecules are readily lost and regained; this accounts for the well-known desiccant properties of zeolites [4].

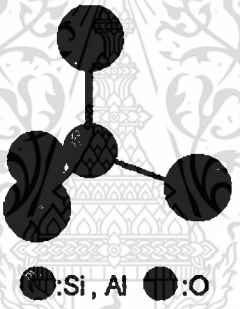

Figure 2.1 Representations of $(SiO_4)^{4-}$ or $(AlO_4)^{5-}$ tetrahedral

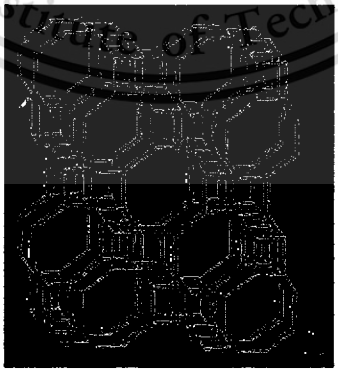

Figure 2.2 The framework structure of chabazite. Each line represents an oxygen atom and each junction a silicon or aluminium (Water molecules fill the space in the cages and cations float in the cages in this aqueous environment)

Many of the natural zeolites can be produced synthetically and several crystalline aluminosilicates with framework structures with no known natural counterpart have been made in the laboratory. The best known example of a synthetic zeolite is zeolite A, which can be related structurally to naturally occurring zeolites. It, like other synthetic zeolites, exhibits the definitive zeolitic properties of ion exchange and reversible water loss.

Another characteristic zeolite property arises from their molecular framework structures in that the combining of tetrahedral creating their porous structure happen to create regular arrays of apertures. These apertures are of such a size as to be able to selectively take up some molecules into their porous structure, whilst rejecting others on the basis of their larger effective molecular dimensions. This is the property of 'molecular sieving', which is largely unique to zeolites and responsible for their first commercial success.

2.2 The structure of zeolites

As stated earlier all zeolites have framework (three-dimensional) structures constructed by joining together $(SiO_4)^{4-}$ and $(AlO_4)^{5-}$ coordinated polyhedral. By definition these tetrahedra are assembled together such that the oxygen of each tetrahedral corner is shared with that in an identical tetrahedral (Si or Al), as shown in Figure 2.3. This corner (or vertex) sharing creates infinite lattices comprised of identical building blocks (unit cells) in a manner common to all crystalline materials.

One way to classify zeolite structure would be to relate them to the symmetry of their unit cells. This would be cumbersome and is much simplified by the observation that structures often have identical (or very similar) repeating structural sub-units which are less complex than their repeating unit cells.

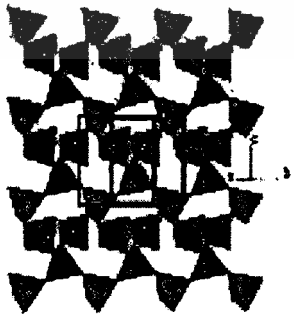

Figure 2.3 Tetrahedral linked together to create a three-dimensional structure

These recurring units are called 'secondary building units' (sbus) and the simplest, classification described all known zeolite frameworks as arrangements linking eight sbus shown in Figure 2.4. These denote only the aluminosilicate skeleton (i.e. the Si, Al and O positions in space relative to each other) and exclude consideration of the cation and water moieties sited within the cavities and channels of the framework. The cation and water sites are complex and only fully defined in certain zeolites as will become apparent later.

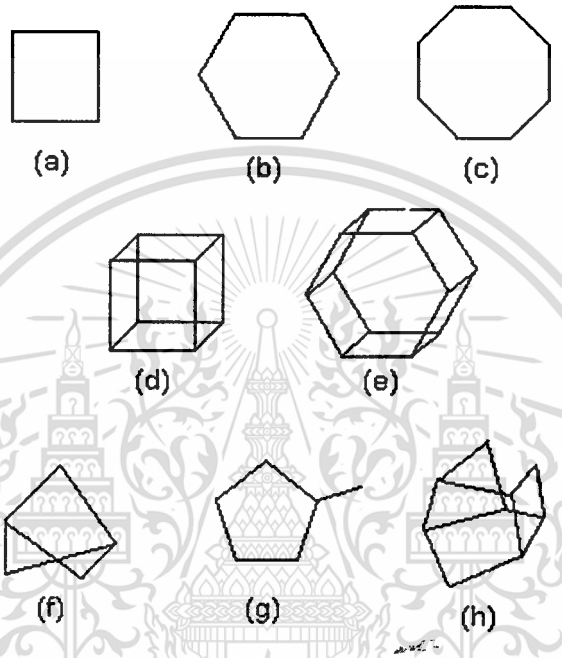

Figure 2.4 The secondary building units (sbus) recognized in zeolite frameworks; (a) single four ring (S4R), (b) single six ring (S6R), (c) single eight ring (S8R), (d) double four ring (D4R), (e) double six ring (D6R), (f) complex4-1, (g) complex 5-1 and (h) complex4-4-1

For the present it should be noted that the number of cations present within a zeolite structure is determined by the number of $(AlO_4)^{5-}$ tetrahedral included in the framework. This arises from the isomorphous substitution of Al^{3+} for Si^{4+} into the component polyhedral, causing a residual negative charge on the oxygen framework. This negative charge is compensated by those cations present in the synthesis and held in the interstices of the structure on crystallization. The extent and location of water molecular incorporation depends upon (i) the overall architecture of

the zeolite molecular structure, i.e. the size and shape of the cavities and channels present, and (ii) the number and nature of the cations in the structure.

The aluminosilicate skeleton can be represented in a number of ways, as for example in the traditional 'ball and stick' model (Figure 2.5). The most favored is the use of tetrahedral arrays, adopted by organic chemists, where the oxygen atoms are drawn as single 'bonds' joining together tetrahedral 'centers' depicting silicon and aluminium. This is the method used in Figure 2.5. Further perusal of Figure 2.4 shows that each sbu contains rings of tetrahedral which are equivalent to rings of oxygen atoms described as 'single six rings' etc. (Figure 2.6). When the sbus are joined to create the infinite lattices they can proscribe larger rings containing 8, 10 or 12 linked tetrahedral (i.e. rings of 8, 10 or 12 oxygen atoms). These rings are obviously important structural features and are often called 'oxygen windows'.

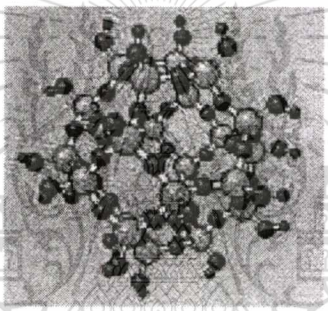

Figure 2.5 A 'ball and stick' representation of the structure of the sodalite unit (left) with a framework diagram (like Figure 2.2) for comparison

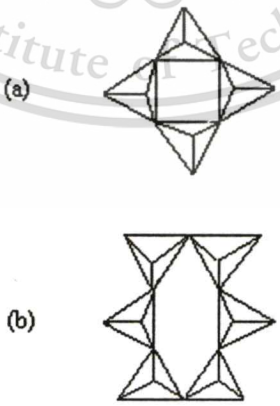

Figure 2.6 The arrangement of tetrahedral in the (a) S4R and (b) S6R sbu

2.3 Zeolites X and Y (Faujasites) [5]

The zeolites finding more application in the catalysis belong to the family of faujasites, including zeolite X and zeolite Y. Having 0.74-nm apertures (12 membered oxygen rings) and a three-dimension pore structure, they admit even hydrocarbon molecules larger than naphthalene. Their chief application is in catalytic cracking of petroleum molecules (primary in the heavy distillated fraction), giving smaller, gasoline-range molecules.

The framework structure of zeolites X and Y (Figure 2.7) is closely related to that zeolite A. The sodalite cages in faujasites are arranged in an array with greater spacing than in zeolite A. Each sodalite cage is connected to four other sodalite cages; each connecting unit is six bridging oxygen ions linking the hexagonal faces of two sodalite units, as shown in Figure 2.7. The bridging oxygens form what is called a hexagonal prism. The high-resolution electron micrograph of Figure 2.8 shows the regularity if the pores in a crystal of zeolite Y.

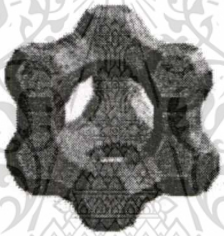

Figure 2.7 Structure of faujasite.

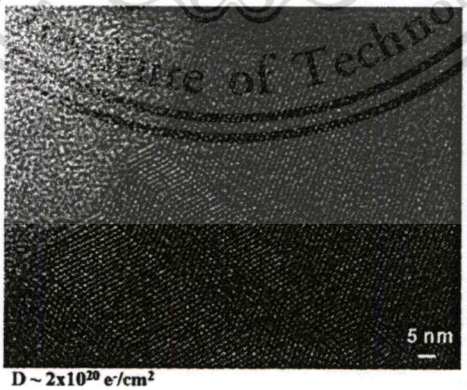

Figure 2.8 High-resolution transmission electron micrograph of crystalline NaY zeolite.

(S. X. Wang, L. M. Wang and R. C. Ewing)

There is a range of faujasite compositions, with a typical unit cell formula being $Na_j[(AlO_2)_j(SiO_2)_{192-j}].zH_2O$, where z is about 260. The value of j is between 48 and 76 for zeolite Y and between 77 and 96 for zeolite X. X-Ray diffraction and NMR data have determined the structures of faujasites, showing, for example, that the unit cell dimension decreases slightly as the Si/Al ratio increases. The X-ray data have also determined the exact positions of cations present to balance the excess negative charge of the AlO_4 tetrahedra. Four cation sites are illustrated in Figure 2.9. Type I sites are located at the centers of the hexagonal prisms, type I' sites are located in the sodalite cages across the hexagonal faces from type I sites, type II sites are located in the supercages near the unjoined hexagonal faces, and type II' sites are located in the supercages, farther from the hexagonal faces than the type II sites.

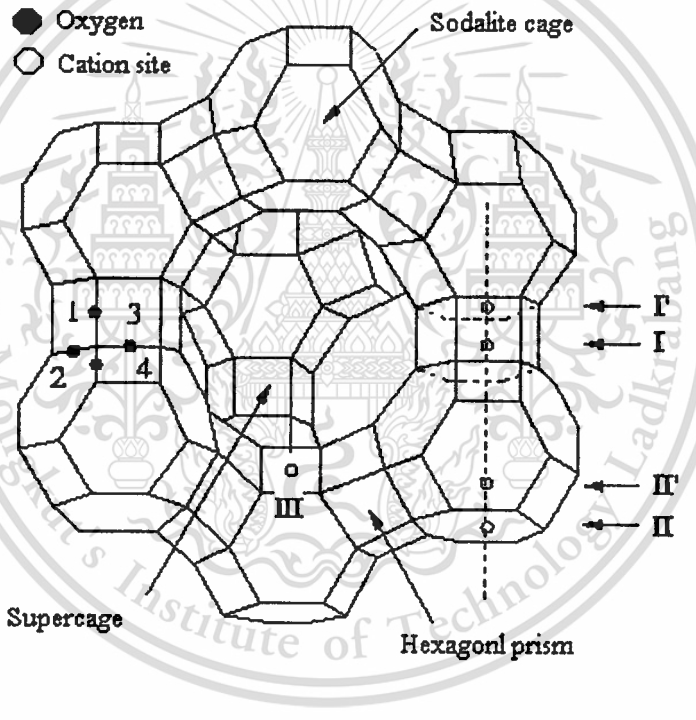

Figure 2.9 Locations of cation sites in X and Y zeolites.

2.4 Solid base catalysis

2.4.1. Solid base and basic sites [6]

Solid bases are defined as solids that serve as base by either the definition of Brønsted or that of Lewis. According to their functions, they are classified into Brønsted bases and Lewis bases. On the surface of solid bases, there are specific sites or centers that function as base. The

sites are called basic sites. For example, isomerisation of alkenes proceeds via allylic carbanions that are formed by abstraction of a proton from the reactant molecules.

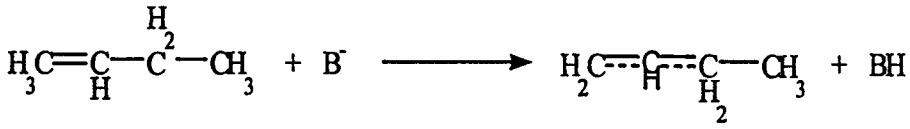

Here, the basic site B^- on the solid surface acts as a Brønsted base. In the reactions of ketones or aldehydes, the reactants are often activated by bases without proton transfer.

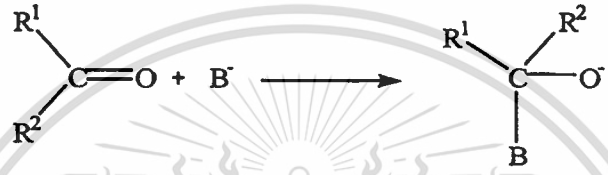

Here, the basic site B^- acts as a Lewis base. It should be noted that the same surface sites could serve as the Brønsted base as well as Lewis base, depending on the nature of the adsorbate. The classification has to be made only after the mode of interaction with an adsorbate is clarified.

2.4.2. Basic strength of basic sites.

The H_acidity function is defined as a measure of the ability of the basic solution to abstract a proton from an acidic neutral solute.

$$H\_ = pK_a - \log([AH]/[A^-])$$

To determine the H_value of the solution, the concentrations of AH and A^- have to measured accurately. When one half of a solute AH is deprotonated in the solution, i.e., $[A^-] = [AH]$, the H_value of the solution is equal to the pK_a value of AH.

It was proposed that the H_scale can be used as the measure of the strength of solid bases [7]. The basic strength of solid bases is expressed by means of the H_value, equated to the highest among the pK_a values of the adsorbates from which the basic site is able to abstract a proton.

Two important points should be noted. In the discussion of solid base, the H_scale is treated as a parameter to describe the nature of individual basic sites [8]. It is often assumed that

there are a certain number of basic sites on the solid surfaces, each of the basic sites has its own basic strength. In the original definition, the H_scale is used to describe basic (or acidic) property of solution, not that of individual basic molecules (or ions) in the solution. In the principle, the idea of the H_scale is only capability of the sites as Lewis bases.

Apart from the appropriateness of applying the concept of the H_scale to basic sites on the surfaces, the pK_a values of the adsorbates (or reactants) is good measure of the ability of the basic sites to abstract a proton from an adsorbate (or reactant).

2.4.3 Basic zeolite catalysts

2.4.3.1 Generation of basic sites in zeolite catalysts

Basicity in zeolites can arise from either the framework oxygen or the incorporated basic species. It has been shown by X-ray photoelectron spectroscopy that, in high aluminium-content zeolites, a decrease in O_{1s} binding energy of the framework oxygen is observed with increase in the size of the exchangeable alkali cations. Since, the electrostatic field strength is reduced when the cations become larger [9], the Lewis acidity of the exchangeable cations is decreased. This means that there is less electron donor interaction of the framework oxygen with the cations. In other words, the large exchangeable cations donate more electrons to the framework oxygen than the smaller cations. Consequently, there should be a concentrated electron density localized on the framework oxygen where Lewis basicity is generated. This is indicated by the highly negative charge of the framework oxygen which can be estimated by the electronegativity equalization method (Sanderson intermediate electronegativity). According to the above discussion and the fact that low binding energy is observed over species with high electron density [10], exchange with large alkali cations results in a lower binding energy of the framework oxygen. This is especially strong in zeolites with high-aluminium content because the adjacent exchangeable cations give an increased interaction to the neighbor oxygens. This leads to in a significant shift in O_{1s} binding energy for cation exchanged zeolite X and zeolite Y but a negligible change for cation exchanged ZSM-5 [11].

2.4.3.2 Basicity in alkali cation-exchanged zeolites [12]

It is generally accepted that the basic sites on the surface of solid catalysts are of the Lewis type, and can, therefore, be defined as sites able to donate an electron pair to an adsorbed molecule. In zeolites Lewis basicity is associated with the framework oxygens bearing the

negative charge of the lattice and consequently the density of negative charge on given oxygen, i.e. its basicity, will depend both on the chemical composition and on the structure of the zeolite. It can generally be said that the lower the average Sanderson electronegativity of the system the higher the basicity of the zeolite.

Catalytic activity : Model catalytic reactions

Knovenagel condensation between benzaldehyde and molecules containing activated methylene groups with different pK_a values has been used as a test reaction to gain insight into the basic properties of solid [13]. In this way it was established that the reaction in solution as it is when solid catalysts are used; it was found that the rate-controlling step of the condensation reaction on basic zeolites is not proton abstraction, as was first proposed for other basic catalysts [14], but attack by the carbanion intermediate on the carbonyl group (scheme 1)

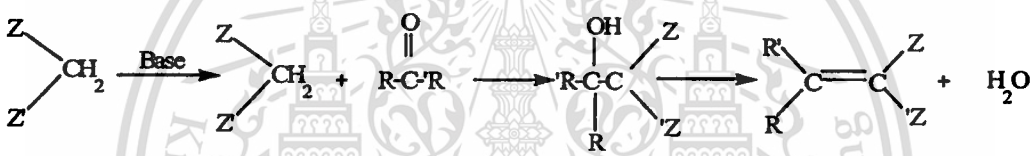

Scheme 1.

When, on the other hand, the Knovenagel condensation is performed between benzaldehyde and a series of methylenic compounds with different pK_a values, e.g. ethyl cyanoacetate (pK_a 9.0), ethyl acetoacetate (pK_a 10.7), and ethyl malonate (pK_a 13.3) it is not only possible to measure the total number of basic sites, but also their strength distribution. This study has shown that alkali-exchanged zeolites have a large number of basic sites able to abstract a proton from organic molecules with pK_a in the range $9 < pK_a < 13.3$ [15].

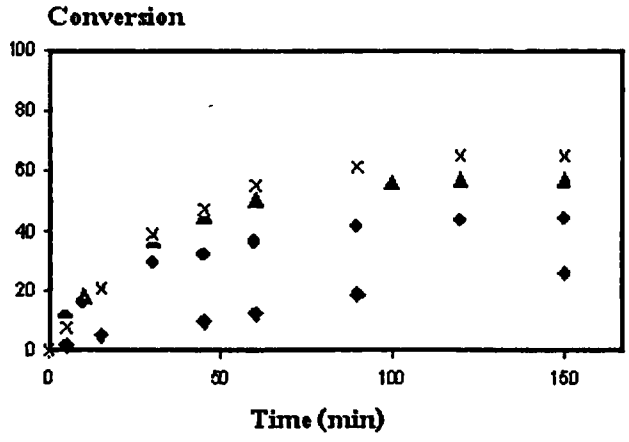

Figure 2.10 Condensation of benzaldehyde and ethyl cyanoacetate on exchanged X zeolites: LiX (◆), NaX (●), KX (▲), and CsX (X)

Table 2.1 Kinetic rate constants (K) for the condensation of benzaldehyde with ethyl cyanoacetate (pK_a 9.0), ethyl acetate (pK_a 10.7), and ethyl malonate (pK_a 13.2) on alkaline-exchanged zeolites, NaGeX, cesium-exchanged sepiolite, and calcined Mg-Al hydrolactice.

Catalyst	RCH_2COOEt	T (K)	K ($mols^{-1}m^{-2} \times 10^{-4}$)
Hydrolactice	R = -CN	363	89.7
CsSep			4.6
NaGeX			4.2
CsX			0.24
KX			0.22
LiX			0.037
CsY			0.019
KY			0.017
LiY			0.011
Hydrotalcite	R = -COOEt	443	7.9
CsSep			0.4
NaGeX			0.8
CsX			0.3
Hydrotalcite	R = -COCH3	413	not reported
CsSep			6.5
NaGeX			5.1
CsX			2.8

Figure 2.10 compares the progress of the Knoevenagel condensation between ethylcynoacetate and benzaldehyde on different exchanged X zeolites, and in Table 2.1 are summarized the rates calculated for the Knoevenagel condensation of different methylenic compounds on basic catalysts [15].

From these results it is possible to concluded that the activity of the exchanged zeolites increases with decreasing framework Si/Al ratio and increasing counter cation radius. With regard to proton-abstracting capacity, alkali-exchanged zeolites have basic sites with a strength distribution in the range of $9.0 < pK_a < 10.7$; only a few centers with higher basicities, in the range $10.7 < pK_a < 13.3$, were detected on the most basic zeolite XCs. Table 1. includes results obtained with a cesium-exchanged sepiolite and a mixed aluminium-magnesium hydrotalcite.

Substitution of Si by Ge in the framework of faujasite substantially increases the catalytic activity of Knoevenagel condensations [16]. Thus, the rates of the reaction between benzaldehyde and ethyl cyanoacetate are one order of magnitude larger over NaGeX than over NaSiX. Significant catalytic activity was, moreover, observed on NaGeX when the methylene-active compound is diethyl malonate (pK_a 13.3) indicating that incorporation of Ge into the zeolite framework increases the relative proportion of strongly basic sites. The increased activity in this material cannot be related to increased base strength, because a decrease in the average Sanderson electronegativity (calculated by taking into account only the electronegativity of the composition elements) is also related to the T-O-T angle. Consistent with this it has been found that despite its low Al content, Na-exchanged beta zeolite is a more active catalyst of the Knoevenagel condensation than NaY or NaX. This is related to the relatively small T-O-T angles when exchanging the H-beta zeolite by Na^+. In common with faujasites, Ge-beta, and Ga-beta zeolites in which some Si is replaced by Ge, or Al is substituted by Ga, respectively, are more active than the corresponding Si-Al form, indicating that introduction of Ga and Ge increases the basicity.

NaY has also been exchanged with Ca, La, Ce, and Re, and a systematic and comparative study of their catalytic activity in the Knoevenagel condensation between banzaldehyde and malononitrile has been conducted by Reddy et al. [17]. Two of the catalysts, La (70%) NaY and Ce (70%) NaY afforded moderate yields but rare-earth (Re)-exchanged NaY was found to be the optimum zeolite for this condensation in terms of yield, mass balance, and selectivity.

2.5 Alkylation Reaction

Alkylation reactions are reactions where an alkyl group is introduced into a molecule. Many different types of alkylation reactions are known. For example, alkyl groups can be introduced into aliphatic hydrocarbons or aromatic hydrocarbons by alkylation reactions. Alkylation reactions can also be used to prepare ethers from alkyl alcohols or aromatic alcohols. Alkylated amines can be prepared by alkylation; however, special methods are normally required to control the number of alkyl groups introduced onto nitrogen. Important synthetic methodology also exists for the alkylation of enolate ions. Alkylation is often promoted through the use of heat or of an appropriate catalyst such as an acid catalyst.

One very important alkylation reaction is the Friedel Crafts alkylation reaction, used for the alkylation of aromatic species, which was discovered in 1877. Many alkyl halides, alcohols, or alkenes can be reacted with benzene in the presence of certain catalysts to give alkyl benzene. Other aromatic hydrocarbons give similarly substituted alkyl aromatic products. A Lewis acid, such as aluminum chloride, is often the catalyst used for this reaction. This reaction is used industrially for the synthesis of hydrocarbons. If the reaction is carried out at high temperatures, rearrangement of the alkyl group may occur. For example reaction of n-propyl halides with benzene at low temperatures affords mainly n-propyl benzene but at higher temperatures the major product is isopropyl benzene. In Friedel-Crafts reactions, alkyl chlorides are more reactive than alkyl bromides and alkyl iodides react only with difficulty. Alkylation is used industrially to produce basic building blocks for the synthesis of more elaborate materials. One commonly used application is in the production of anti-knock gasoline

2.6 Base-catalyzed Alkylation

In contrast to acid-catalyzed alkylation of arenes where alkylation of aromatic nucleus occurs, the base-catalyzed reaction of alkylarenes leads to alkylation of the side chain [18]. Alkenes (straight-chain 1 alkenes, isobutylene), conjugated dienes (1,3-butadiene, isoprene), and styrene and its derivatives can react with alkylarenes possessing a benzylic hydrogen. In contrast, arylalkanes that do not have reactive benzylic hydrogens yield only ring alkylated products in very low yields.

Sodium and potassium are the two most frequently used alkali metals in side-chain alkylation. Sodium usually requires a promoter (*o*-chlorotoluene, anthracene) to form an organosodium intermediate which is the true catalyst of the reaction. A temperature range of 150-

250 °C is usually required for alkylation with monoolefins, whereas dienes and styrene are reactive at lower temperatures.

Selective acid-base poisoning of the alkylation of toluene with methanol was studied over alkali and alkaline-earth exchanged Y zeolites. Zeolites are attractive materials for alkylation reactions because their acid-base properties can be easily modified by dealumination, isomorphorus substitution or ion-exchange. Although base catalysts such as MgO and CaO were successfully used for side-chain alkylation, recent studies indicate that the zeolite pores might be indispensable to efficiently catalyze the reaction. Alkali-exchanged zeolites have demonstrated the highest activities and selectivities for side-chain alkylation of toluene with methanol. Particularly, the side-chain alkylation of toluene with methanol requires basic sites to activate the carbon atom in the methyl group of toluene and also to dehydrogenate methanol to formaldehyde, which is generally believed to be the actual alkylating agent to form styrene. On the other hand, strong base sites also catalyze methanol decomposition to form carbon monoxide, which is the major side reaction during toluene alkylation with methanol.

2.7 Literature reviews

In the recent forty years, the catalytic properties of zeolites have been one of the most studied subjects in the field of catalysis. Investigations on the structural nature and catalytic properties of zeolites were specially intense.

In fact, some zeolites have also basic properties. X and Y zeolites that have been modified through conventional ion exchange with alkali metal cation solutions indeed exhibit basic properties useful for catalysis, as shown by their effectiveness for various test reactions which include side-chain alkylation of toluene [19]. The *N*-alkylation of aniline [20], the dehydrogenation of isopropanol or other alcohols Knoevenagel condensations [21], and double bond isomerizations[22]. A number of trends have been observed in the catalytic activities of such samples but these trends are not entirely consistent. In 1987, Giordano investigated the alkylation of toluene have shown that the yield of the side chain alkylation products styrene and ethylbenzene, indicative of base catalysis, could be correlated with the intermediate Sanderson electronegativity (S_{int})[23]; the formation of these products becomes significant at S_{int}<3.6. The yield of styrene and ethylbenzene was found to increase with increasing cation size, i.e. in the order Na<K<Rb<Cs, except for CsX due to stability problems, and zeolites X were found to be more active than zeolites Y [24]. In 1979, Sefcik investigated the rotational freedom of

aromatics adsorbed on modified zeolite X with nuclear magnetic resonance spectroscopy and concluded that cations as large as Cs^+ in the supercages sterically hinder ring alkylation while the side chain can be alkylated. In 1987, Engelhardt et al. found that NaX, KX, and CsX that were obtained through exchange with alkali metal hydroxides were more active than samples obtained with other alkali metal salts, concluding that small amounts of occluded hydroxides have a positive effect [25].

The reaction of isopropanol dehydrogenation to acetone indicates the presence of strongly basic sites, with cation exchanged zeolites X and Y as catalysts [26].In 2000, P. Concepción-Heydorn found that the yield of acetone increased with cation size, but for this reaction, zeolite Y was more active than zeolite X when the cation was K, Rb, or Cs [27]. Jacobs and Uytterhoeven suggested that the rate of acetone formation was related to the concentration of iron impurities rather than to the alkali metal cations [28]. In 1989, Hathaway and Davis used various alkali metal salts for the conventional ion exchange, to investigate the zeolite samples in an unrinsed and a rinsed state, and perform not only the isopropanol dehydrogenation but also chemical and spectroscopic analysis of the materials to identify occluded species. These in formed that unrinsed samples prepared from alkali metal acetates and hydroxides were more active for acetone formation than the samples prepared from alkali metal nitrates, and the samples prepared from alkali metal chlorides were entirely inactive for isopropanol dehydrogenation. Catalytic activity was, at least in part, attributed to the occluded salts, whose presence was confirmed by infrared (IR) spectroscopy and chemical analysis which sometimes revealed a cation excess ($n_{M+}/n_{Al}>1$). Unrinsed zeolites Y with potassium or cesium, prepared from hydroxides, had a higher rate of formation of acetone and a higher selectivity for acetone than the corresponding zeolite X samples. Rinsing the samples with deionized water increased the activity towards propene formation, which was explained with re-exchange of alkali metal cations by protons [29].

The strength of basic sites in zeolites that have been modified with alkali metal salts has been investigated using the adsorption of probe molecules in combination with various methods, e.g. the adsorption of pyrrole in combination with IR spectroscopy, or X-ray photoelectron spectroscopy (XPS), or the adsorption of carbon dioxide in combination with IR spectroscopy, microcalorimetry, or temperature-programmed desorption (TPD) [30]. In 1992, D. Barthomeuf derived from IR spectra taken after adsorption of pyrrole that the basic strength of the framework oxygen increases depending on the cation in the order of Cs>Rb>K>Na. For any given cation, the

basicity was found to increase with increasing Al contents [31], consistent with IR measurements by J.Xie who adsorbed pyrrole on NaY and NaX. XPS spectra of the N_{1s} level of adsorbed pyrrole and the Cl_{2p} level of adsorbed chloroform confirm the ranking of alkali metal cations and also show that zeolite X is more basic than zeolite Y [31]. In 1999, Doskil and Davis investigated carbonate species formed upon CO_2 adsorption and their thermal stability with IR spectroscopy; the results indicated that KX had stronger basic sites than CsX [32]. Laspéras et al. concluded from TPD measurements that CO_2 adsorption cannot be related to framework basicity but rather to cation polarizing power. Occlusion of cesium oxide in alkali metal cation exchanged zeolites created basic sites [33]. Direct spectroscopic measurements of the negative charge on the framework oxygen with XPS by Okamoto et al. showed that the charge increases with increasing Al content and with an increasing fraction of Na replaced by Cs in NaY [34].

In 1998, P.Kazansky studied hydrogen adsorption on Li, Na and Cs forms of X zeolite with a silicon to aluminium ratio of 1.4. The results obtained indicated that the adsorption sites are represented by alkali metal cations. It was also found that the rotation of hydrogen molecules adsorbed on CsX was almost free, but was substantially hindered in case of adsorption on LiX. This obviously indicates a stronger interaction of hydrogen with Li cations. On the other hand, the adsorption isotherms for LiX, NaX and CsX zeolites were almost identical, indicating close-lying values of the heats of adsorption [35].

In previous work, T.sooknoi and J.Dwyer used basic zeolite catalysts, to investigate the role of substrate's electrophilicity by competitive adsorption and catalytic alkylation of acetonitrile. Adsorption strength of the substrates was found to depend largely on their electrophilicity and basicity of the zeolite framework. The strong adsorption of acetonitrile on basic zeolite catalysts also leads to an increased alkylation activity, but reduce the decomposition of methanol to carbon monoxide and hydrogen [36].

CHAPTER 3

EXPERIMENTAL DETAILS

3.1 Reagents

1. Air Zero (TIG)
2. Acetonitrile (Fluka), 99.5%
3. Acetonylacetone (Fluka), $\geq$ 97%
4. Acrylonitrile (Fluka), $\geq$ 99%
5. Cesium acetate (Fluka)
6. 2-Cyclohexen-1-one (Fluka), $\geq$ 95%
7. Distilled water
8. 2,5-Dimethylfuran (Fluka), $\geq$ 97%
9. Hydrogen gas (TIG)
10. Molecular sieve 13X, pellet (UOP)
11. Molecular sieve 13X, powder (Aldrich)
12. Methanol (Carlo Erba), 99%
13. 3-Methyl-2-cyclopentenone (Fluka), $\geq$ 97%
14. Nitrogen gas (TIG)
15. Potassium nitrate (Carlo Erba)
16. Propionitrile (Fluka), $\geq$ 99%

3.2 Apparatus

1. Basic bench centrifuge (MSB 020.CX1.5, Centaur 2)
2. Catalytic test rig
3. Condenser
4. CHNS/O analyzer (CHNS/O 2400, Perkin Elmer, Mahidol university)
5. Furnace (Vecstar Furnaces)
6. Gas Adsorption Analyzer (Autosorb-1C, Quantrachrome)
7. Gas Chromatograph (Buck scientific, model 910)
8. Gas Chromatograph (3800 Gas Chromatograph, Varian)

9. Gas Chromatograph/Mass spectrometer (6890N/5973N, Agilent, Scientific Instruments Service Centre, KMITL)
10. Heating mantle
11. Hotplate
12. Laboratory glassware
13. Magnetic stirrer
14. Oven
15. Scanning Electron Microscope (LEO 1455VP, LEO Electron Microscopy, Scientific Instruments Service Centre, KMITL)
16. Syringe pump (Razel Syringe pump, model 99)
17. Sieve (U.S.A. standard sieve, AASHO N-92)
18. Thermogravimetric Analyzer (Pyris 1 TG, Perkin Elmer, Scientific Instruments Service Centre, KMITL)
19. Vial
20. Water circulator
21. X-Ray Fluorescense Spectrometer (SRS 3400, Bruker AG, Scientific Instruments Service Centre, KMITL)
22. X-Ray Powder Diffractometer D8 Advance, Bruker AG, Scientific Instruments Service Centre, KMITL)

3.3 Experiment procedure

3.3.1 Preparation of basic zeolite catalysts.

3.3.1.1 Cesium cation exchanged Zeolite X

3.3.1.2 Potassium cation exchanged Zeolite X

3.3.2 Characterization of zeolites catalysts.

3.3.2.1 Crystal morphology using Scanning Electron Microscope (SEM)

3.3.2.2 Zeolite structure using X-ray Power Diffractrometer (XRD)

3.3.2.3 Chemical composition of the zeolite samples using X-ray Fluorescense Spectrometer (XRF)

3.3.2.4 Surface area using Gas Adsorption Analyzer

3.3.2.5 Carbon dioxide Adsorption

3.3.3 Acid – Base Catalytic Characterization by Cyclisation

3.3.4 Catalytic testing

3.3.3.1 The activity of the catalyst on the alkylation of acetonitrile with methanol

3.3.3.2 The activity of the catalyst on the hydrogenation of acrylonitrile

3.3.3.3 The activity of the catalyst on the hydrogenolysis of propionitrile

3.4 Experimental details

3.4.1 Preparation of basic zeolites catalysts.

3.4.1.1 Cesium cation exchanged Zeolite X

Cesium exchanged zeolite X incorporated with cesium cation was prepared by ion exchange of NaX (molecular sieve 13X) with cesium acetate aqueous solution (1g NaX in 100 ml, 0.1 M $C_2H_3CsO_2$) at 80 ^{0}C for 24 hours. After that, this sample was filtrated without washing and dried at 105 ^{0}C overnight. This sample was designated as CsNaX30. CsNaX20, CsNaX15 and CsNaX10 were prepared with the same procedure as used for the preparation of CsNaX30 except that washing with deionised water for 4, 7 and 10 times was applied, respectively. After that, these samples were calcined in dry air at 450 ^{0}C (heating rate at 2 ^{0}C/min) for an hour.

3.4.1.2 Potassium cation exchanged Zeolite X

Partially exchanged potassium zeolite X was prepared by ion exchanged of commercial NaX. Molecular sieve 13X (5.0g), obtained from Aldrich, was stirred in potassium nitrate solution (500 ml, 0.1 M KNO_3) at 80 ^{0}C for 3 hours. The procedure was repeated three times. After that, this sample was filtrated and dried at 105 ^{0}C overnight and is designated as KX. KNaX was prepared with the same procedure as used for the preparation of KX except that washing with deionised water was included. Finally, these samples were calcined in dry air at 400 ^{0}C (heating rate at 2 ^{0}C/min) for an hour.

3.4.2 Characterization of zeolites

3.4.2.1 Crystal morphology of zeolites

The crystal morphology and crystal size were determined by scanning electron microscope, equipped with an energy dispersive X-ray fluorescence spectroscopy (EDS) accessories. The sample was prepared by thoroughly placing dried zeolite onto the sample holder. It was then coated with gold thin film by ion sputtering. The sample was placed in the sample chamber of scanning electron microscope and evacuated from ambient pressure to 10^{-4} torr. The

scanning electron micrographs were taken at the magnification of 500, 1000, 2000, and 3000 times.

3.4.2.2 Zeolites structure

The zeolites structure were determined by X-ray diffractometer (D8 Advance, Bruker). The sample was prepared by packing the zeolite in the sample holder. CuKα X-ray beam was used for analysis at 40 kV, 40 mA. The sample were scanned from 2 angle of 5^0 to 60^0. X-ray diffraction pattern of sample was compared with X-ray diffraction pattern of standard zeolite for determining the structure.

3.4.2.3 Chemical composition of the zeolite samples

The chemical composition of zeolite catalysts can be determined by X-ray fluorescence spectrometer (SRS 3400, Bruker). The sample was prepared by mixing 4.5 grams of boric acid and 0.5 grams of zeolites and sent to a grinder. The mixer was packed onto sample holder and then compressed at 150 kN. The sample was placed in the sample chamber. Rhodium was used as X-ray source for measuring at 50 kV, 60 mA.

3.4.2.4 Surface area

Surface area of zeolites was determined by Gas Adsorption Analyzer (Autosorb-1C, Quantachrome). The sample was prepared by weighing approximately 20 mg of zeolites into the cleaned and dried sample cell. The sample cell was attached to the out gassing station. Heating mantle was installed and the temperature was raised to 350^0C. The sample cell was then removed from the out gassing station after the nitrogen was filled and was attached to the analysis station. The equilibration time is set to 3 minutes and the adsorption was tested at the partial pressure (P/P_0) range of 10^{-6} to 1.0.

3.4.2.5 Carbon dioxide Adsorption

Carbon dioxide adsorption is the technique using for determination of the basicity and basic strength of the catalyst. This technique was done according to the following procedure: the zeolite sample was weighed accurately about 20 mg and transferred to a clean, dry empty sample cell. This sample cell was attached to the outgassing station. Then, a heating mantle was installed with the sample cell and the temperature was raised to 350 °C. After the residual

adsorbate was removed by temperature and reduced pressure. The carbon dioxide adsorbate was filled by open the gas inlet valve. The sample cell was attached to the sample station. In the initiate adsorption, a ice bath of ice was placed around the sample cell and the measurement of carbon dioxide adsorption was set with 3 minutes equilibration time. When adsorption was complete, the sample cell was removed from the sample station and dried thoroughly.

3.4.3 Acid – Base Catalytic Characterization by Cyclisation

Alkali cations incorporated into zeolites, namely NaX, KX and CsNaX10 were used as catalysts. The powder of sample was prepared by compressing and sent to crashing. After that the resulting solid sample was sieved into 180 – 250 μm "pellet catalyst". The reaction was carried out in a fixed-bed flow reactor at 350^{0}C, as shown in Figure 3.1. Pelleted catalyst (1g) was sandwiched between a packing of inert glass beads in a 40 cm-long Pyrex reactor with a inner diameter of 0.8 cm. Catalysts were preheated prior to the reaction under dried air stream (~30 ml/min) to 450^{0}C. Preheating was carried out for 2 hours, then air was replaced by nitrogen and the reactor temperature was set to 350^{0}C. Nitrogen was used as carrier gas at a flowrate of 35 ml/min and acetonylacetone was continuously fed by syringe pump. The reaction was carried out for 3 hours. Liquid products were collected in a condenser (0^{0}C) every 30 minutes. The product mixture was separated and analysed by gas chromatrography (GC) using a Carbowax 20M column (packed column 1/8" x 6') at 150^{0}C with helium flowrate 30 ml/min as carrier gas. Gas products were not detected.

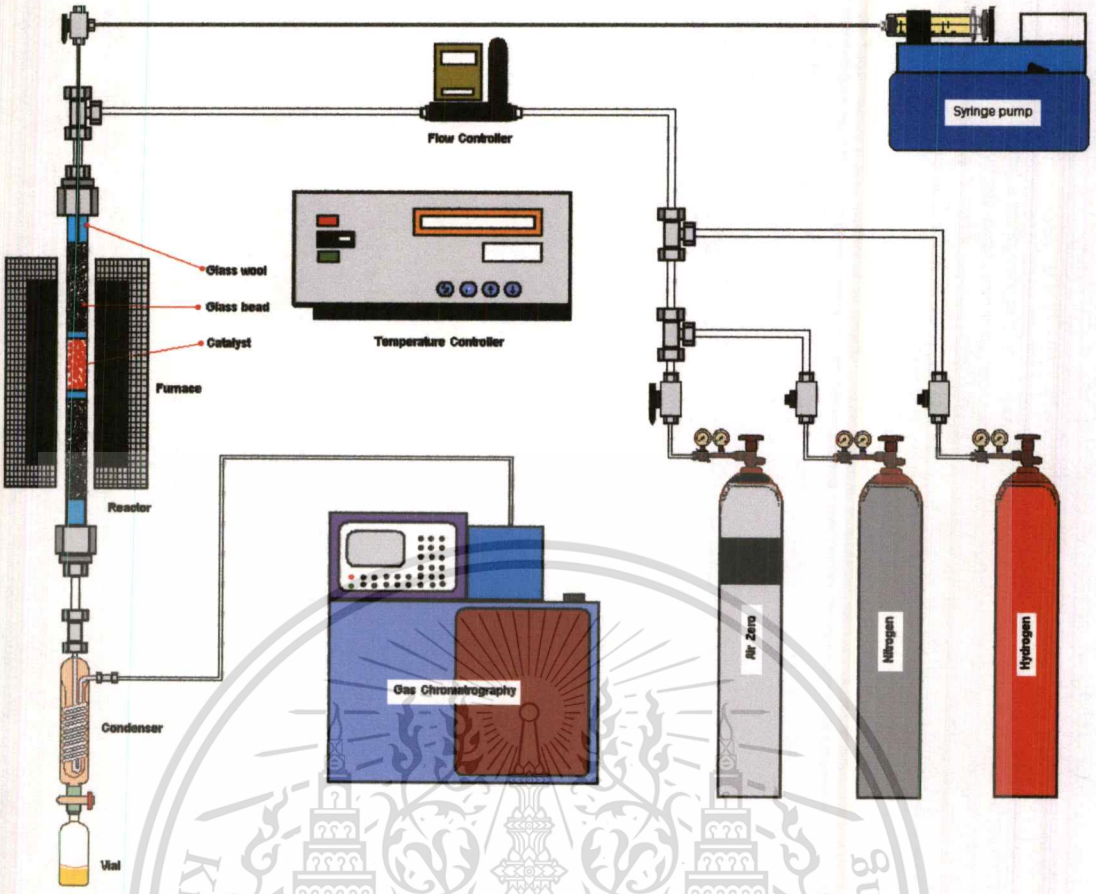

Figure 3.1 The catalytic test rig

3.4.4 Catalytic testing

3.4.4.1 Alkylation of acetonitrile with methanol

NaX, KX, KNaX and CsNaX10, 15, 20 and 30 were used as catalysts. Acetonitrile and methanol were dried and kept over predried Molecular Sieve 13X.

The reactions were carried out using a similar procedure as used for cyclisation in 3.4.3. However the reaction temperature was set to 400^{0}C. Nitrogen was used as carrier gas at a flowrate of 25 ml/min. The mixture of acetonitrile and methanol was fed by syringe pump. A mole fraction of acetonitrile : methanol, 1:10 was usually employed the fed mixture. However, in one experiment, an acetonitrile : methanol mixture in of 1:15 was used as a feed in order to demonstrate the effect of feed composition. The effect of temperature was examined by reactions carried out at 350, 375 and 425 ^{0}C. The effect of contact time was examined using 0.3, 0.5 and 0.7 grams of CsNaX30. Liquid products from the reaction were collected in a condenser (0^{0}C) every

60 minutes and analysed by gas chromatography using a Porapak Q column at 150 ^{0}C with nitrogen as carrier gas at a flow rate of 55 ml/min. Gas products were periodically detected by on-line gas chromatography using a Porapak Q column (packed column 1/8" x 6') at 30 ^{0}C. Nitrogen was again used as carrier gas at the rate of 20 ml/min. The structure of the liquid products were confirmed by GC-MS.

3.4.4.2 Hydrogenation of Acrylonitrile

For hydrogenation of acrylonitrile, Source of hydrogen can be obtained from methanol decomposition and using hydrogen as carrier gas. CsNaX10 and CsNaX20 were used as catalysts. The catalytic reactions were carried out using a similar procedure as used for the alkylation of acetonitrile with methanol in 3.4.4.1. The reactant was continuously fed by syringe pump. The mixture of acrylonitrile and methanol with a mole fraction of acrylonitrile : methanol, 1:50 was used. Also, hydrogen was used as carrier gas at a flowrate of 25 ml/min in reaction using only acrylonitrile as feed. Liquid products from the reaction were collected in a condenser (0^{0}C) every 60 minutes and analyzed by gas chromatrography using a Porapak Q column at 150 ^{0}C using nitrogen as carrier gas with flow rate of 55 ml/min.

3.4.4.3 Hydrogenolysis of Propionitrile

In the hydrogenolysis of propionitrile, Source of hydrogen can be obtained from methanol decomposition. CsNaX10 and CsNaX20 were also used as catalysts. The catalytic reactions were carried out a similar procedure as used for the alkylation of acetonitrile with methanol in 3.4.4.1. The mixture of propionitrile and methanol was fed by syringe pump. A mole of fraction of propionitrile : methanol, 1:50 was used. Liquid and gas products from the reaction were collected and analyzed using the same procedure as used for alkylation in 3.4.4.1.

Catalytic testing parameter are summarized in Table 3.1

Table 3.1 Catalytic test parameter

	Reaction	Catalyst	Feed	ratio (mole/mole)	Reaction temperature (C°)	W/F	Carrier gas
1	Cyclisation	NaX	acetonylacetone	only	350	~75	N_2
2		KX	acetonylacetone	only	350	~75	N_2
3		CsNaX10	acetonylacetone	only	350	~75	N_2
4	Alkylation	NaX	CH_3OH/CH_3CN	10/1	400	~40	N_2
5		KX	CH_3OH/CH_3CN	10/1	400	~40	N_2
6		KNaX	CH_3OH/CH_3CN	10/1	400	~40	N_2
7		CsNaX10	CH_3OH/CH_3CN	10/1	400	~40	N_2
8		CsNaX15	CH_3OH/CH_3CN	10/1	400	~40	N_2
9		CsNaX20	CH_3OH/CH_3CN	10/1	400	~40	N_2
10		CsNaX30	CH_3OH/CH_3CN	10/1	400	~40	N_2
11		CsNaX30	CH_3OH/CH_3CN	10/1	350	~40	N_2
12		CsNaX30	CH_3OH/CH_3CN	10/1	375	~40	N_2
13		CsNaX30	CH_3OH/CH_3CN	10/1	425	~40	N_2
14		CsNaX30	CH_3OH/CH_3CN	10/1	400	~12	N_2
15		CsNaX30	CH_3OH/CH_3CN	10/1	400	~21	N_2
16		CsNaX30	CH_3OH/CH_3CN	10/1	400	~29	N_2
17		CsNaX15	CH_3OH/CH_3CN	15/1	400	~40	N_2
18	Hydrogenation	CsNaX30	CH_2CHCN	only	400	~5	H_2
19		CsNaX30	CH_3OH/CH_2CHCN	50/1	400	~200	N_2
20		CsNaX10	CH_3OH/CH_2CHCN	50/1	400	~200	N_2
21	Hydrogenolysis	CsNaX10	CH_3OH/CH_3CH_2CN	50/1	400	~200	N_2
22		CsNaX30	CH_3OH/CH_3CH_2CN	50/1	400	~200	N_2

CHAPTER 4

RESULTS AND DISCUSSION

4.1 Catalyst characterization

4.1.1 Elementals Analysis

The silicon/aluminium molar ratio, degree of ion exchange and amount of excess cation per unit cell of zeoliteX catalysts were determined by X-ray fluorescence spectroscopy as shown in Table 4.1.

Table 4.1 Determination of silicon, aluminium, potassium and cesium content of zeolites

Zeolite	Si/Al ratio	Degree of ion exchange	Excess cation per unit cell
NaX	1.18	-	-
KNaX	1.16	39.92%	14.47
KX	1.19	100%	28.25
CsNaX10	1.23	36.59%	10.28
CsNaX15	1.21	37.56%	16.27
CsNaX20	1.23	37.21%	22.12
CsNaX30	1.23	36.04%	30.64

These values are calculated from elemental analysis as shown in Appendix A. A degree of ion exchange of cesium in zeolite X is limited at approximately 37%. This is because of size of Cs^+ is much larger than K^+ and Na^+. The cesium cations in this material, designated as "CsNaX", are presumably exchanged cations located mainly in the supercages. However, extra framework Cs^+ is found in all zeoliteX samples, depend on number of washing with deionised water. It is shown that by doing so, degree of ion exchange for all CsNaX are the same. Only excess cesium is varied by number of washings. It is also presumed that the excess of cesium cations are present as cesium oxide (Cs_2O), peroxide (Cs_2O_2) and superoxide (CsO_2)[37]. The occlusion of excess potassium and cesium clusters leads to a moderate decrease in the surface area of the zeolites as shown in Table 4.2.

4.1.2 Specific Surface Area

The BET surface area of zeoliteX catalysts were shown in Table 4.2

Table 4.2 The specific surface area of zeoliteX catalysts

ZeoliteX catalysts	Specific surface area (m^2/g)
NaX	672
KNaX	563
KX	517
CsNaX10	506
CsNaX15	483
CsNaX20	452
CsNaX30	367

The decrease in the specific surface area of Zeolite NaX was obtained after exchange with K^+ and Cs^+ cations into zeolite. The decreased trend in specific surface area as a function of increased size of exchangeable cations and number of cesium excess per unit cell indicated that all the exchanged cations are present in the pore of catalysts.

4.1.3 Catalyst Structure

X-ray diffraction patterns of catalyst were obtained from Bruker X- ray powder diffractometer using CuKα radiation. X-ray diffraction patterns of zeolite NaX, KX and CsNaX10 were shown in Figure 4.1

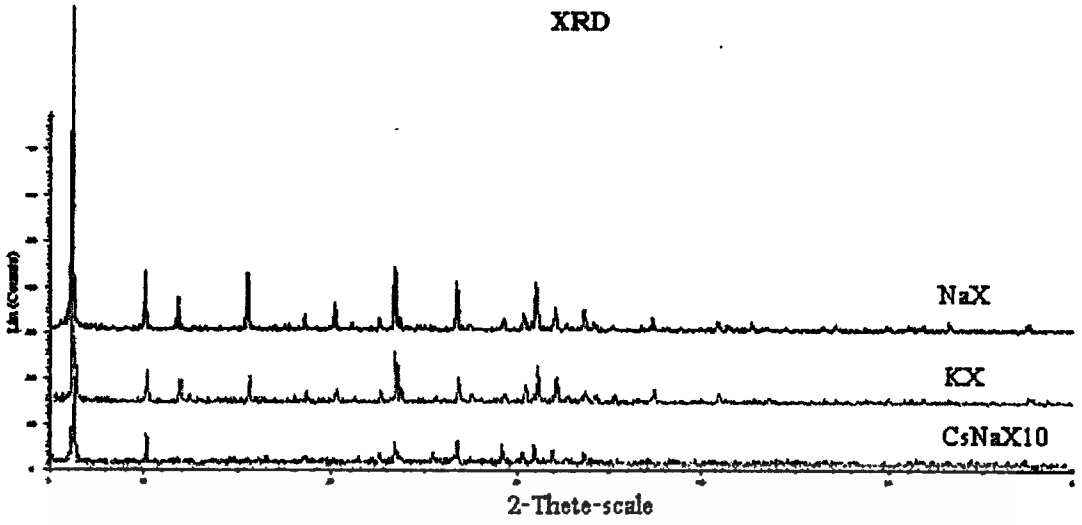

Figure 4.1 X-ray diffraction patterns of NaX, KX and CsNaX10

The results showed the decrease in peak intensity of incorporated potassium and cesium ion into NaX zeolite. This lowering of peak intensity might be contributed from the difference of X-ray adsorption coefficient of the parent catalyst when the larger exchanged cations (K^+ and Cs^+) are incorporated [38]. Large cation can adsorb and scatter X-ray radiation, resulting in reduction of peak intensity. However, this shall not affect crystallinity of the sample. This is because when back-ion exchanged of the cesium containing catalysts with sodium cations. It was found that the peak intensity is recovered [39].Therefore, it was confirmed that the crystallinity and framework structure were retained after ion exchange or incorporation of the cesium cations.

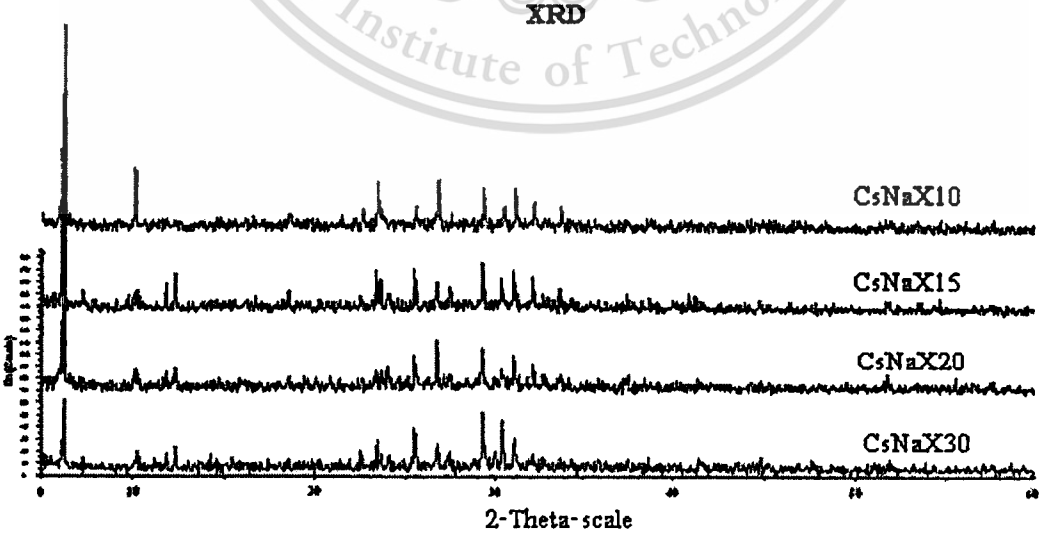

Figure 4.2 X-ray diffraction patterns of CsNaX10, CsNaX15, CsNaX20 and CsNaX30

The X-ray patterns of zeolites X recorded after increasing cesium content show significant changes in the positions and intensities of the reflections (Figure 4.2) These changes are caused by the different scattering coefficients of sodium and cesium cations and the additional reflections of the excess cesium species which render the decrease in peak intensity.

4.1.4 Crystal Morphology

Figure 4.3, 4.4 and 4.5 show scanning electron micrograph of NaX (Molecular sieve 13X), KX and CsNaX30, respectively. The crystal size of all samples are approximately 3.0 μm diameter and appeared to be of quality with regard to the regularity of their shape. It is expected that ion exchange does not affect on crystal sizes.

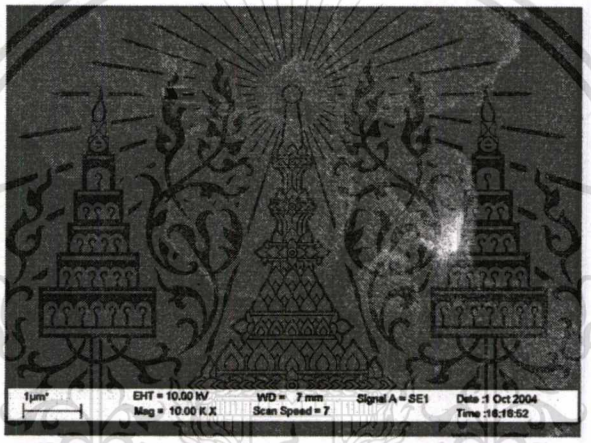

Figure 4.3 Morphology of calcined zeolite NaX

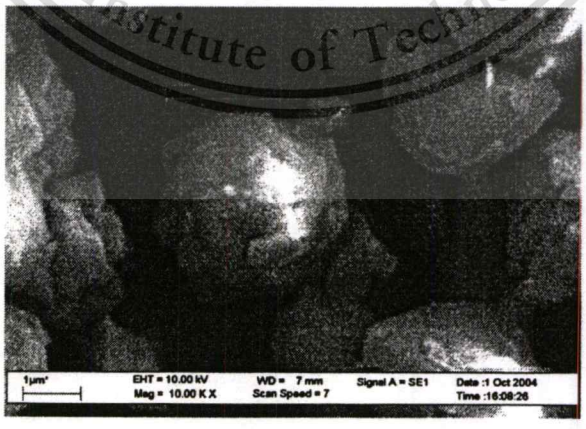

Figure 4.4 Morphology of calcined zeolite KX

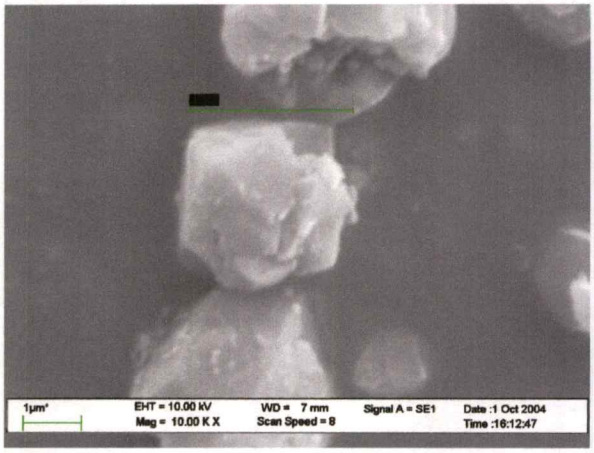

Figure 4.5 Morphology of calcined zeolite CsNaX30

The energy dispersive X-ray fluorescence spectroscopy (EDS) accessory was used to detect the dispersion of metal loading on ZeoliteX as shown in Figure 4.6 and 4.7.

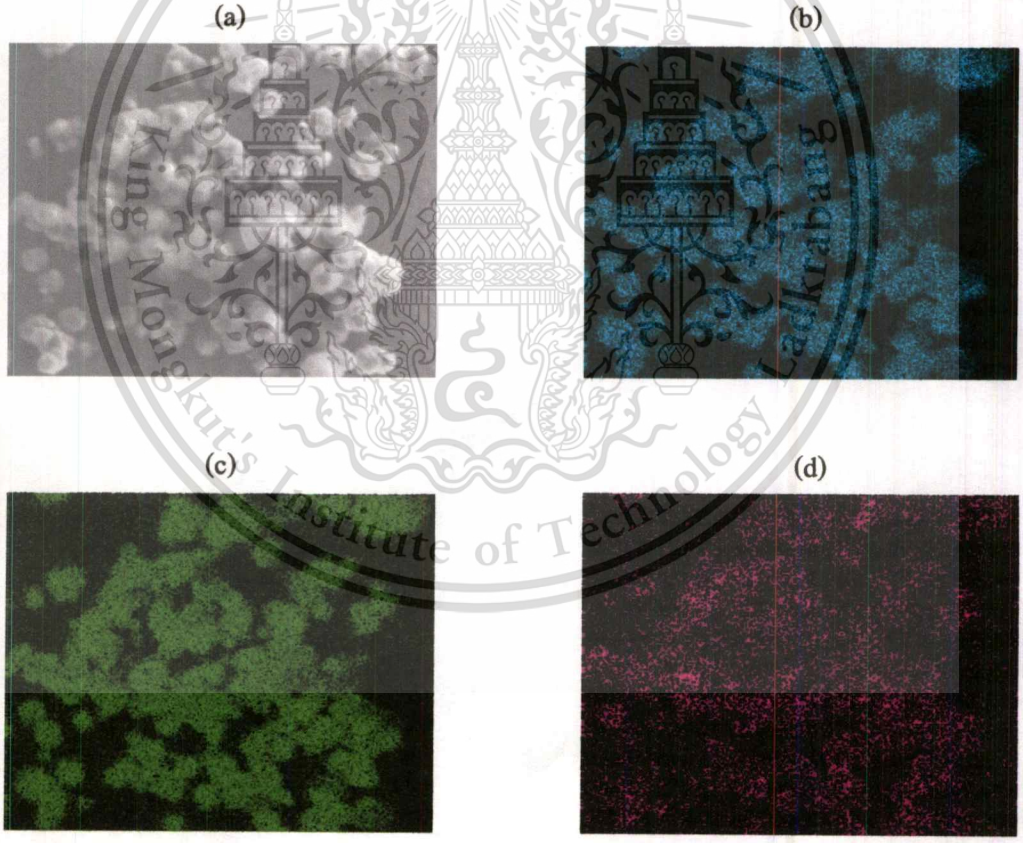

Figure 4.6 EDS images of CsNaX10 (a), Al dispersive on CsNaX10 (b), Si (c), Cs (d)

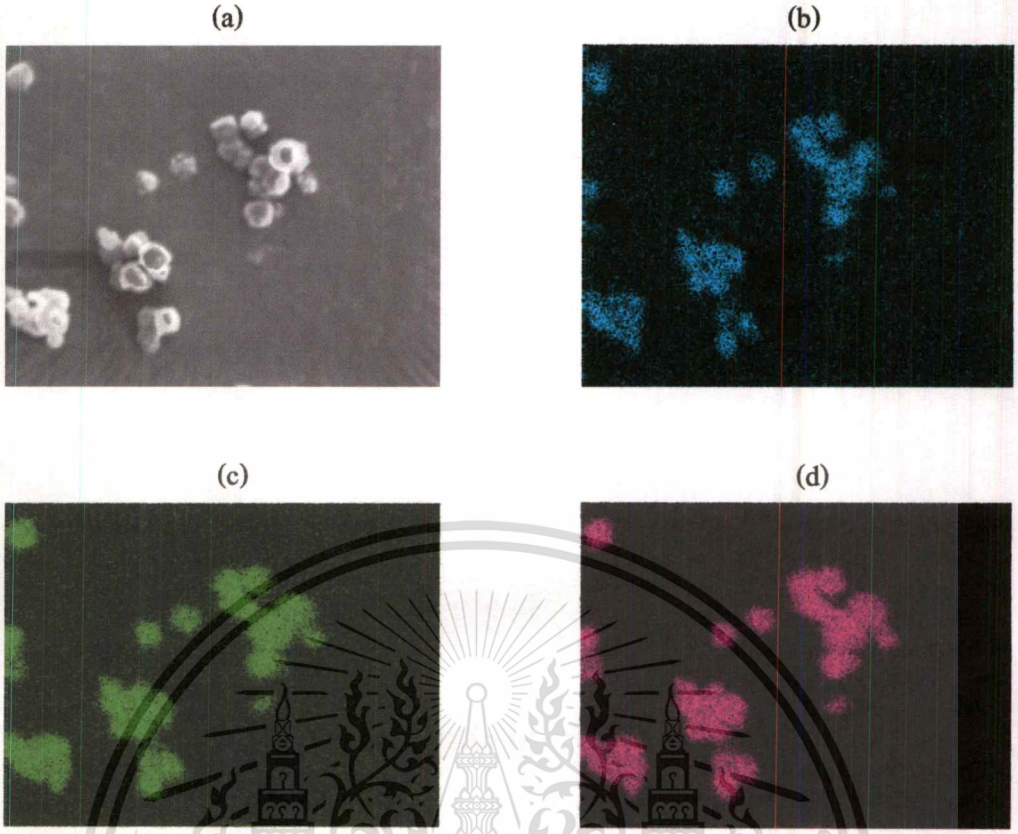

Figure 4.7 EDS images of CsNaX30 (a), Al dispersive on CsNaX30 (b), Si (c), Cs (d)

SEM-EDS shows that Cs^+ is well dispersed on zeolite crystal for the both sample. Moreover, it can be seen that the amounts of Cs^+ in CsNaX30 is proportionally higher than that in CsNaX10 as shown in Figure 4.7d and 4.6d, respectively. No cluster of Cs salts can be individually observed from both samples, it can be seen that Cs^+ is always co-existed with Al and Si. This indicated the occlusion of Cs^+, either as exchangeable cation or excess cesium on the zeolites. It is expected that catalytic activity is only derived from Cs^+ in the zeolite crystals.

4.1.5 Carbon dioxide Adsorption

The basicity of ion-exchanged zeolites arises from the framework negative charge, thus, the relatively high aluminum content of zeolite X results in a substantial framework negative charge, which makes zeolite X one of the most basic zeolites when in the alkali-exchanged form. In addition to reports in the literature [32, 33], the excess cesium "cluster" can provide additional basicity in zeolites.

In order to verify the basicity contributed from the excess cesium "cluster" species in these catalysts, adsorption of carbon dioxide, was tested for CsNaX10 and CsNaX30. It is known that carbon dioxide is a good probe for basicity determination. An interaction of carbon dioxide with zeolite takes place at the framework oxygen adjacent to the charge balancing cations forming a bent configuration species where negative charge from the surface would be distributed in part over the two oxygens of carbon dioxide. This carbonate like species can be stabilized by interaction with the charge balancing exchangeable cations and such interaction is facilitated by both the basicity of the framework oxygen and the polarizing capacity of the exchangeable cation. Since cesium is a highly polarizable cation, carbon dioxide take place on the basic framework of cesium exchanged zeolite X can be demonstrated in Figure 4.8.

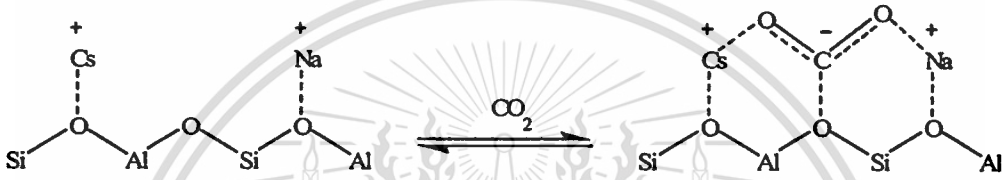

Figure 4.8 Carbon dioxide take place on the basic framework of cesium exchanged zeolite X

In addition, excess cesium cation "cluster" species may also facilitate the formation of carbonate-like structures. Over CsNaX, interaction of carbon dioxide with the excess cesium cation "cluster" can be postulated as follows:

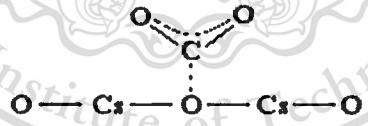

Isotherms for carbon dioxide adsorption on cesium exchanged zeolites X are presented in Figure4.9. The adsorbed amount is expressed in volume of carbon dioxide adsorption per gram of catalysts varies. The result has shown that the adsorption capacity of carbon dioxide on CsNaX30 is higher than that on CsNaX10. This can be attributed to the fact that of CsNaX30 is more basicity than that of CsNaX10. Results of elemental analysis suggest that CsNaX30 contains a larger amount of excess cesium cations per unit cell as compared to CsNaX10 (Table4.1). From the results, it indicated that the basicity of CsNaX increases with the amount of excess cesium per unit cell.

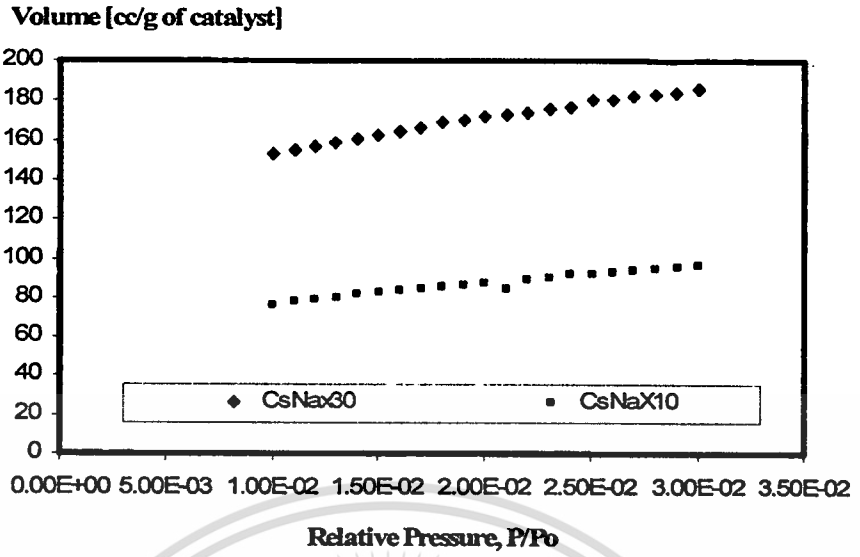

Figure 4.9 Isotherms concerning the adsorption of carbon dioxide measured on CsNaX30 and CsNaX10.

The isotherm equation describing adsorbed molecules on sites which are independent of each other and are energetically equivalent. This monolayer adsorption is well fitted with Langmuir adsorption isotherm as shown in Appendix D. The adsorption equilibrium constants determined by Langmuir plot are summarized in Table 4.3.

Table 4.3 Langmuir adsorption equilibrium constant

Catalysts	Langmuir constant (*K*)
CsNaX10	1.91E+02
CsNaX30	2.41E+02

It can be seen that Langmuir adsorption equilibrium constant (K) of CsNaX30 is higher than that of CsNaX10. It is indicated that the adsorption strength of carbon dioxide on CsNaX30 is stronger than that on CsNaX10. This implies that the basic strength of catalyst depends on the amounts of excess cesium per unit cell. From the results, it can be concluded that the basicity and basic strength of the zeolite catalyst increases with the amounts of excess cesium per unit cell.

4.2 Acid-Base Catalytic Characterization by Cyclisation

Acetonylacetone (2, 5-hexanedione) can undergo intramolecular cyclisation in the presence of either acid or base catalysts. 2, 5-Dimethylfuran is formed from the acid catalysed cyclisation whilst, in the presence of base catalysts, 3-methyl-2-cyclopentenone is produced. The fact that, in the presence of acid, the carbonyl groups of acetonylacetone can readily be protonated, arises from the enolisation of carbonyl group which, then, undergoes O-alkylation with the other protonated carbonyl carbon. The cyclic ketal formed rapidly dehydrates to give a heterocycle aromatic compound, 2, 5-dimethylfuran. (Figure 4.10)

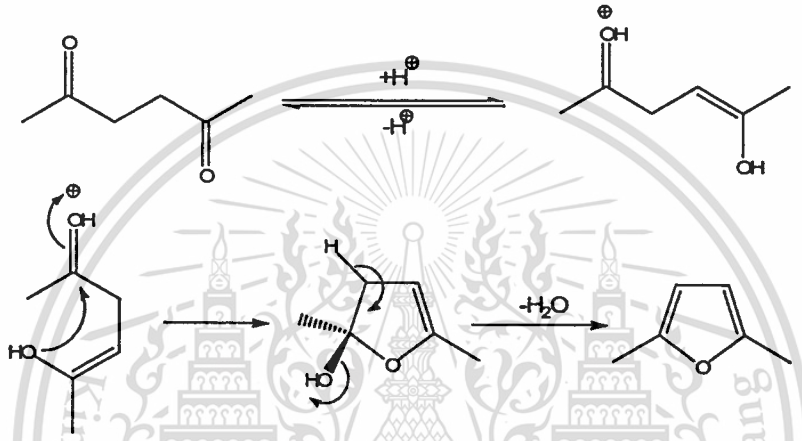

Figure 4.10 Formation of 2, 5-Dimethylfuran in acid catalysted cyclisation

However, in basic catalyst, the less sterically restricted enolated carbanion can be formed and undergoes cyclisation at the other carbonyl carbon. The resulting β-hydroxyl cyclic ketone is subsequently dehydrated to the α, β-unsaturated cyclic ketone, 3-methyl-2-cyclopentenone. (Figure 4.11)

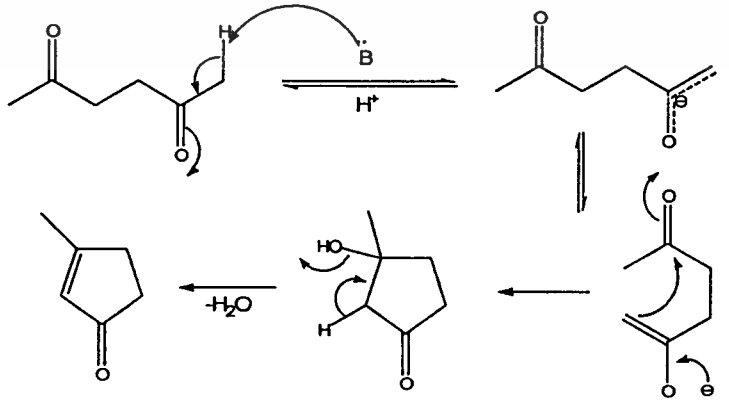

Figure 4.11 Formation of 3-methyl-2-cyclopentenone

The fact that the cyclisation of acetonylacetone can be catalysed by both acid and base catalysts, provides a catalytic probe for determining the acid-base catalytic behavior of zeolite X catalysts. In the present work, zeolite X containing sodium, potassium and cesium in the framework were used to investigated the role of the alkali cations in the cyclisation of acetonylacetone.

Table4.4 shows the results from reactions over various alkali cations incorporated into zeolite X catalysts. It was shown that the cyclisation of acetonylacetone over all alkali zeolite X catalysts produced, selectively, 3-methyl-2-cyclopentenone as a major product. Whilst 2, 5-dimethylfuran was found in small amounts. Therefore, zeolites incorporated with alkali cations are basic catalyst. Over zeolite X, the basicity of the catalysts appears to increase with the size of alkali cations incorporated.

Table 4.4 Results from the cyclisation of acetonylacetone

Catalyst	Time on stream	Acetonylacetone Conversion	2,5 Dimethylfuran Yield	3-Methyl-2-cyclopentenone Yield
NaX	60	98.9	0.5	95.6
	90	67	0.2	65.8
	120	40.1	0.1	38.7
	150	22.6	0.2	21.9
	180	16.3	0.1	16.1
KX	60	99.3	1.4	96.3
	90	86	2.1	83.2
	120	43.2	1.9	39.8
	150	35.1	1.7	33.6
	180	28.7	1.9	25.4
CsNaX10	60	100	0.9	97.8
	90	95.2	1.1	93.6
	120	77.3	1.2	75.1
	150	50.1	0.5	48.2
	180	40.4	0.6	38.7

It was previously suggested that the basicity of zeoliteX arises from the cations which play an important role in polarization of the basic sites. As the exchangeable cations become larger, its lewis acidity is decreased leading to a reduced ability to stabilize enolisation of acetonylacetone. This results in a decreased activity for 2, 5-dimethylfuran but an increased activity in cyclisation via base catalysed pathway as shown in Figure 4.11.[40]

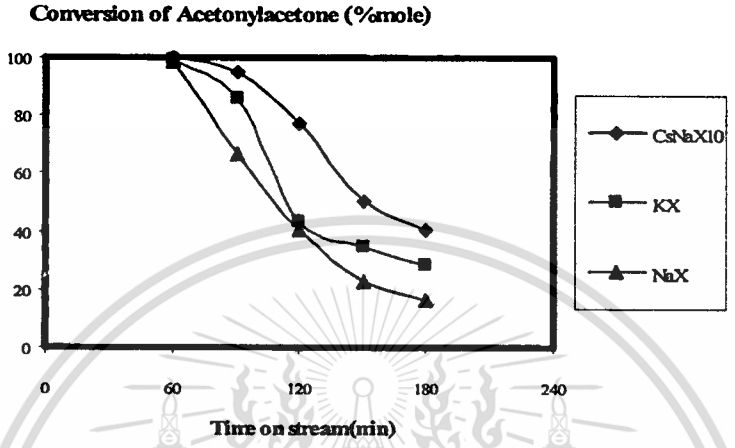

Figure 4.12 Conversion of acetonylacetone over alkali cation incorporated Zeolite X

In addition, the conversion of acetonylacetone over alkali cation incorporated suggests that CsNaX possess high activity and deactivates slowly, as compared to KX and NaX. This supports the above conclusion that the basicity of the catalysts depend on the cation, in the order of $Cs^+ > K^+ > Na^+$ (Figure 4.12).

The above observation is in accordance with previous reports which employ various technique such as adsorption of carbon dioxide in combination with IR spectroscopy [41], microcalorimetry, or temperature-programmed desorption (TPD) [42] to investigate basic site of catalyst. It was agreed with the present study that the basicity and basic strength of catalysts is enhanced when the cationic size is increased.

4.3 Alkylation of Acetonitrile with Methanol

From the Figure 4.13, the conversion of methanol and acetonitrile obtained from the alkylation of acetonitrile with methanol over basic zeolite (CsNaX10) catalyst are plotted.

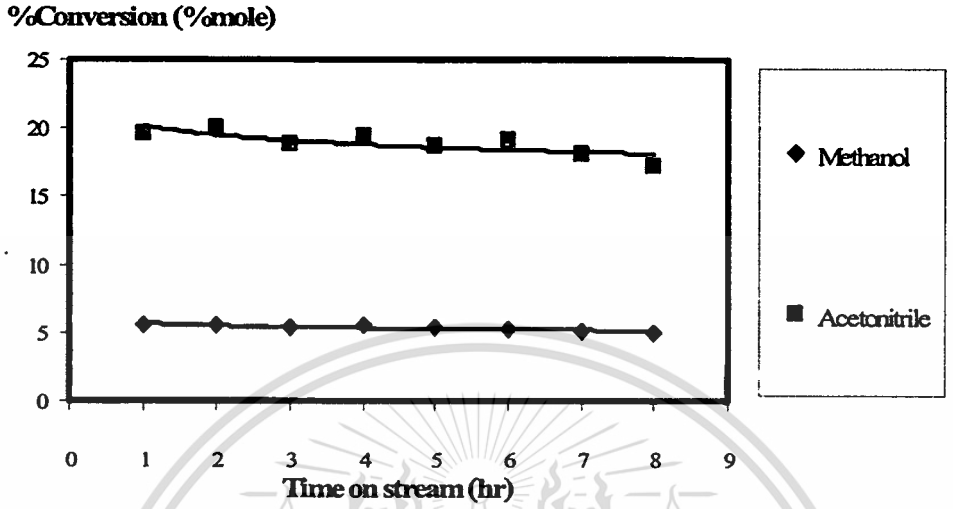

Figure 4.13 Conversion of methanol and acetonitrile at 400 °C over CsNaX10.
(Reaction temperature; 400°C, W/F; ~41g.hr.mol^{-1}, Carrier gas; nitrogen flow rate 25ml/min; feed; methanol/acetonitrile: 10/1)

The result shows that the methanol conversion exhibits steady state at about 5% throughout the reaction whereas acetonitrile conversion shows a somewhat decrease with time on stream. This result indicates that the catalyst is slightly deactivated. The fact that conversion of acetonitrile appears to be higher than that of methanol is because, in this experiment, the methanol to acetonitrile ratio of 10:1 was used as a feed

$$(n)CH_3OH + (n)CH_3CN \longrightarrow \underset{\text{(propionitrile)}}{(m)CH_3CH_2CN} + \underset{\text{(acrylonitrile)}}{(n-m)CH_2{=}CHCN} + H_2O$$

Figure 4.14 The pattern for alkylation of methanol with acetonitrile.

According to of the stoichiometric conversion shown in Figure 4.14, the conversion of methanol should be the same as acetonitrile which can be calculated to about 2% (20% x 0.1; ratio of acetonitrile/methanol). However, methanol conversion found in the experiment was approximately 5%.

This result suggested that, methanol not only converted into alkylated product but also decomposes into formaldehyde, carbon monoxide, and hydrogen as shown in Figure 4.15. These components can be detected by on-line Gas chromatography in small amounts.

$$CH_3OH \longrightarrow HCHO \longrightarrow CO$$

$$CH_3OH \longrightarrow CO + 2H_2$$

Figure 4.15 Stoichiometric equations for the decomposition of methanol to formaldehyde, carbon monoxide and hydrogen [43]

The alkylation of acetonitrile with methanol over basic catalysts results in a mixture of liquid products content consist of propionitrile, acrylonitrile and other products. Yield of these products are shown in Figure 4.16.

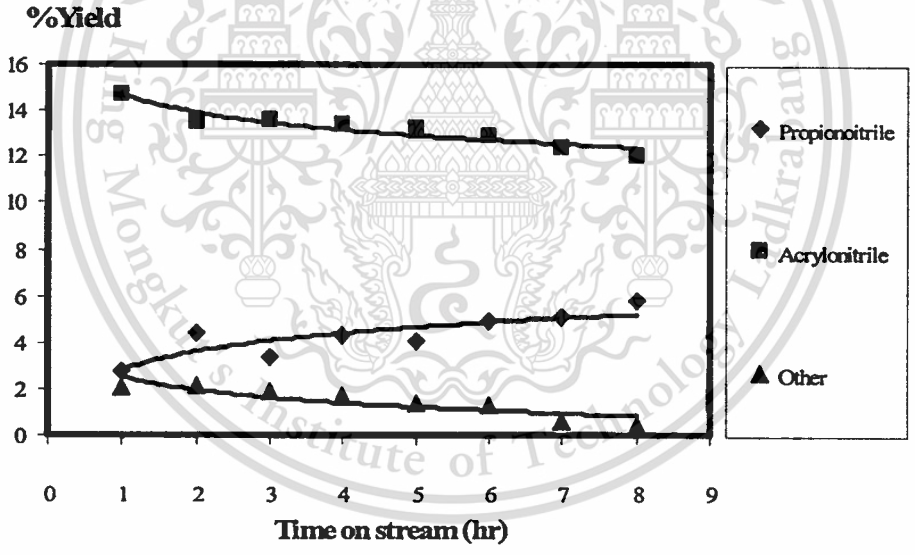

Figure 4.16 Products distribution from the alkylation of acetonitrile with methanol over CsNaX10.

It can be seen that high yield of alkylated products (acrylonitrile and propionitrile) was obtained over cesium exchanged zeolite X (conversion of acetonitrile is 20%). These products can be formed by reaction of acetonitrile with methanol as shown in Figure 4.17.

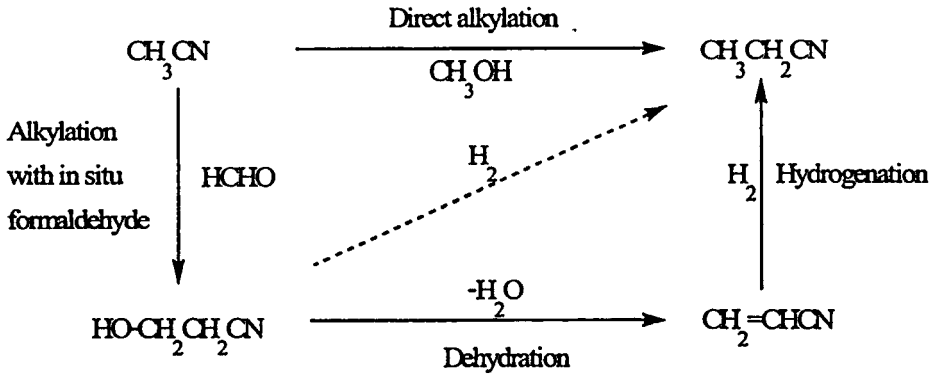

Figure 4.17 Reaction pathways for the alkylation of acetonitrile with methanol

It is proposed that acetonitrile can be strongly adsorbed on basic sites which facilitates proton abstraction, at the α-carbon of acetonitrile, subsequently forming a carbanion intermediate. The carbanion species formed can be stabilized by both resonance and inductive effects, associated with the presence of the –CN group (a strong electron withdrawing group), providing stability and activity to react with an appropriate electrophile.

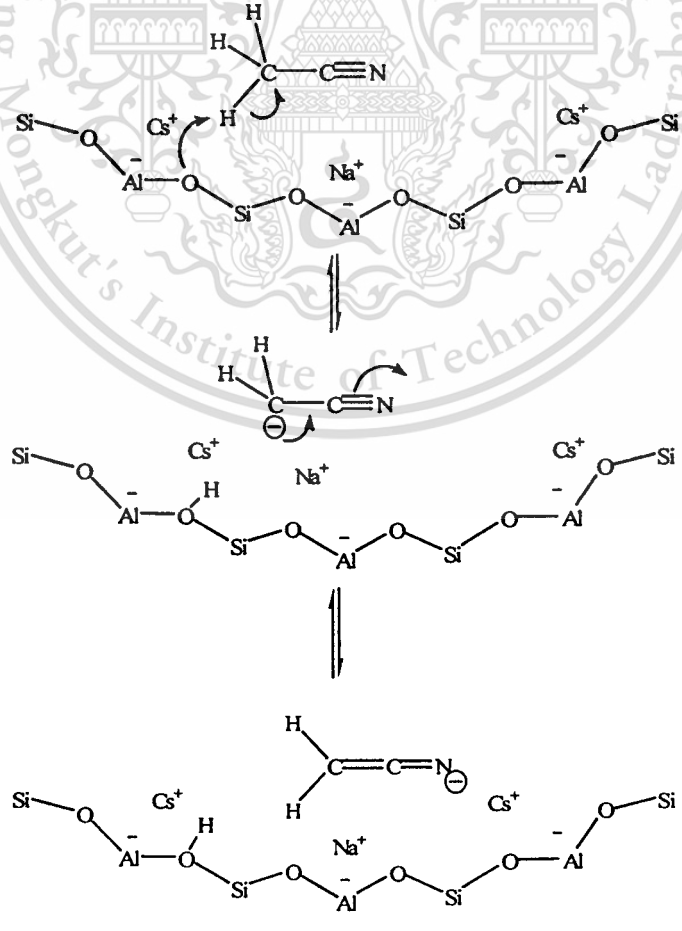

This is likely to be formaldehyde and methanol. The formation of unsaturated product (acrylonitrile) should be produced via alkylation of acetonitrile with formaldehyde. Whilst the saturated product (propionitrile) is likely to produced by direct alkylation with methanol or hydrogenation of acrylonitrile with hydrogen, primarily formed by methanol decomposition.

In addition, other products are found in the product mixture. Gas Chromatograph/Mass spectrometer confirms that they are butanedinitrile, 2-butenenitrile and butanenitrile. Chromatograms of these components are shown in Figure C.1. Butanedinitrile is a coupling product from propionitrile. In the thermal process, cleavage of propionitrile created free radical, which subsequently coupled with each other to produce butanedinitrile as proposed in Figure 4.18.

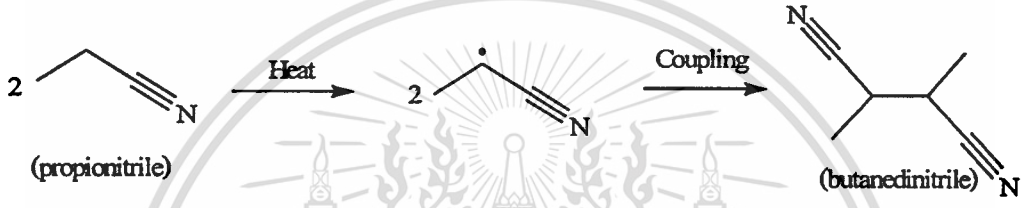

Figure 4.18 Possible pathway for coupling of propionitrile into butanedinitrile via a free radical intermediates

2-Butenenitrile and butanenitrile were found in larger quantity. They were products from side reaction of acetonitrile and their formation can be proposed according to the following scheme (Figure 4.19)

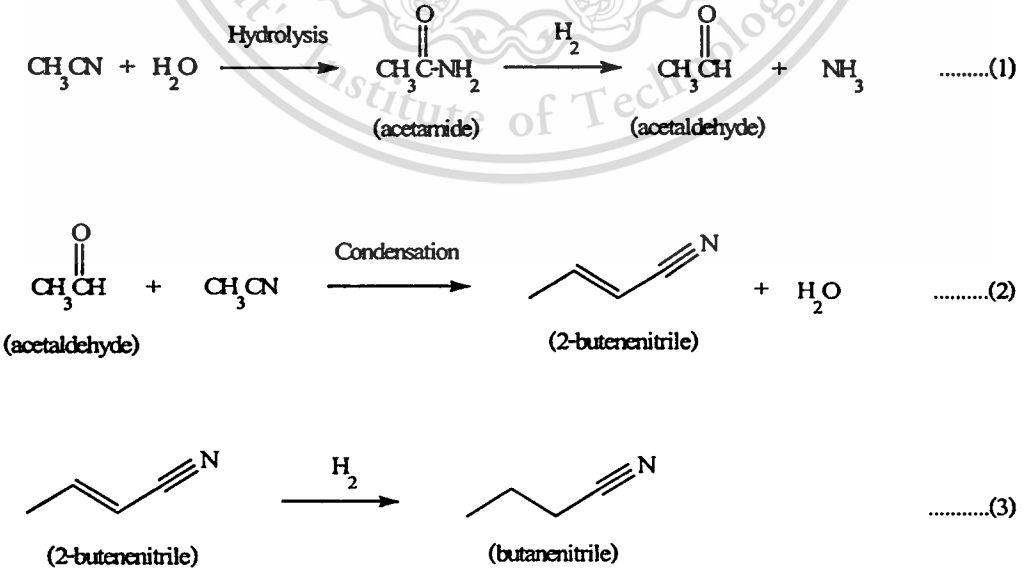

Figure 4.19 The formation of 2-butenenitrile and butanenitrile

According to the fact that the product mixture contains water as co-product from alkylation reaction, acetonitrile can undergo hydrogenolysis to acetaldehyde as shown in equation (1). Acetonitrile then react with acetaldehyde to form 2-butenenitrile through condensation as shown in equation (2). This reaction may occur substantially if base is used as catalysts. This is because base catalysts will promote proton abstraction at α-carbon of acetonitrile, producing carbanion intermediate that will react with acetaldehyde. In addition, 2-butenenitrile can undergo hydrogenation to give butanenitrile (equation (3)), employing hydrogen produced from decomposition of methanol.

Based on the preceding discussion, it is plausible to suggest that the side reaction of alkylation take place when water, hydrogen and base catalyst are involved in the reaction.

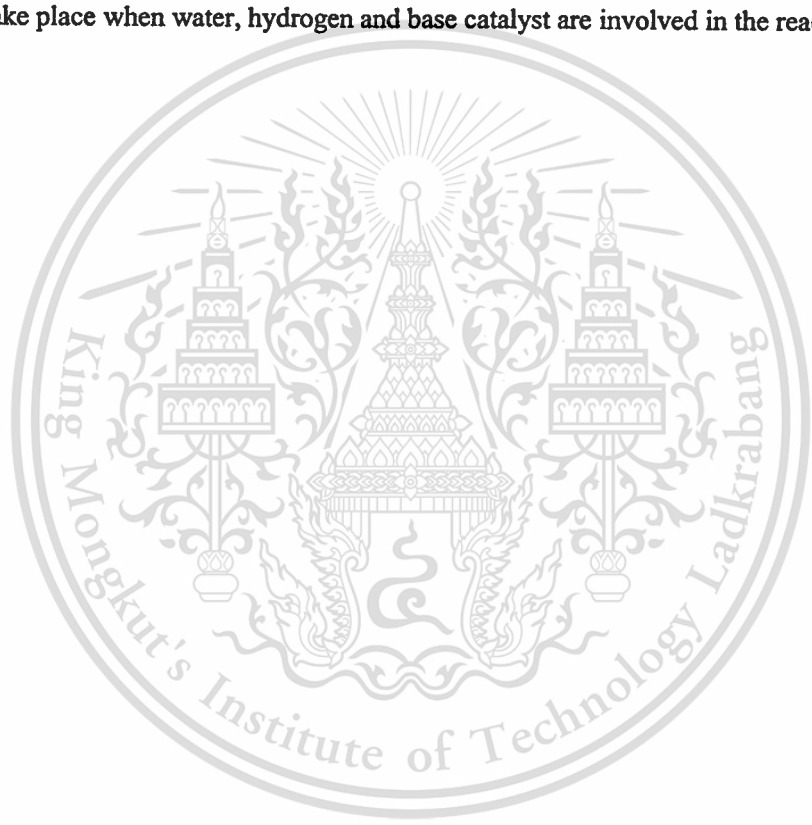

4.3.1 Effect of Cation Exchange

In previous work [44], base catalysts can be used for alkylation of toluene into styrene and ethylbenzene (side chain alkylation products). Yields of alkylated products were found to increase with increasing cation size, in the order $Cs^+ > Rb^+ > K^+ > Na^+$ and zeoliteX was found to be more active than zeoliteY. Thus, zeoliteX is used as solid base catalyst due to its low Si/Al ratio and ease to be modified by ion exchange.

In this works, the effect of cation species was primarily investigated by using zeolite NaX, KX, CsNaX10 as catalysts which were tested for alkylation of acetonitrile with methanol at 400°C. The conversion of methanol versus time on stream is presented in Figure 4.20. NaX, KX and CsNaX10 showed gradual decrease of the conversion of methanol with reaction time.

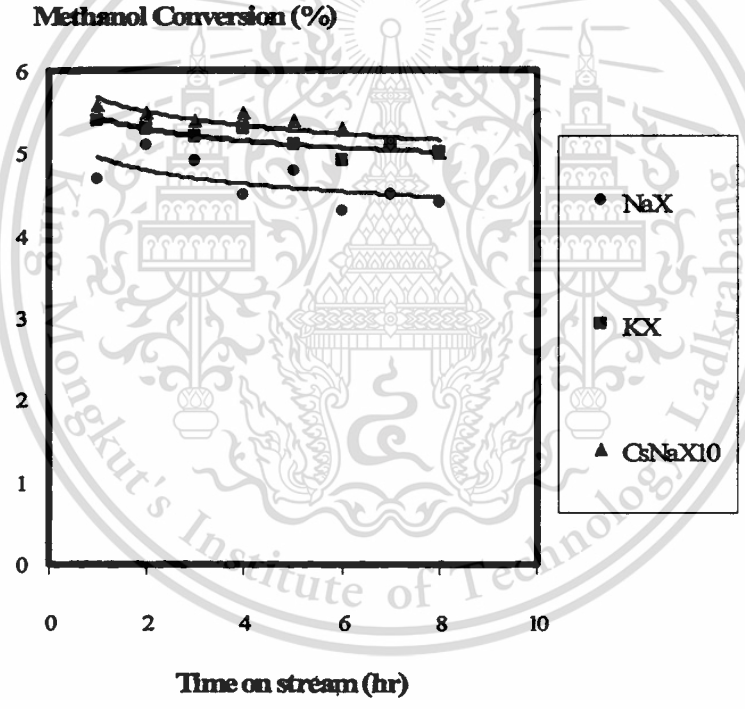

Figure 4.20 Conversion of methanol over NaX, KX and CsNaX10.

(Catalysts; NaX, KX and CsNa10, W/F;~41g.hr.mol^{-1}, Carrier gas; nitrogen flow rate 25 ml/min, Feed; methanol / acetonitrile: 10/1mole/mole)

The initial activities of the catalysts is in the order of CsNaX10 > KX > NaX, which is consistent with the results of cyclisation (section 4.2). It is clear that the basicity of the catalysts depends on the size of exchangeable cation in the order of $Cs^+ > K^+ > Na^+$. Consequently, the methanol decomposition which produced hydrogen and formaldehyde can be increased when the basicity of catalysts is increased. This is because the strength of adsorption of methanol in CsNaX10 is much higher than in KX and NaX. As basicity is increased, the hydrogen bonding formed by the interaction between the alcoholic hydrogen of methanol and the basic sites in zeolite leads to an increase catalytic conversion of methanol over CsNaX, as compared to KX and NaX. Accordingly, an increased formation of formaldehyde, which is served as alkylating agent, can be expected. This would result in a high conversion of acetonitrile to the alkylated products when the basicity of the catalysts is increased as shown in Figure 4.21.

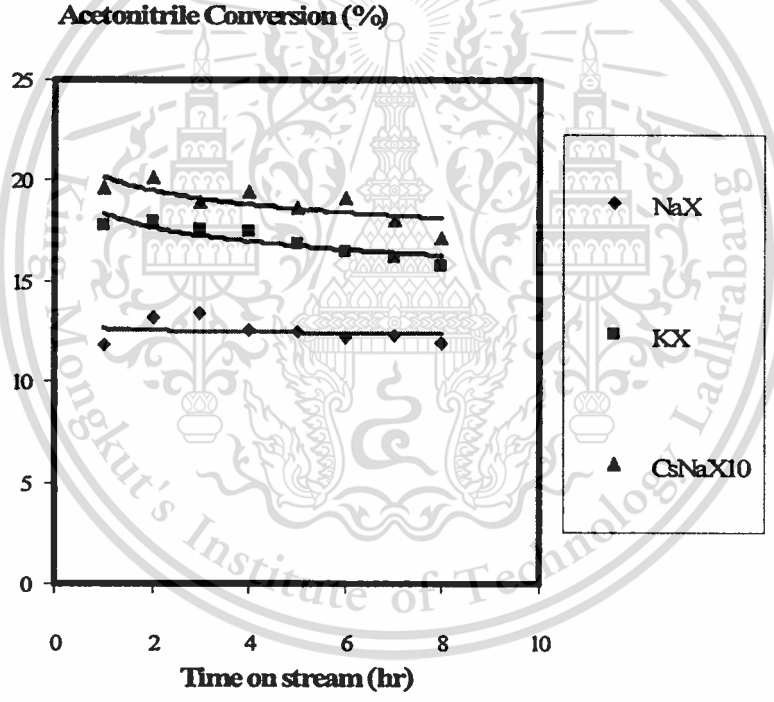

Figure 4.21 Conversion of acetonitrile over NaX, KX and CsNaX10.

(Catalysts; NaX, KX and CsNa10, W/F;~41g.hr.mol^{-1}, Carrier gas; nitrogen flow rate 25 ml/min, Feed; methanol / acetonitrile: 10/1mole/mole)

It can be seen that the Cs^+ exchanged zeolite X shows the highest activity, as compared to other alkali cation exchanged catalysts. This is due to the strong interaction of acetonitrile on the active basic site, associated with Cs^+. The adsorbed species of acetonitrile in basic zeolite catalysts can be proposed as in Figure 4.22. The localized electrons of the –CN group would interact with the exchangeable cation, Cs^+, and the acidic α-hydrogen would interact with the oxygen bridge, subsequently leading to the proton abstraction.

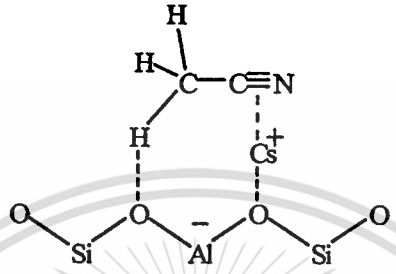

Figure 4.22 Proposed adsorbed species of acetonitrile in cesium exchanged zeolites [45].

From the result, it can be concluded that the proton abstraction of acetonitrile which plays an important role for the alkylation activity, depends on basicity of the catalyst. Therefore, the adsorption of acetonitrile on basic sites is quite essential.

Product distribution from the reactions using NaX, KX and CsNaX10 are shown in Figure 4.23. Over the strong basic catalyst, CsNaX, it is found that the increase in selectivity to propionitrile and other products are observed whereas selectivity of acrylonitrile is decreased. As selectivity of propionitrile is increased with catalyst basicity, it can be assumed that propionitrile is generated from hydrogenation of acrylonitrile which is primarily produced from the alkylation of acetonitrile with formaldehyde. This is because decomposition of methanol is largely promoted over highly basic catalyst, CsNaX. This results in large amount of hydrogen which can be dissociated over basic site into $H^{\delta-}$ and $H^{\delta+}$. Acrylonitrile can be readily hydrogenated by such species producing propionitrile. Figure 4.24 shows possible reaction pathway for the formation of propionitrile over alkali cation exchanged zeoliteX.

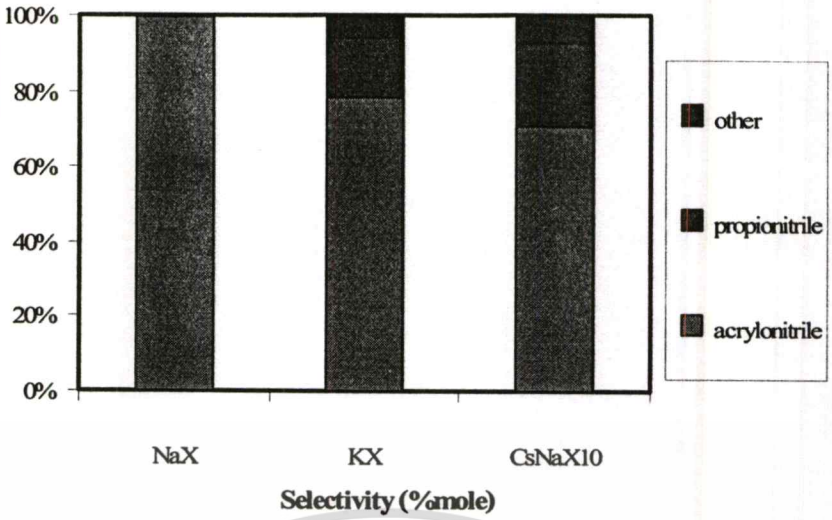

Figure 4.23 Products distribution from the alkylation of acetonitrile with methanol over NaX, KX and CsNaX10 as function of time.*(Catalysts; NaX, KX and CsNa10, W/F;~41g.hr.mol^{-1}, Carrier gas; nitrogen flow rate 25 ml/min , Feed ; methanol / acetonitrile : 10/1mole/mole)*

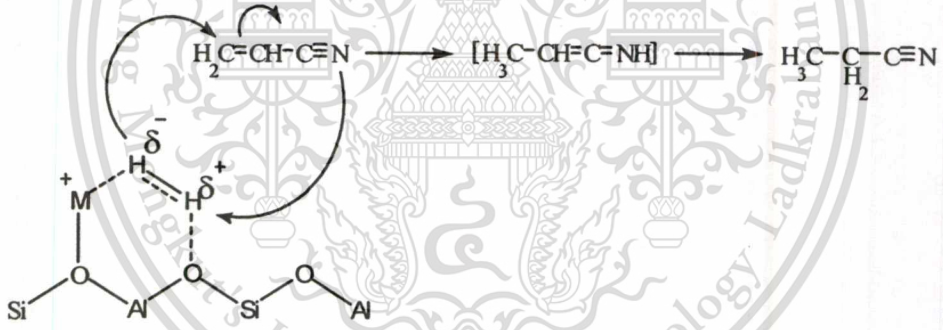

Figure 4.24 Reaction of dissociated hydrogen over basic site with acrylonitrile to form propionitrile.

The hydrogenation of acrylonitrile should be enhanced when the basicity of catalyst is increased. This fact can be demonstrated later in detail by the hydrogenation of acrylonitrile (section 4.4.).

In addition, as the basicity increases, the amount of water eliminated from alkylation of acetonitrile with formaldehyde would be increased. Consistent with this view, increase in selectivity to other products is attributed to the additional hydrogen and water in the reaction.

4.3.2 Effect of Degree of Ion Exchange

The effect of degree of ion exchange was studied by reactions using KNaX and KX as catalysts. Degree of ion exchange of KNaX and KX amount 39.92% and 100%, respectively. (from Table 4.1).

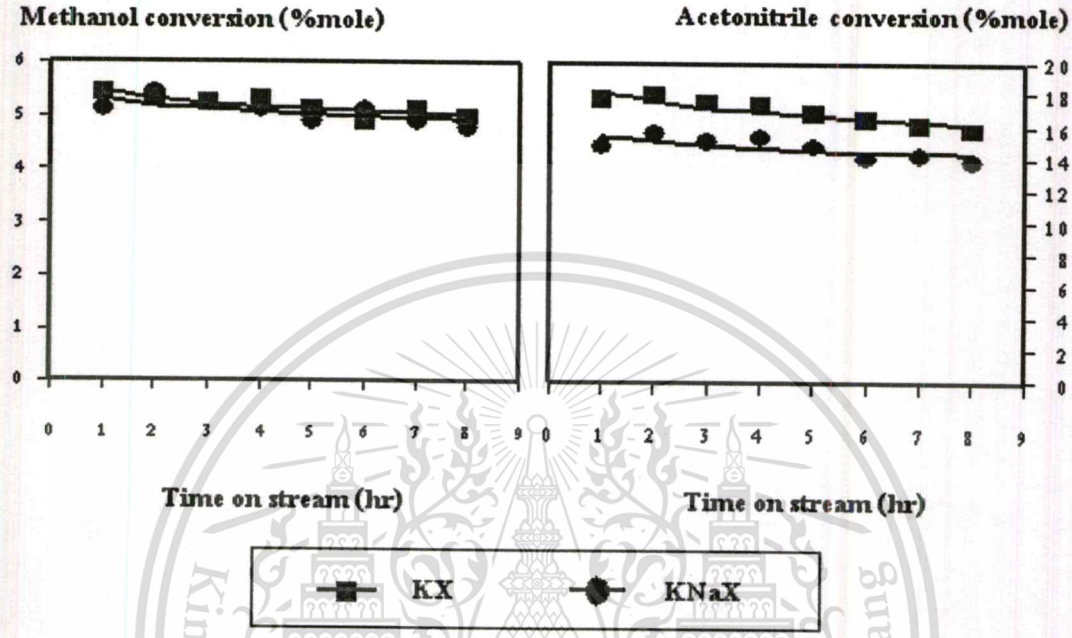

Figure 4.25 Conversion of methanol and acetonitrile over KX and KNaX
(Catalysts; KNaX and KX, W/F;~41g.hr.mol^{-1}, Carrier gas; nitrogen flow rate 25 ml/min, Feed; methanol / acetonitrile: 10/1mole/mole)

In Figure 4.25, the conversion of methanol and acetonitrile from KNaX was compared with KX. The result showed a gradual decrease in activity of both substances with time on stream, and KX showed higher activity than KNaX. This is because numbers of the degree of ion exchange in KNaX less than that in KX. It can be described that the basicity of K^+ is much higher than that of Na^+. As number of K^+ is increased, the basicity of catalysts is pronounced, which leads to an increased conversion of both substrates. This result indicated that, increase in number of basic cation, i.e. K^+, into the zeolite, would increase total electron density of the framework. Therefore, the conversion of methanol and acetonitrile depend on the degree of ion exchange with highly basic cation.

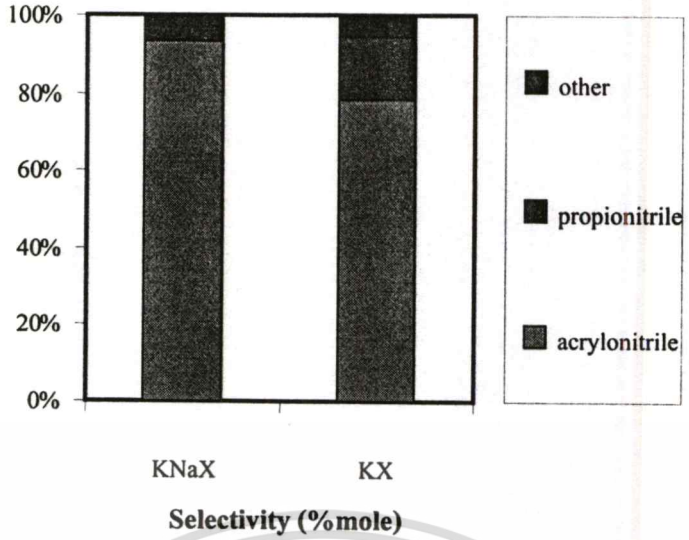

Figure 4.26 Products distribution from the alkylation of acetonitrile with methanol over KNaX and KX.

(Catalysts; KNaX and KX, W/F;~41g.hr.mol^{-1}, Carrier gas; nitrogen flow rate 25 ml/min, Feed;methanol/ acetonitrile : 10/1mole/mole)

Product distribution of the reactions using KNaX and KX were shown in Figure 4.26. At the higher degree of ion exchange, it found that the increase in selectivity to propionitrile and other products were observed whereas acrylonitrile was decreased. This result indicated that the effect on product selectivity was found to depend on degree of ion exchange of the zeolite catalyst. Due to the fact that the basicity of the catalyst increases with amount of K^+ exchanged with Na^+ in zeolite X, hydrogen from methanol decomposition is also increased with the degree of ion exchange. Therefore, the hydrogenation of acrylonitrile to propionitrile is enhanced and the selectivity of propionitrile is increased. This is also the case for the increased selectivity of other products when basicity of catalyst is increased.

4.3.3 Effect of Excess Cesium Cation per Unit cell

The effect of excess cesium cation per unit cell was studied by reactions using CsNaX10, CsNaX 15, CsNaX20 and CsNaX30 as catalysts. All catalysts possess the same degree of ion exchange (approximately 37%). The chemical composition of this material determined by elemental analysis (Table 4.1), shows that there is an excess of cesium cations over the stoichiometric requirement and the excess cesium cations are referred to as cesium cation

"cluster" in zeolite catalysts. It is possible that these species may be in formed cesium oxide (Cs_2O), peroxide (Cs_2O_2) and superoxide (CsO_2) providing that their preparation and calcination are carried out in the presence of oxygen [37].

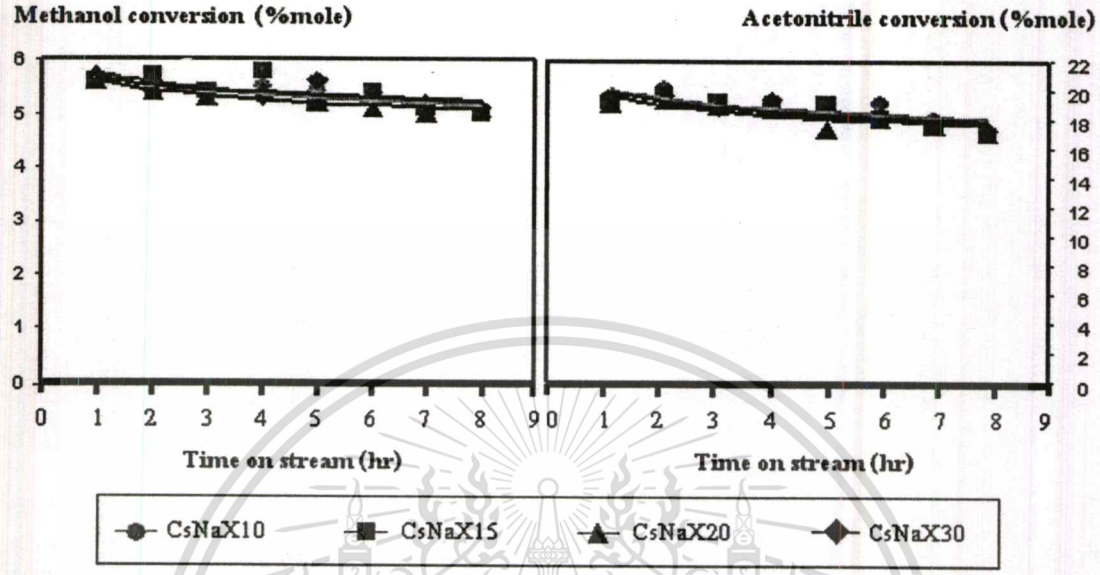

Figure 4.27 Conversion of methanol and acetonitrile over CsNaX10, 15, 20 and 30 *(Catalysts; CsNaX10, 15, 20 and 30, W/F;~41g.hr.mol^{-1}, Carrier gas; nitrogen flow rate 25 ml/min, Feed; methanol / acetonitrile: 10/1mole/mole)*

The conversion of methanol and acetonitrile show that similar activity is observed for all reactions using zeolites CsNaX10, 15, 20 and 30, as presented in Figure 4.27. It indicated that the conversion of both substrates is independent of the excess cesium cation. From the result, it can be concluded that carbanion formation is not promoted by the excess cesium cation. This is because the polar environment in the micropore is required for stabilization of carbanion intermediate formed. Therefore, only basic site in zeolite framework is responsible for the alkylation activity.

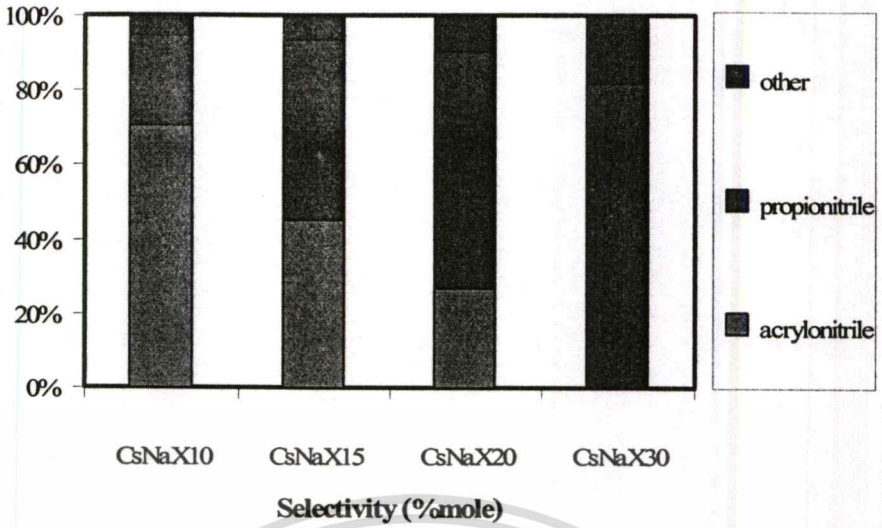

Figure 4.28 Products distribution over CsNaX10, 15, 20 and 30.

Although, the excess cesium cation does not affect the alkylation activity, it is strongly affect selectivity of the saturated (acrylonitrile) and unsaturated (propionitrile) products as shown in Figure 4.28. Increasing the basicity of CsNaX by incorporation of excess cesium cation substantially reduces the selectivity of acrylonitrile, but instead, increased propionitrile selectivity. It can be assumed that the formation of propionitrile is resulted from the hydrogenation of acrylonitrile over excess cesium cation "cluster" as shown in Figure 4.29. The adsorption and subsequently heterolytic dissociation of hydrogen can be facilitated over excess cesium cation. Acrylonitrile which is primary product formed by alkylation of acetonitrile with methanol, can be readily adsorbed on excess cesium cation site, where hydrogenation with dissociated hydrogen can take place. Hence, the more excess cesium cation, the more basicity and the higher hydrogenation activity. Indeed, catalyst with excess cesium cation was found to be active in the hydrogenation of acrylonitrile to propionitrile (section 4.4).

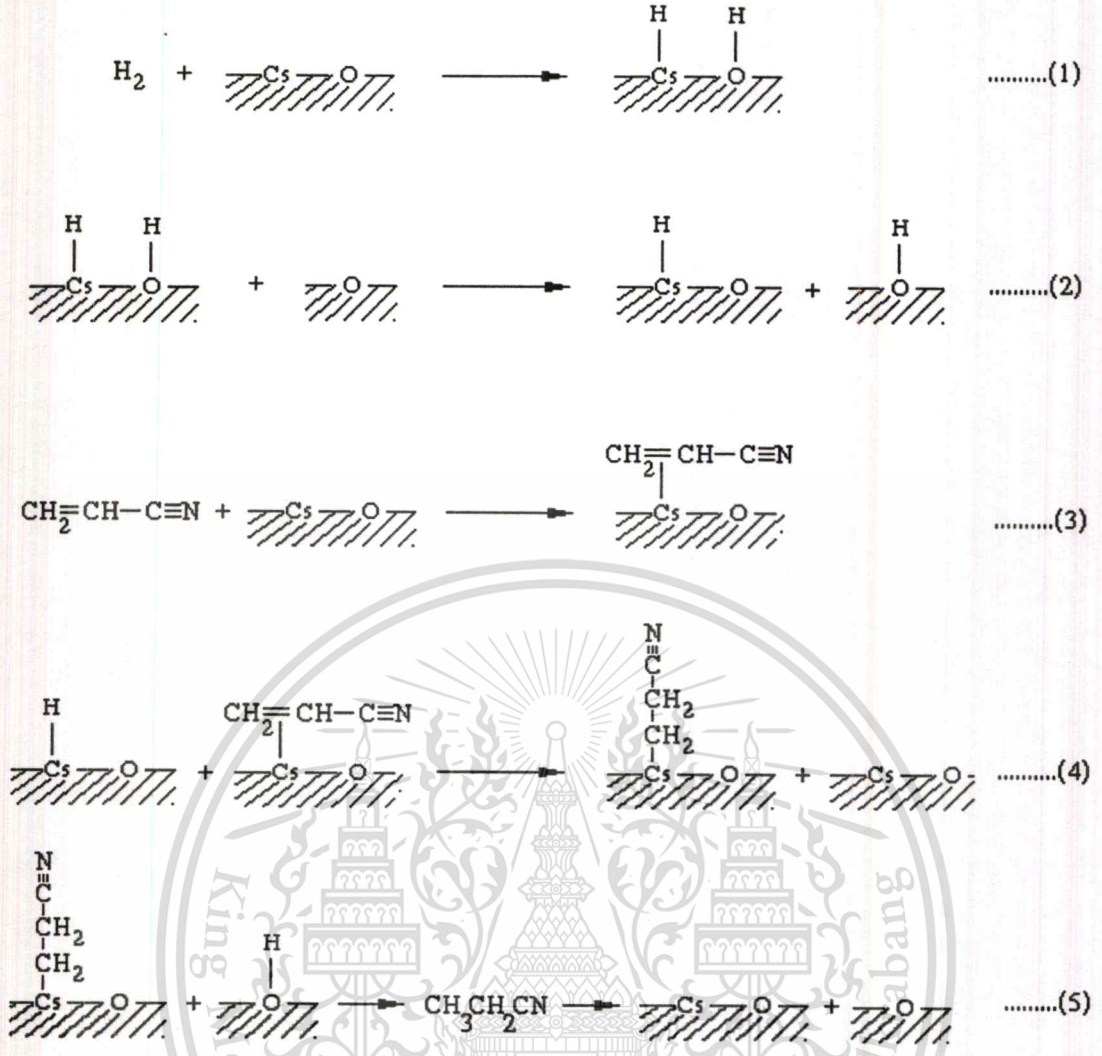

Figure 4.29 Formation of propionitrile from the hydrogenation of acrylonitrile over excess cesium cation "cluster".

4.3.4 Effect of Feed Ratio, Methanol: Acetonoitrile

The effect of feed ratio, methanol: acetonitrile mixture was investigated for insight into the rate determining step in the alkylation of acetonitrile with methanol based on proton abstraction of acetonitrile. The reaction employ feeding ratio of 10:1 and 15:1 ratios with W/F ~ 41 (based on acetonitrile). The experiments were carried out at 400°C using CsNaX15 as catalyst. Effect of methanol and acetonitrile conversion at different feed ratios are shown in Figure 4.30 and 4.31

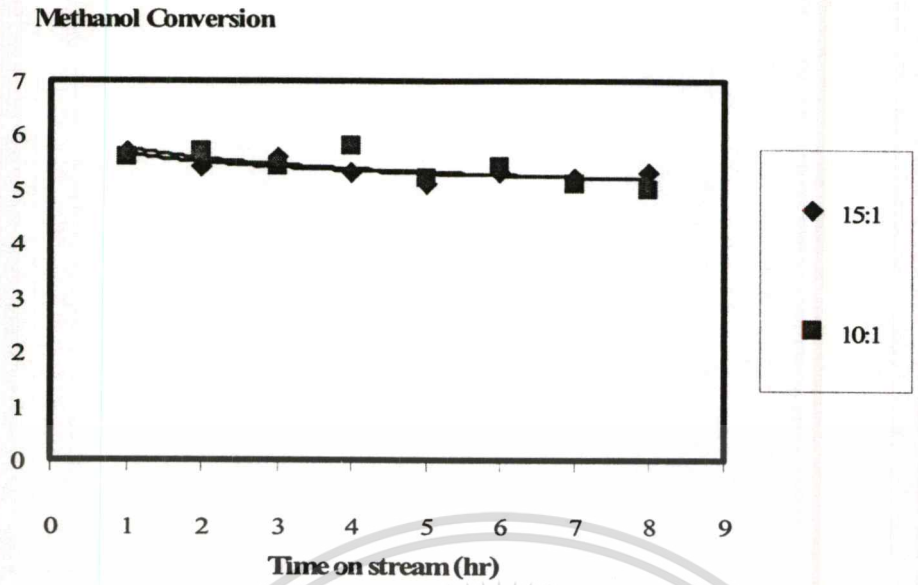

Figure 4.30 Effect of methanol conversion at different feed ratio of methanol:acetonitrile.

(Catalyst; CsNaX15, W/F; ~41, Carrier gas; nitrogen flow rate 25 ml/min, temperature; 400 °C)

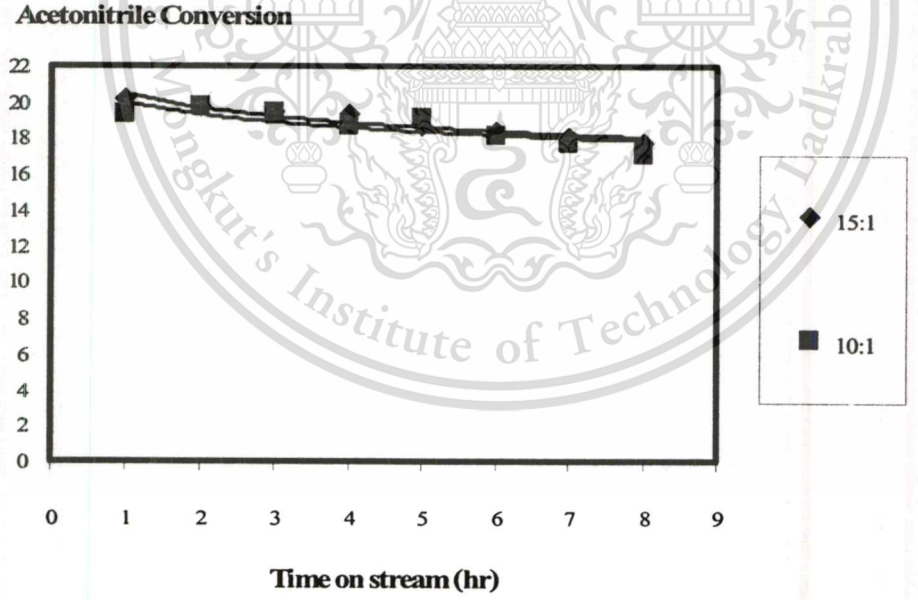

Figure 4.31 Effect of acetonotrile conversion at different feed ratio of methnol:acetonitrile.

(Catalyst; CsNaX15, W/F; ~41, Carrier gas; nitrogen flow rate 25 ml/min, temperature; 400 °C)

Increase in methanol concentration in feed resulted in no changes of both conversion of methanol and acetonitrile. Figure 4.32, it is shown that the methanol decomposition was increased whereas alkylation activity of acetonitrile remains the same in the reaction using feed ratio of 15:1. It is suggested that, in addition to active basic site in the framework, decomposition of methanol can be promoted by the surface of catalyst and excess cesium cation "cluster". It seems that no competitive adsorption of methanol over acetonitrile takes place over active basic site. This is because a stronger interaction for acetonitrile than methanol with the active basic site. The strong interaction of acetonitrile with the active basic site is attributed to the greater electron withdrawal by the –CN group, as opposed to the -OH group, which increases the polarity and α-hydrogen acidity of acetonitrile, as compared to methanol and also provides an electron-donor interaction (either from π electrons or lone-pair electrons) for possible bonding to surface cations. Since the reaction is promoted by basic sites, adsorption of acetonitrile, which is the most electrophilic species in the system, would be favored. The localized electrons of the –CN group would interact with the exchangeable cation and the acidic α-hydrogen would interact with the oxygen bridge subsequently leading to the proton abstraction. Since it appears that adsorption strength of acetonitrile is higher than methanol on CsNaX-CsOH [37], it can be presumed that, the proton abstraction of acetonitrile may well be the rate determining step for the alkylation of acetonitrile with methanol.

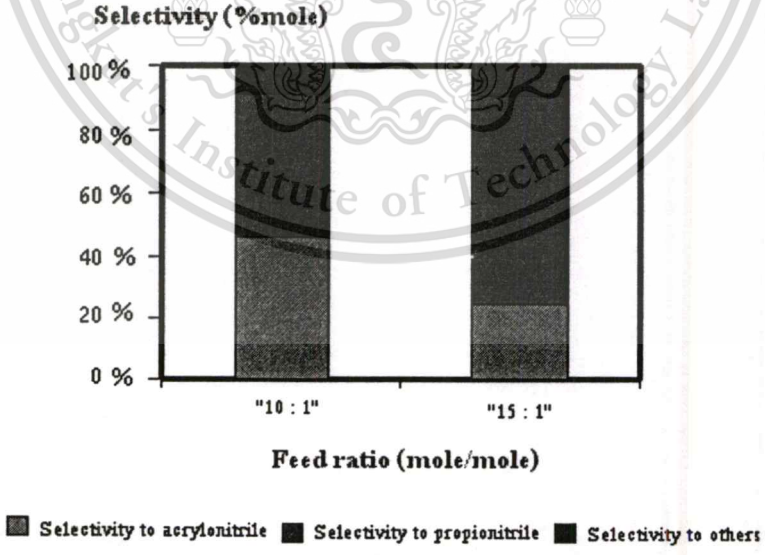

Figure 4.32 Selectivity of acrylonitrile, propionitrile and other from alkylation of acetonitrile with methanol at different feed ratio. (Data from appendix B) *(Catalyst; CsNaX15, W/F; ~41, Carrier gas; nitrogen flow rate 25 ml/min, temperature; 400 °C)*

However, selectivity of the products was affected by feed ratio of methanol: acetonitrile as observed in Figure 4.32. As the feed ratio of methanol: acetonitrile increased, selectivity of propionitrile increased whilst selectivity of acrylonitrile decreased. This is consistent with previous discussion that the decomposition of methanol is enhanced, producing higher yield of hydrogen in the reaction using 15:1 methanol/acetonitrile, as compared to that using 10:1. Hence, hydrogenation of acrylonitrile to propionitrile is increased.

4.3.5 Effect of Reaction Temperature

It can be seen that rate of methanol decomposition determine product selectivity. Since decomposition of methanol is governed by reaction temperature, the alkylation of acetonitrile with methanol over basic catalyst has been investigated using various temperatures. The reactions are tested at 350, 375, 400, 425 °C using CsNaX30 as catalyst. This is because CsNaX30 contribute a relatively stronger basicity, as compred to other catalysts (see in section 4.1.5). Effect of methanol and acetonitrile conversion at different reaction temperatures are shown in Figure 4.33 and 4.34, respectively.

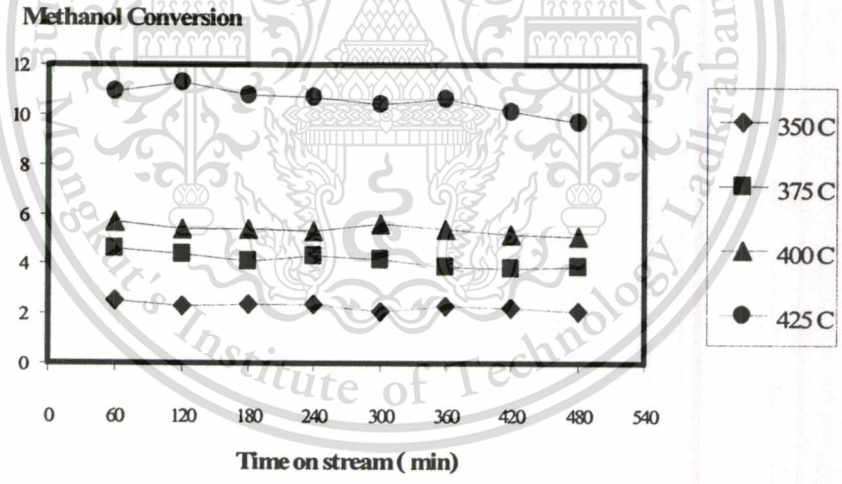

Figure 4.33 Effect of methanol conversion at different reaction temperature.

(Catalyst; CsNaX30, W/F~41g.hr.mol^{-1}, Carrier gas; nitrogen flow rate 25 ml/min Feed; methanol / acetonitrile: 10/ 1mole/mole)

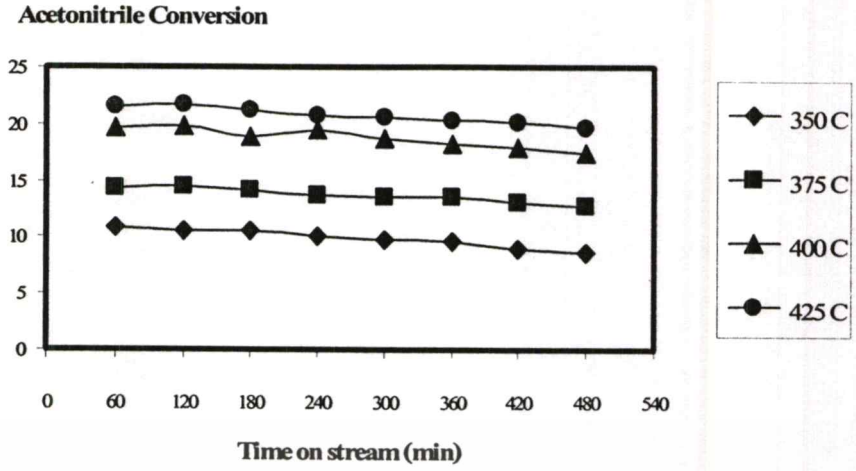

Figure 4.34 Effect of acetonitrile conversion at different reaction temperature.

(Catalyst; CsNaX30, W/F;~41g.hr.mol^{-1}, Carrier gas; nitrogen flow rate 25 ml/min, Feed; methanol / acetonitrile: 10/1mole/mole)

The result shows that the conversion of both methanol and acetonitrile increased with increasing the reaction temperature. The marked increased in methanol conversion at temperature is higher than 400 °C can be observed. As, methanol decomposition is endothermic, previous work also reveals that methanol dehydrogenation occurs substantially at the temperature above 400 °C [46]. Our experiment provided a consistent evidence showing that methanol conversion significantly increased when the reaction temperature was at 425 °C. As such, one may conclude that an increase in methanol conversion can increase the amount of formaldehyde and hydrogen in the reaction. It can be seen that the conversions of acetonitrile also increase with the reaction temperature. This facilitates the conversion of acetonitrile to the alkylted products as observed in Figure 4.34.

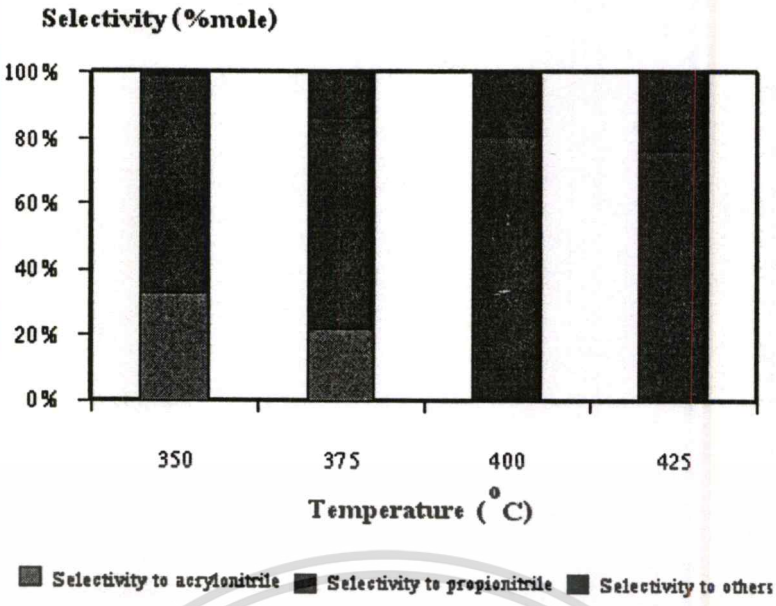

Figure 4.35 Selectivity of acrylonitrile, propionitrile and other from alkylation of acetonitrile with methanol at different reaction temperature. (Data from appendix B)

In Figure 4.35, it can be observed that the increase in temperature causes the decrease in the selectivity of acrylonitrile and the increase of the selectivity of propionitrile and other products. This is very well agreed with the observed higher decomposition of methanol at high temperature. As more hydrogen is produced, acrylonitrile which is primary product formed by alkylation of acetonitrile with methanol, can be readily hydrogenated to propionitrile. However, the selectivity of propionitrile is decreased at the 425°C. While the selectivity of other products increased with the reaction temperature. This is presumably, because hydrogen (from methanol decomposition) and water (by product from alkylation) are increased in the reaction at higher temperature. Moreover, the increase of temperature would allow easier cleavage of C-H bond in propionitrile to free radical. Therefore, these can lead to higher productivity of 2-butenenitrile, butanenitrile and butanedinitrile.

According to the above discussion, it can be suggested that, the formation of acrylonitrile should arise from the reaction between acetonitrile with formaldehyde, which is generated in situ via decomposition of methanol. However, propionitrile is not a direct alkylated product, but is likely to form by hydrogenation of acrylonitrile with hydrogen generated *in situ* via decomposition of methanol. Figure 4.36 demonstrates a possible pathway for the formation of acrylonitrile and propionitrile.

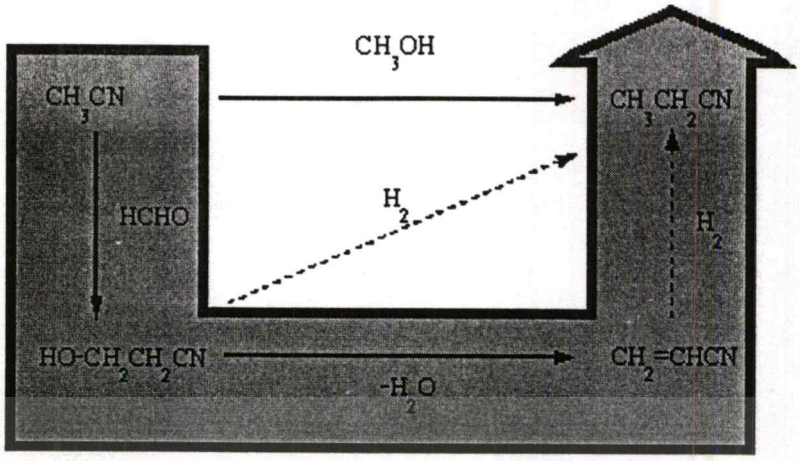

Figure 4.36 Formation of acrylonitrile and propionitrile from the alkylation of acetonitrile

In the present study, reaction temperature of 400 °C will be used for further investigation. The underlying reasons for that are, (i) the reaction lower than 400°C presented low conversion of acetonitrile, and (ii) an attempt to avoid function of 2-butenenitrile, butanenitrile and butanedinitrile at high temperature.

4.3.6 Effect of W/F

The results discussed above suggest that the reaction pathway for the alkylation of acetonitrile with methanol is likely to be a series reaction in which acrylonitrile is the primary product and propionitrile is the secondary product. In attempting to gain insight into the reaction pathway, W/F was varied by using different amounts of catalyst. This can be used to determine changes in the product selectivity of the reaction. The assumption is that a reduction in W/F would cause a decrease in the selectivity of propionitrile, and the selectivity of acrylonitrile to propionitrile would be increased. The reaction was carried out at 400 °C, and used CsNaX30 as catalyst.

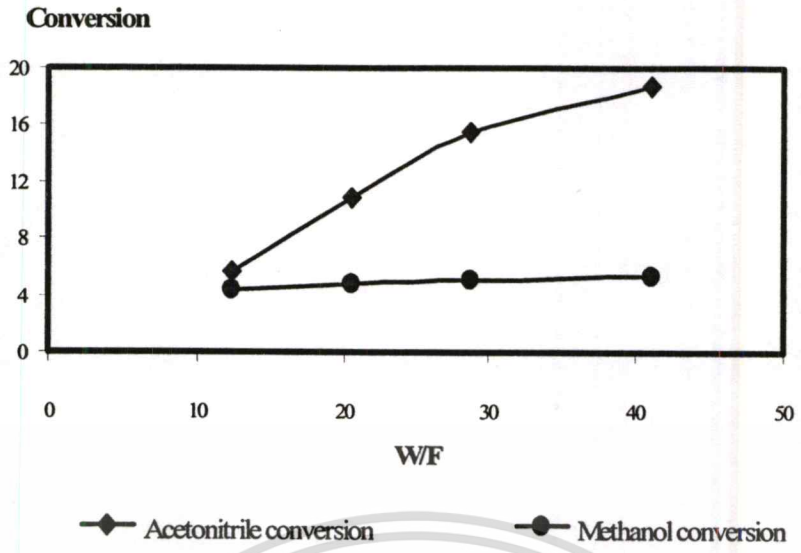

Figure 4.37 Effect of acetonitrile and propionitrile conversion at various contact time.
(Catalyst; CsNaX30, Reaction temperature; 400°C, Carrier gas; nitrogen flow rate 25 ml/min, Feed; methanol / acetonitrile: 10/1mole/mole)

Figure 4.37 shows the experimental results of methanol and acetonitrile conversion at various W/F. As seen the conversion of methanol and acetonitrile are increased with W/F as expected. In addition, it is found that propionitrile selectivity and selectivity of other products tended to increased whereas acrylonitrile selectivity decreased, respectively (Figure 4.38).

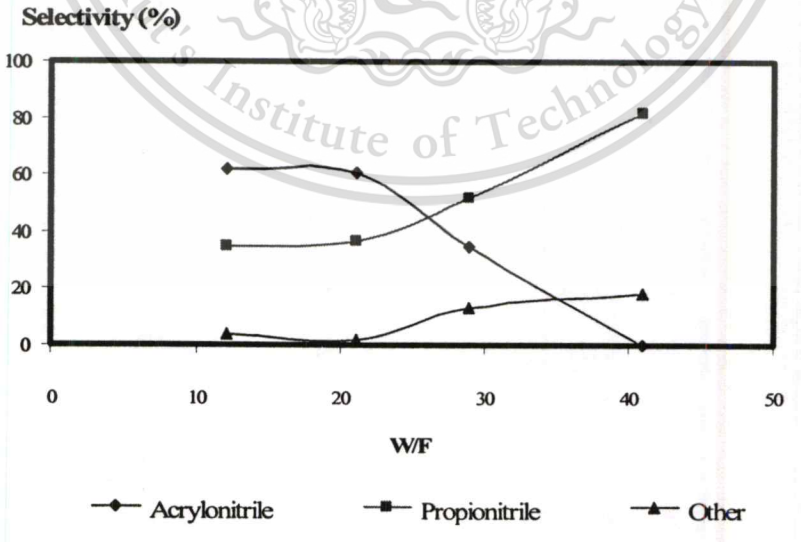

Figure 4.38 Selectivity of acrylonitrile, propionitrile and other from alkylation of acetonitrile with methanol at various contact time. (Data from appendix B)

This result indicated that the alkylation of acetonitrile with methanol proceed in a series of reactions. At low W/F, acrylonitrile is primarily formed by alkylation of acetonitrile with methanol, higher W/F allows acrylonitrile to readily further with hydrogen from methanol decomposition to form propionitrile. In addition, at high W/F, acrylonitrile can not be found in the reaction. This is because acrylonitrile can be completely hydrogenated to propionitrile. This is consistent with earlier discussion that the hydrogenation of acrylonitrile (primary product) to propionitrile (secondary product) is increased when W/F is enhanced. Moreover, the selectivity of other products is increased due to the fact that hydrogen and water are increased in the reaction at higher W/F.

4.4 Hydrogenation and Hydrogenolysis

Hydrogenation of Acrylonitrile

The reaction pathway for formation of propionitrile is proposed to proceed via acrylonitrile hydrogenation. This can be confirmed by the reaction of acrylonitrile in the presence of hydrogen. This reaction is investigated using only acrylonitrile as a feed, and hydrogen as carrier gas. From the Figure 4.39, the conversion of acrylonitrile and selectivity of products obtained from hydrogenation of acrylonitrile over zeolite CsNaX30 catalyst is plotted.

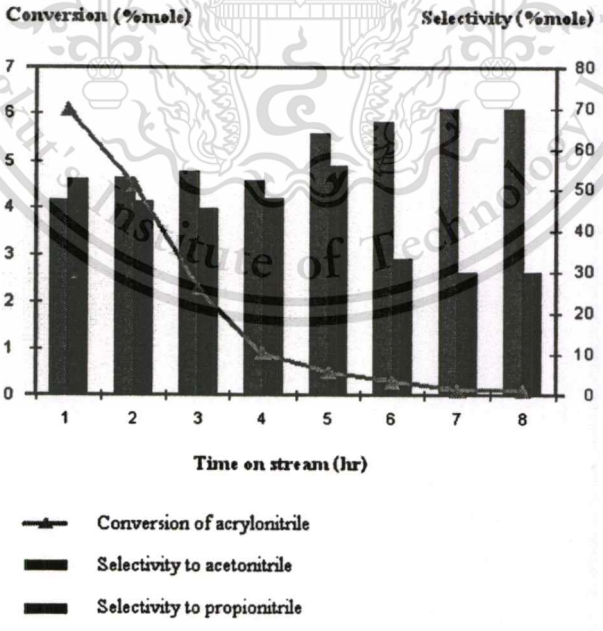

Figure 4.39 Conversion of acrylonitrile and selectivity to propionitrile and acetonitrile over CsNaX30, acrylonitrile as feed. *(Catalysts; CsNa30, Carrier gas; hydrogen flow rate 25 ml/min, Feed; acrylonitrile, Reaction temperature; 400 °C)*

It is found that the conversion is rapidly decreased. This indicates the deactivation of the catalyst when only acrylonitrile is used as feed. This is because acrylonitrile is a high polar, unsaturated compound. Strongly adsorption of acrylonitrile over CsNaX can be expected, and this would result in the formation of high molecular weight products, due to oligomerization of acrylonitrile monomer over basic catalyst. It is noted that acrylonitrile can be easily polymerization using anionic initiator [47].

The hydrogenation of acrylonitrile initially results in a mixture containing propionitrile and acetonitrile. From the result, it is confirmed that propionitrile can be produced by hydrogenation of acrylonitrile. However, acetonitrile can also be produced from the reaction of acrylonitrile with hydrogen. It is postulated that the formation of acetonitrile occur by hydrogenolysis of propionitrile, the product from hydrogenation. The hydrogenolysis activity of the CsNaX catalyst can be proved by reaction of propionitrile with hydrogen *in situ* produced from decomposition of methanol. The mixtures of methanol and propionitrile (methanol/ propionitrile ~ 50/1 mole/mole) were used as feed. The propionitrile conversions over CsNaX10 and CsNaX30 as catalysts at 400 °C with time on stream were shown in Figure 4.40.

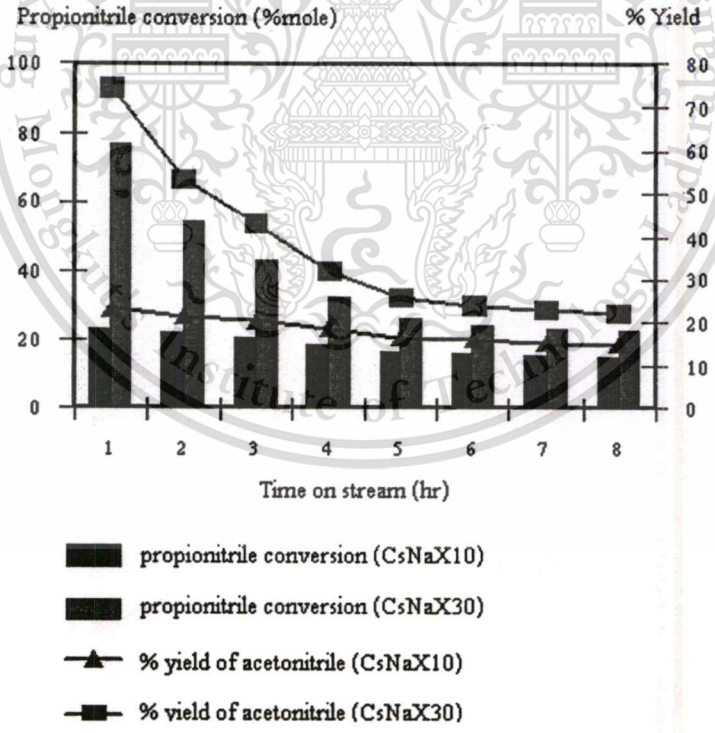

Figure 4.40 Conversion of propionitrile and selectivity to acetonitrile over CsNaX10 and CsNaX30. *(Catalysts; CsNa10 and CsNaX30, Carrier gas; nitrogen flow rate 25 ml/min, Feed; methanol/propionitrile; 50/1, Reaction temperature; 400 °C)*

Indeed, it is clear that propionitrile can be hydrogenolysed to acetonitrile over basic catalyst. The conversion of propionitrile was found to depend on the amounts of excess cesium cation "clusters" present in the zeolite framework. This indicates that the hydrogenolysis activity also depend on basicity of catalyst. As basicity is increased, decomposition of methanol is enhanced, hydrogen is also increased and propionitrile can be readily hydrogenolysis to acetonitrile. In the presence of hydrogen, there appears to be a possibility that propionitrile may react with the hydrogen dissociated over basic sites. The reaction with hydride anion would take place at the methyl group forming methane and acetonitrile as shown in Figure 4.41

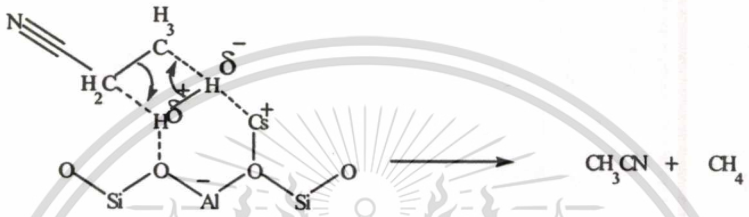

Figure 4.41 Formation of acetonitrile occur from hydrogenolysis of propionitrile.

The deactivation of catalyst in hydrogenolysis of propionitrile is also observed in the same manner as hydrogenation of acrylonitrile. However, less severity is obtained since propionitrile is relatively more saturated, than acrylonitrile.

From the above results, it can be confirmed at this stage that the hydrogenation of acrylonitrile to propionitrile and also hydrogenolysis of propionitrile to form acetonitrile can be postulated as follows:

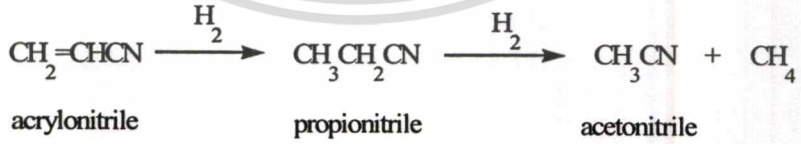

However, the conversion of acrylonitrile (Figure 4.39) was considered to be low. This is because contact time used in this study is far from that used in the alkylation of acetonitrile. Acrylonitrile produced in the alkylation of acetonitrile is relatively small, as compared to that used as feed in the hydrogenation. In addition, hydrogen in the alkylation of acetonitrile is can be produced by methanol decomposition. Unlike this reaction, hydrogen is used as carrier gas.

Therefore, the mixtures of methanol and acrylonitrile (50/1 mole/mole) are instead used as feed. This is calculated based on yield of alkylated products (approximately 20%) from the reaction using mixtures of methanol and acetonitrile (10/1: mole/mole) as feed. In this reaction, hydrogen would be produced from the methanol decomposition in a manner similar to that produced in the alkylation of acetonitrile. The result is shown in Figure 4.42.

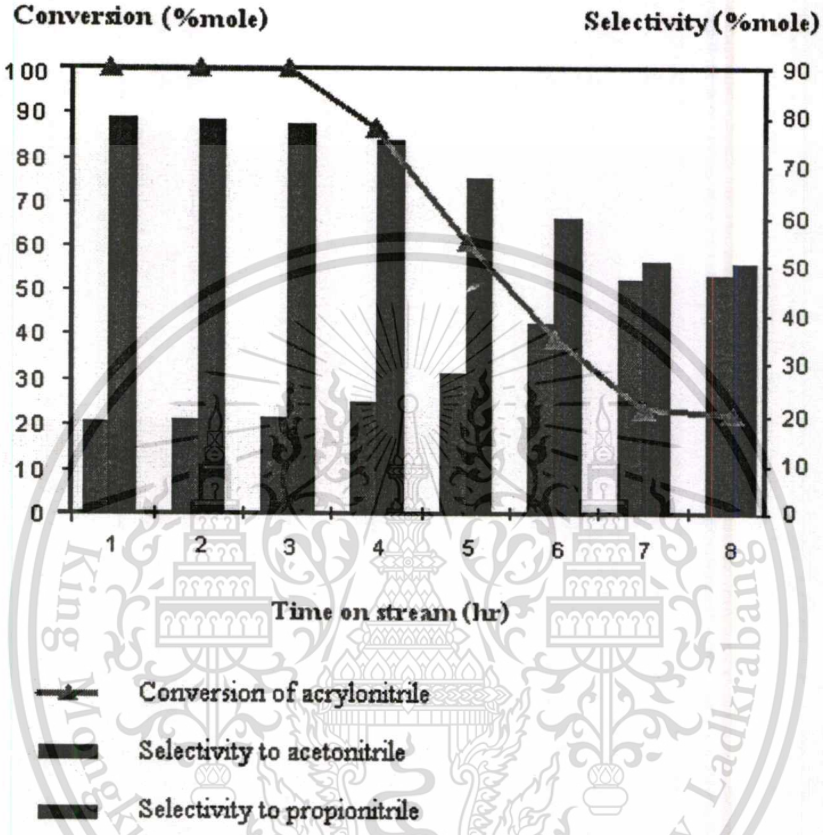

Figure 4.42 Conversion of acrylonitrile and selectivity to propionitrile and acetonitrile over CsNaX30, methanol/acrylonitrile mixture as feed. *(Catalysts; CsNa30, Carrier gas; nirogen flow rate 25 ml/min, Feed; methanol/acrylonitrile; 50/1, Reaction temperature; 400 °C)*

It can be seen that under the condition investigated, acrylonitrile was completely converted for the first three hours of the reaction and the conversion is rapidly decreased afterwards. This again confirmed that, propionitrile is produced from acrylonitrile hydrogenation. Although acetonitrile is found to be a major product, it is subsequently produced from hydrogenolysis of propionitrile, a product from hydrogenation of acrylonitrile, as discussed earlier. Once the catalyst is deactivated, the hydrogenolysis activity is also depressed. Therefore,

selectivity of acetonitrile is decreased whilst propionitrile selectivity is increased at the end of runs.

Nevertheless, it is found that, after three hours on stream, the conversion of acrylonitrile and selectivity of acetonitrile decreased to a certain value after 7 hours on stream and vice versa for propionitrile. This suggests that a part of active site is deactivation while others remain active. It is likely that the active sites derived from excess cesium cation "cluster" are primarily deactivated. It is confirmed by comparing the results of acrylonitrile conversion over CsNaX10 and CsNaX30. The activities of these catalysts are shown in Figure 4.43

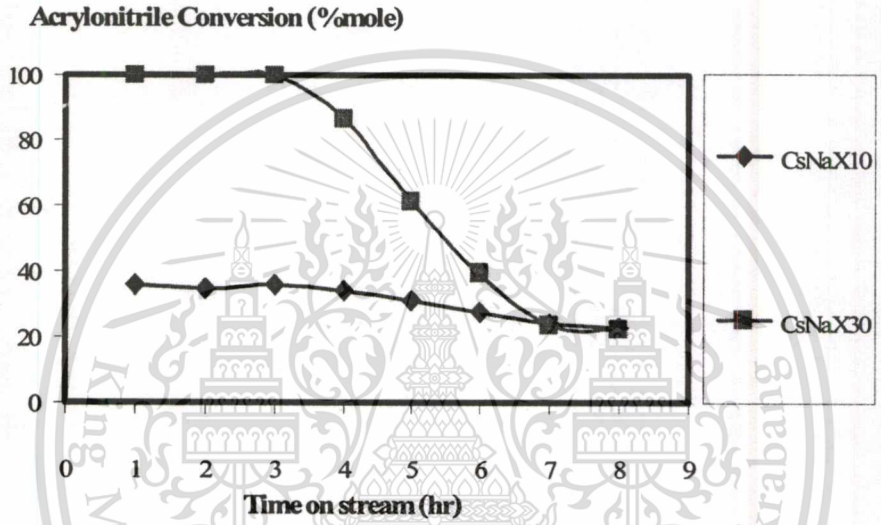

Figure 4.43 Conversion of acrylonitrile from hydrogenation of acrylonitrile over CsNaX10 and CsNaX30. *(Carrier gas; nitrogen flow rate 25 ml/min, Feed; methanol/acrylonitrile; 50/1, Reaction temperature; 400 °C)*

It can be seen that, CsNaX30 initially showed higher activity than CsNaX10. This is because the amounts of the excess cesium cation "cluster" in CsNaX30 is higher than that in CsNaX10, indicating that the hydrogenation activity depend on basicity of catalyst. However, the acrylonitrile conversions of both catalysts are decreased to a certain value after 7 hours on stream. This suggests that the active sites arised from the excess cesium cation "clusters" are primarily deactivated. The observed activity after 7 hours on stream is likely to be derived from the active basic sites in the zeolite framework. It can be noted that the excess cesium cation "clusters" particularly promotes the hydrogenation activity of the catalysts which determined product selectivity (acrylonitrile/propionitrile). However, this type of active site is not responsible for alkylation activity as discussed earlier.

CHAPTER 5

CONCLUSION AND SUGGESTION

5.1 Conclusion

The basicity of the zeolite catalysts can arise from the anionic framework of the alkali cation exchanged zeolites. The size of alkali cation shows significant effect on activity for cyclisation of acetonylacetone and selectivity of the products. The basicity of catalysts is increased with the size of alkali cation incorporated, in the order of $Cs^+ > K^+ > Na^+$, and also with degree of ion exchange. Moreover, the incorporation of cesium cation, in excess of their stoichiometric requirement into zeolites, results in the enhancement of their basicity and basic strength.

The proton abstraction of acetonitrile which plays an important role for the alkylation activity, depends on basicity of the catalyst. Therefore, the adsorption of acetonitrile on basic sites is quite essential. However, the adsorption of methanol is also indispensable because the alkylation requires bimolecular adsorption of the both substrates.

The alkylation of acetonitrile with methanol over basic catalysts proceed via a series of reactions, which results in a mixture containing saturated and unsaturated products, namely acrylonitrile and propionitrile. The formation of acrylonitrile, a primary product, is derived from the reaction between acetonitrile and formaldehyde, which is generated in situ via decomposition of methanol. Propionitrile is formed by hydrogenation of acrylonitrile with hydrogen from the methanol decomposition.

The effects on product selectivity, particularly the saturation/unsaturation ratio was found to increase with increasing reaction temperature and catalyst basicity, which depends on degree of ion exchange and size of the exchangeable cation. Moreover, increasing the basicity of CsNaX by incorporation of excess cesium cation "cluster" increases the hydrogenation activity of catalyst. Therefore, selectivity of saturated product depends on excess cesium cation "cluster". However, the excess cesium cation "cluster" does not affect the alkylation activity. This is because the carbanion intermediate formed, require polar environment in the micropore for its stabilization.

Further, investigation on the hydrogenation activity of CsNaX shows that propionitrile and acetonitrile can be obtained from reaction of acrylonitrile with hydrogen. From the result, it is confirmed that propionitrile can be produced by hydrogenation of acrylonitrile, and some of propionitrile can also be hydrogenolysed to acetonitrile. From the results, it can be concluded that the basic zeolite catalysts can readily promote hydrogenation and hydrogenolysis of polar compounds at low pressure.

5.2 Suggestion for Further Studies

1 Both products from alkylation of acetonitrile with methanol are economically valuable, Acrylonitrile is a monomer for various polymer materials, i.e. acrylic fibers, ABS resins, barrier resin, nitrile rubber and SAN resin. Propionitrile is also a raw material for pharmaceutical. To maximizes acrylonitrile yield, excess cesium cation "cluster" present in the zeolite framework should be reduced and *vice versa* for propionitrile.

2. It was found from the present study that CsNaX with excess cesium cation "cluster" increases the hydrogenation of acrylonitrile at low pressure. Thus, this catalyst should be tested for hydrogenation activity of other polar compounds.

3. The nature of excess cesium cation "cluster" incorporated zeolite X cannot be clarified in this work. Further investigation on the form of this catalyst should be performed to identify using various spectroscopic techniques, i.e. EXAFS.

REFERENCE

[1] D. Barthomeuf, "Framework induced basicity in zeolites" **Microporous and Mesoporous Materials,** Volume 66, Issue 1, 2003, pp. 1-14

[2] R. Heidler, O. Geert, A. Janssens, J. Wilfried, Mortier and A. Robert, Schoonheydt, "Charge sensitivity analysis of the interaction of pyrrole with basic FAU-type zeolites using the electronegativity equalization method" **Microporous Materials,** Volume 12, Issues 1-3,1997, pp. 1-11

[3] J. Robert, Davis, J. Eric, Doskocil, S. Bordaweaker, "Structure/function relationships for basic zeolite catalysts containing occluded alkali species" **Catalysis Today,** Volume 62, 2000, pp. 241-247

[4] A. Dyer, **An introduction to Zeolite Molecular Sieves,** John Wiley & Sons, UK, 1988

[5] Bruce C. Gates, **Catalytic Chemistry,** John Wiley & Sons, Canada, 1992

[6] I. T. Horvath, **Encyclopedia of catalysis,** John Wiley & Sons, USA, 2003

[7] K. Tanabe, M. Misono, Y. Ono and H. Hattori, **New Solid Acids and Bases,** Kodansha, Japan, 1990

[8] C.H. Rochester, **Acidity Functions,** Academic Press, UK, 1970

[9] G. Tchobanoglous and F. Burton, **Wastewater engineering : Treatment, Disposal and Resue.,** Mcgraw-Hill, inc., New York, 1991

[10] C. Wagner, W. Riggs, L. Davis, J.Moulder and G. Muilenberg, **Handbook of X-Ray Photoelectron Spectroscopy,** Perkin-Elmer Corporation, Minnesota, 1979

[11] M. Huang, S. Kaliaguine and A. Auroux, Stud. **Surf. Sci. Catal.,** volume 97, 1995, pp. 311-318

[12] R. A. Sheldon, H. Bekkum, **Fine chemicals through Heterogeneous Catalysis,** Wiley-VCH, Germany, 2001

[13] A. Corma, V. Fornés, R. M. Martín-Aranda, H. García and J. Primo, "Zeolites as base catalysts: Condensation of aldehydes with derivatives of malonic esters", **Applied Catalysis,** volume 59, 1990, pp. 237-248

[14] J. March, **Advanced Organic Reactions: Reactions, Mechanisms and Structure 4th ED.,** Wiley-Interscience, 1992, 945

[15] I. Rodriguez, G. Sastre, A. Corma and S. Iborra, "Catalytic Activity of Proton Sponge: Application to Knoevenagel Condensation Reactions", **Tetrahedron Letters**, Volume 40, 1999, pp. 1621-1622

[16] A. Corma, R. M. Martín-Aranda and F. Sánchez, "Zeolites as base catalysts: Condensation of benzaldehyde derivatives with activated methylenic compounds on Germanium-substituted faujasite ",**Journol of Catalysis**, volume 126, 1990, pp.192-198

[17] R. Indrasena and S. Rajender, Varma, "Rare-earth (RE) exchanged NaY zeolite promoted knoevenagel condensation", **Tetrahedron Letters**, volume 38, 1997, pp.1721-1724

[18] H. Pines and W. M. Stalick, **Base-catalyzed Reactions of Hydrocarbons and Related Compounds**, Academic Press, New York, 1997

[19] P. Kovacheva, K. Arishtirova and N. Davidova, "Oxidative methylation of toluene with methane catalyzed by cesium modified molecular sieves ", **Journal of Catalysis A**: General, volume 178, 1999, pp. 111-115

[20] B. Lian Su and D. Barthomeuf, "Alkylation of aniline with methanol: change in selectivity with acid-basicity of faujasite catalysts ", **Applied Catalysis**, volume 124, 1995, pp. 73-80

[21] J. Eric, Doskocil and J. Robert, Davis, "Spectroscopic Characterization and Catalytic Activity of Zeolite X Containing Occluded Alkali Species ", **Journal of Catalysis**, volume 188, 1999, pp. 353-364

[22] D. Shailendra, W. Bordawekar and J. Robert, Davis, "Probing the Basic Character of Alkali-Modified Zeolites by CO_2 Adsorption Microcalorimetry, Butene Isomerization, and Toluene Alkylation with Ethylene ",**Journal of Catalysis**, volume 189, 2000, pp. 79-90

[23] N. Giordano, L.Pino, S. Cavallaro, P. Vatarelli, B.S. Rao, "Alkylation of toluene with methanol on zeolites. The role of electronegativity on the chain or ring alkylation ", **Zeolites**, volume 7, 1987, pp.131-134

[24] T. Yashima, K. Sato, T. Hayasaka and N. Hara, "Alkylation on synthetic zeolites: III. Alkylation of toluene with methanol and formaldehyde on alkali cation exchanged zeolites ", **Journal of Catalysis**, volume 26, 1972, pp. 303-312

[25] J. Engelhardt, J. Szanyi and J. Valyon, "Alkylation of toluene with methanol on commercial X zeolite in different alkali cation forms", **Journal of Catalysis**, volume 107, 1987, pp. 296-306

[26] E. Paul, K. Hathaway and E. Davis," Base catalysis by alkali-modified zeolites: I. Catalytic activity ", **Journal of Catalysis**, volume 116, 1981, pp. 263-278

[27] P. Concepción-Heydorn, C. Jia, D. Herein, N. Pfänder, H. G. Karge and F. C. Jentoft, "Structural and catalytic properties of sodium and cesium exchanged X and Y zeolites, and germanium-substituted X zeolite ", **Journal of Molecular Catalysis A:** Chemical, Volume 162, 2000, pp. 227-246

[28] P. A. Jacobs, M. Tielen and B. Jan, A. Uytterhoeven, "Active sites in zeolites: Part 6. Alcohol dehydration over alkali cation-exchanged X and Y zeolites", **Journal of Catalysis**, Volume 190, 2000, pp. 98-108

[29] E. Paul, K. Hathaway and E. Davis, "Base catalysis by alkali-modified zeolites: II. Nature of the active site", **Journal of Catalysis**, Volume 116, 1989, pp. 279-284

[30] M. Laspéras, H. Cambon, D. Brunel, I. Rodriguez and P. Geneste, "Cesium oxide encapsulation in faujasite zeolites effect of framework composition on the nature and basicity of intrazeolitic species", **Microporous Materials**, Volume 7, 1996, pp. 61-72

[31] J. Xie, Minming, S. Huang and S. Kaliaguine, "Characterization of basicity in alkali cation exchanged Faujasite zeolites: an XPS study using chloroform as a probe molecule ", **Applied Surface Science**, volume 115, 1997, pp. 157-165

[32] J. Eric, A. Doskocil and R.J. Davis, "Spectroscopic Characterization and Catalytic Activity of Zeolite X Containing Occluded Alkali Species", **Journal of Catalysis**, Volume 188, 1999, pp. 353-364

[33] M. Laspéras, H. Cambon, D. Brunel, I. Rodriguez and P. Geneste, "Characterization of basicity in alkaline cesium-exchanged X zeolites post-synthetically modified by impregnation: A TPD study using carbon dioxide as a probe molecule ",**Microporous Materials**, Volume 1, 1993, pp. 343-351

[34] Y. Okamoto, M. Ogawa, A. Maezawa and T. Imanaka, "Electronic structure of zeolites studied by X-Ray photoelectron spectroscopy ", **Journal of Catalysis**, Volume 112, 1988, pp. 427-436

[35] V. B. Kazansky, V. Yu. Borovkov, A. Serich, H. G. Karge, "Low temperature hydrogen adsorption on sodium forms of faujasites: barometric measurements and drift spectra", **Microporous and Mesoporous Materials**, volume 22, 1998, pp. 251-259

[36] T. sooknoi, J. Dwyer, "Role of substrate, electrophilicity in base catalysis by zeolites: alkylation of acetonitrile with methanol", **Journal of Molecular Catalysis**, 2003

[37] T. sooknoi, "Basic zeolite catalysts", **Conversion of methanol over basic zeolite catalysts**, 1996

[38] P. Concepción-Heydorn, C. Jia, D. Herein, N. Pfänder, H. G. Karge and F. C. Jentoft, "Structural and catalytic properties of sodium and cesium exchanged X and Y zeolites, and germanium-substituted X zeolite" **Journal of Molecular CatalysisA:Chemical** Volume 162, Issues 1-2, 2000, pp. 227-246

[39] M. L. Occelli and P. Ritz, "The effects of Na ions on the properties of calcined rare-earths Y (CREY) zeolites", **Applied Catalysis A: General**, Volume 183, Issue 1, 5 July 1999, pp. 53-59

[40] M. A. Aramendía, V. Boráu, I. M. García, C. Jiménez, A. Marinas, J. M. Marinas, A. Porras and F. J. Urbano, "Comparison of different organic test reactions over acid–base catalysts", **Applied Catalysis A: General**, Volume 184, Issue 1, 2 August 1999, pp. 115-125

[41] E. J. Doskocil and R. J. Davis, "Spectroscopic Characterization and Catalytic Activity of Zeolite X Containing Occluded Alkali Species", **Journal of Catalysis**, Volume 188, Issue 2 , 1999, pp. 353-364

[42] H. Cambon, D. Brunel, I. Rodriguez and P. Geneste, "Cesium oxide encapsulation in faujasite zeolites effect of framework composition on the nature and basicity of intrazeolitic species" ,**Microporous Materials** , Volume 7, Issues 2-3 ,1996, pp. 61-72

[43] R.Newton and B.Dodge, Journal of American Chemistry Society, Volume 55, 4747, 1933

[44] K. Sefcik, D. Michael, "Investigation of the zeolite catalyzed of toluene using arbon-13 nuclear magnetic resonance", **Journal of American Chemistry Society**, Volume 101, Issue 8 , 11 April 1979, pp. 2164-2170

[45] T. Sooknoi and J. Dwyer, "Role of substrate's electrophilicity in base catalysis by zeolites: alkylation of acetonitrile with methanol", **Journal of Molecular Catalysis A: Chemical**, Volume 211, Issues 1-2, 2004, pp. 155-164

[46] M. Huang, P. A. Zielinski, J. Moulod and S. Kaliaguine, "Vapour-phase reaction of methanol with acetone over alkali containing zeolites", **Applied Catalysis A: General**, Volume 118, Issue 1, 1994, pp. 33-49

[47] V. Vijayabaskar, V.K. Tikku and Anil K. Bhowmick, "Electron beam modification and crosslinking: Influence of nitrile and carboxyl contents and level of unsaturation on structure and properties of nitrile rubber", **Radiation Physics and Chemistry**, Volume 75, Issue 7, 2006, Pages 779-792

[48] [online] Available : http//www.iza-online.org

APPENDICES

APPENDIX A

CALCULATION

Example 1: Calculations of catalytic parameters

W/F, conversion, yield and selectivity

Example 2: Calculations of chemical composition

Si/Al ratio

Degree of ion exchange

Unit cell composition

Total cesium cations and excess cesium cation per unit cell

Calculations of catalytic parameters

Conversion

Conversion could be calculated by the ratio between molar flow rate of the reactant converted and molar flow rate of the reactant fed. The difference between molar flow rate of reactant fed and the molar flow rate of unreacted feed left in the product mixtures from both gas and liquid fractions, were defined as the amounts of reactant converted. %Conversion can be calculated from the following equation.

$$\%\text{Conversion} = \frac{(M_f - M_u)}{M_f} \times 100$$

M_f = molar flow rate of feed

M_u = molar flow rate of unreacted feed in products

Yield

Yield of each product is defined as percentage of molar ratio of particular product obtained and the reactant fed during a certain period of time.

$$\%\text{Yield} = \frac{\text{mole of product}}{\text{mole of feed}} \times 100$$

The % weight of liquid products obtained from the analysis can be used to calculate the % yield using the following equation.

$$\%\text{Yield}_i = \frac{F_i W}{100 M_i F_o} \times 100$$

F_i = %weight of product (i) from the analysis (%)

W = weight of total liquid collected per hour (g/hour)

M_i = molecular weight of the product (i) (g/mol)

F_o = mole of reactant fed in hour (mol/hour)

In the case that more than one reactant are present in the feed, yield is generally calculated based on the limited reactant.

Selectivity

Selectivity of the products was defined as the ratio of mole of particular product and the total mole of the reactant converted. High selectivity of a desired product was preferred. %Selectivity can be obtained from the following equation.

$$\%\text{Selectivity} = \frac{\%\text{Yield}}{\%\text{Conversion}} \times 100$$

Example 1: Calculations of catalytic parameters

W/F, conversion, yield and selectivity

Reaction conditions

The reaction conditions of sample from alkylation of acetonitrile with methanol at 400 °C using CsNaX10 as catalyst on 3 hour of time on stream.

Mass flow rate of methanol (F_m)	0.7090	g/hour
Molar flow rate of methanol feed (M_m)	0.0221	mole/hour
Mass flow rate of acetonitrile (F_a)	0.0908	g/hour
Molar flow rate of acetonitrile feed (M_{ace})	0.0022	mole/hour
Reaction temperature	400	°C
Weight of catalyst; CsNaX10 (W_c)	0.9987	g
Weight of liquid collected in 1 hour (W)	0.7673	g

Analysis of the products mixture from Gas Chromatography

Methanol (%W_m)	87.4104	%weight
Acetonitrile (%W_{ace})	9.5921	%weight
Propionitrile (%W_p)	0.5343	%weight
Acrylonitrile (%W_{acr})	2.0722	%weight
Other (%W_o)	0.3910	%weight

Molecular weight of substance

Molecular weight of methanol	=	32.04
Molecular weight of acetonitrile	=	41.05
Molecular weight of acrylonitrile	=	53
Molecular weight of propionitrile	=	55

W/F

$W/F = (W_c)/(M_m + M_m)$

$= (0.9987)/(0.0221 + 0.0022)$

$= 41.10\ g.h.mole^{-1}$

%Conversion

%Conversion of Methanol

Methanol in product $= (\%W_m W)/100M_w$

$= (87.4104 \times 0.7673)/ (100 \times 32.04)$

$= 0.0209$ mole

%conversion of methanol $= [(M_m - \text{methanol in product})/ (M_m)] \times 100$

$= [(0.0221 - 0.0209)/0.0221] \times 100$

$= 5.43$

%Conversion of Acetonitrile

Acetonitrile in product $= (\%W_{ace} W)/100M_w$

$= (9.5921 \times 0.7673)/ (100 \times 41.05)$

$= 0.0018$ mol

%conversion of acetonitrile $= [(M_{ace} - \text{acetonitrile in product})/ (M_{ace})] \times 100$

$= [(0.0022 - 0.0018)/0.0022] \times 100$

$= 18.90$

%Yield

%Yield of Acrylonitrile $= [(\%W_{acr} \times W)/100M_w M_{ace}] \times 100$

$= [(2.0722 \times 0.7673)/ (100 \times 53 \times 0.0022)] \times 100$

$= 13.63$

%Yield of Propionitrile = $[(\%W_p W)/100M_w M_{acc}] \times 100$

= $[(0.5343 \times 0.7673)/ (100 \times 55 \times 0.0022)] \times 100$

= 3.39

%Selectivity

%Selectivity of Propionitrile = (%Yield/%Conversion) x 100

= (3.39/18.9) x 100

= 17.98

%Selectivity of Acrylonitrile = (%Yield/%Conversion) x 100

= (13.63/18.9) x 100

= 71.97

Example 2: Calculations of chemical composition

Si/Al ratio

Degree of ion exchange

Unit cell composition

Total cesium cations and excess cesium cation per unit cell

Data from XRF, calculations of chemical composition of CsNaX20

CsNaX20	SiO_2	Al_2O_3	Cs_2O	Na_2O
%Weight (W) of elements	31.8	21.9	37.8	8.4

Molar Composition

Mole of silicon = $[(W_{SiO2} \times MW_{Si})/MW_{SiO2})]/MW_{Si}$

= [(31.8 x 28)/60]/28

= 0.53

Mole of aluminium = $[(W_{Al2O3} \times 2MW_{Al})/MW_{Al2O3})]/MW_{Al}$

= [(21.9 x 54)/102]/27

= 0.43

Mole of cesium = $[(W_{Cs2O} \times 2MW_{Cs})/MW_{Cs2O})]/MW_{Cs}$

= [(37.8 x 266)/282]/133

= 0.27

Mole of sodium = $[(W_{Na2O} \times 2MW_{Na})/MW_{Na2O})]/MW_{Na}$

= [(8.4 x 46)/62]/23

= 0.27

Si/Al ratio

Si/Al ratio = (mole of Si / mole of Al)

= 0.53/0.43

= 1.23

Degree of ion exchange

$$\text{Degree of ion exchange} = \frac{\text{mole of Al} - \text{mole of Na} \times 100}{\text{mole of Al}}$$

$$= \frac{0.43 - 0.27 \times 100}{0.43}$$

$$= 37.21\ \%$$

Unit cell composition

$$\text{Unit cell composition} = T_{192}O_{384}$$

$$T = Al + Si$$

$$192 = Al + (Si/Al \times Al)$$

$$192 = Al + (1.23Al)$$

$$= 2.23Al$$

$$\therefore \textit{Aluminium atom per unit cell} = 192/2.23$$

$$= 86$$

$$\therefore \textit{Silicon atom per unit cell} = T - Al$$

$$= 192 - 86$$

$$= 106$$

$$\text{Mole of sodium} = \text{mole of Al} \times \frac{100 - \text{degree of ion exchange}}{100}$$

$$= 86 \times \frac{100 - 37.21}{100}$$

$$\therefore \textit{Sodium atom per unit cell} = 54$$

$$\text{Exchangeable cesium atom/unit cell} = \text{Al atom per unit cell} - \text{Na atom per unit cell}$$

$$= 86 - 54$$

$$\therefore \textit{Cesium atom per unit cell} = 32$$

Unit cell composition of CsNaX30 can be expressed as; $\boxed{Na_{54}Cs_{32}(Al_{86}Si_{106}O_{384})}$

Total cesium cations and excess cesium cation per unit cell

Total cesium per unit cell $= \dfrac{\text{Al per unit cell x molar composition of Cs}}{\text{molar composition of Al}}$

$= \dfrac{86 \times 0.27}{0.43}$

$= 54$

Excess cesium per unit cell $=$ total Cs per unit cell – exchangeable Cs per unit cell

$= 54 - 32$

$= 22$

APPENDIX B

REACTION DATA

Cyclisation: Table B.1- Table B3

Alkylation: Table B.4 – Table B.17

Hydrogenation: Table B.18 – Table B. 20

Hydrogenolysis: Table B.21 – Table B.22

Table B.1 Results from the cyclisation of acetonylacetone at 350°C, over NaX

Reaction Condition	Catalyst		Time on Stream (min)				
			60	90	120	150	180
Reaction temperature 350 °C	NaX	Acetonylacetone Conversion	98.9	67	40.1	22.6	16.3
W/F~75 g.h.mol-1		3-Methyl-2-cyclopentenone Yield	95.6	65.8	38.7	21.9	16.1
Nitrogen carrier gas flow rate 35 ml/min		2,5-Dimethylfuran Yield	0.5	0.2	0.1	0.2	0.1

Table B.2 Results from the cyclisation of acetonylacetone at 350°C, over KX

Reaction Condition	Catalyst		Time on Stream (min)				
			60	90	120	150	180
Reaction temperature 350 °C	KX	Acetonylacetone Conversion	99.3	86	43.2	35.1	28.7
W/F~75 g.h.mol-1		3-Methyl-2-cyclopentenone Yield	96.3	83.2	39.8	33.6	25.4
Nitrogen carrier gas flow rate 35 ml/min		2,5-Dimethylfuran Yield	1.4	2.1	1.9	1.7	1.9

Table B.3 Results from the cyclisation of acetonylacetone at 350°C, over CsNaX10

Reaction Condition	Catalyst		Time on Stream (min)				
			60	90	120	150	180
Reaction temperature 350 °C	CsNaX10	Acetonylacetone Conversion	100	95.2	77.3	50.1	40.4
W/F~75 g.h.mol-1		3-Methyl-2-cyclopentenone Yield	97.8	93.6	75.1	48.2	38.7
Nitrogen carrier gas flow rate 35 ml/min		2,5-Dimethylfuran Yield	0.9	1.1	1.2	0.5	0.6

Table B.4 Conversion of methanol, acetonitrile and yield, selectivity of products from alkylation of acetonitrile with methanol at 400 °C, over NaX

Reaction Condition	Catalyst		Time on Stream (hours)							
			1	2	3	4	5	6	7	8
Reaction temperature at 400 °C W/F ~ 41 g.h.mol-1 Methanol/Acetonitrile ratio 10/1 Nitrogen carrier gas flow rate ~25 ml/min	NaX	Methanol Conversion	4.7	5.1	4.9	4.5	4.8	4.3	4.5	4.4
		Acetonitrile Conversion	11.8	13.2	13.4	12.6	12.5	12.2	12.3	11.9
		Propionitrile Yield	0	0	0	0	0	0	0	0
		Acrylonitrile Yield	11.8	13.2	13.4	12.6	12.5	12.2	12.3	11.9
		Others Yield	0	0	0	0	0	0	0	0
		Selectivity of Propionitrile	0	0	0	0	0	0	0	0
		Selectivity of Acrylonitrile	98.4	98.9	98.8	98.6	98.7	98.9	98.8	98.3

Table B.5 Conversion of methanol, acetonitrile and yield, selectivity of products from alkylation of acetonitrile with methanol at 400 °C, over KX

Reaction Condition	Catalyst		Time on Stream (hours)							
			1	2	3	4	5	6	7	8
Reaction temperature at 400 °C W/F ~ 41 g.h.mol-1 Methanol/Acetonitrile ratio 10/1 Nitrogen carrier gas flow rate ~25 ml/min	KX	Methanol Conversion	5.1	5.4	5.2	5.1	4.9	5.1	4.9	4.8
		Acetonitrile Conversion	14.9	15.6	15.2	15.4	14.9	14.1	14.3	13.9
		Propionitrile Yield	1.3	1.6	1.3	1.2	1	0.7	0.9	0.8
		Acrylonitrile Yield	13.6	14	13.9	14.2	13.9	13.4	13.4	13.1
		Others Yield	0	0	0	0	0	0	0	0
		Selectivity of Propionitrile	8.7	10.3	8.6	7.8	6.7	5.0	6.3	5.8
		Selectivity of Acrylonitrile	91.3	89.7	91.4	92.2	93.3	95.0	93.7	94.2

Table B.6 Conversion of methanol, acetonitrile and yield, selectivity of products from alkylation of acetonitrile with methanol at 400 °C, over KNaX

Reaction Condition	Catalyst		Time on Stream (hours)							
			1	2	3	4	5	6	7	8
Reaction temperature at 400 °C W/F ~ 41 g.h.mol-1 Methanol/Acetonitrile ratio 10/1 Nitrogen carrier gas flow rate ~25 ml/min	KNaX	Methanol Conversion	5.4	5.3	5.2	5.3	5.1	4.9	5.1	5
		Acetonitrile Conversion	17.8	18	17.6	17.5	16.9	16.5	16.2	15.8
		Propionitrile Yield	1.8	2.1	2.6	2.8	2.7	2.3	2.5	2.6
		Acrylonitrile Yield	14.8	14.7	13.9	13.7	13.2	13.3	13.1	12.7
		Others Yield	1.2	1.2	1.1	1	1	0.9	0.6	0.5
		Selectivity of Propionitrile	10.1	11.7	14.8	16.0	16.0	13.9	15.4	16.5
		Selectivity of Acrylonitrile	83.1	81.7	79.0	78.3	78.1	80.6	80.9	80.4

Table B.7 Conversion of methanol, acetonitrile and yield, selectivity of products from alkylation of acetonitrile with methanol at 400 °C, over CsNX10

Reaction Condition	Catalyst		Time on Stream (hours)							
			1	2	3	4	5	6	7	8
Reaction temperature at 400 °C W/F ~ 41 g.h.mol-1 Methanol/Acetonitrile ratio 10/1 Nitrogen carrier gas flow rate ~25 ml/min	CsNaX10	Methanol Conversion	5.6	5.5	5.4	5.5	5.4	5.3	5.1	5
		Acetonitrile Conversion	19.6	20.1	18.9	19.4	18.7	19.1	18.1	17.2
		Propionitrile Yield	2.8	4.4	3.4	4.3	4.1	4.9	5.1	4.8
		Acrylonitrile Yield	14.7	13.5	13.6	13.4	13.2	12.9	12.4	12
		Others Yield	2.1	2.2	1.9	1.7	1.4	1.3	0.6	0.4
		Selectivity of Propionitrile	14.3	21.9	18.0	22.2	21.9	25.7	28.2	27.9
		Selectivity of Acrylonitrile	75.0	67.2	72.0	69.1	70.6	67.5	68.5	69.8

Table B.8 Conversion of methanol, acetonitrile and yield, selectivity of products from alkylation of acetonitrile with methanol at 400 °C, over CsNaX15

Reaction Condition	Catalyst		Time on Stream (hours)							
			1	2	3	4	5	6	7	8
Reaction temperature at 400 °C W/F ~ 41 g.h.mol-1 Methanol/Acetonitrile ratio 10/1 Nitrogen carrier gas flow rate ~25 ml/min	CsNaX15	Methanol Conversion	5.6	5.7	5.4	5.8	5.2	5.4	5.1	5
		Acetonitrile Conversion	19.3	19.8	19.4	18.7	19.1	18.2	17.7	17.1
		Propionitrile Yield	8.2	9.2	9	8.5	9.3	8.6	8.2	8
		Acrylonitrile Yield	8.9	8.8	8.7	8.6	8.6	8.6	8.6	8.4
		Others Yield	2.2	1.8	1.7	1.6	1.2	1	0.9	0.7
		Selectivity of Propionitrile	42.5	46.5	46.4	45.5	48.7	47.3	46.3	46.8
		Selectivity of Acrylonitrile	46.1	44.4	44.8	46.0	45.0	47.3	48.6	49.1

Table B.9 Conversion of methanol, acetonitrile and yield, selectivity of products from alkylation of acetonitrile with methanol at 400 °C, over CsNaX20

Reaction Condition	Catalyst		Time on Stream (hours)							
			1	2	3	4	5	6	7	8
Reaction temperature at 400 °C W/F ~ 41 g.h.mol-1 Methanol/Acetonitrile ratio 10/1 Nitrogen carrier gas flow rate ~25 ml/min	CsNaX20	Methanol Conversion	5.6	5.4	5.3	5.4	5.2	5.1	5	5.1
		Acetonitrile Conversion	19.1	19.5	19	19.3	17.4	18.2	17.7	17.2
		Propionitrile Yield	10.2	11.9	11.8	12.5	11	12.7	12.5	12.8
		Acrylonitrile Yield	6.8	5.5	5.4	5.2	4.7	4.1	3.7	3.1
		Others Yield	2.1	2.1	1.8	1.6	1.7	1.4	1.5	1.3
		Selectivity of Propionitrile	53.4	61.0	62.1	64.8	63.2	69.8	70.6	74.4
		Selectivity of Acrylonitrile	35.6	28.2	28.4	26.9	27.0	22.5	20.9	18.0

Table B.10 Conversion of methanol, acetonitrile and yield, selectivity of products from alkylation of acetonitrile with methanol at 400 ^{0}C, over CsNaX30

Reaction Condition	Catalyst		Time on Stream (hours)							
			1	2	3	4	5	6	7	8
Reaction temperature at 400 ^{0}C W/F ~ 41 g.h.mol-1 Methanol/Acetonitrile ratio 10/1 Nitrogen carrier gas flow rate ~25 ml/min	CsNaX30	Methanol Conversion	5.7	5.4	5.4	5.3	5.6	5.4	5.2	5.1
		Acetonitrile Conversion	19.7	19.8	18.9	19.5	18.7	18.3	17.9	17.4
		Propionitrile Yield	15.5	16.0	15.0	15.7	15.3	15.5	15.8	15.7
		Acrylonitrile Yield	0.1	0.0	0.0	0.0	0.0	0.0	0.0	0.0
		Others Yield	4.1	3.8	3.9	3.8	3.4	2.8	2.1	1.7
		Selectivity of Propionitrile	78.8	80.6	79.2	80.4	81.6	84.6	88.1	90.1
		Selectivity of Acrylonitrile	0.4	0.2	0.1	0.1	0.2	0.1	0.2	0.2

Table B.11 Conversion of methanol, acetonitrile and yield, selectivity of products from alkylation of acetonitrile with methanol at 350 ^{0}C, over CsNaX30

Reaction Condition	Catalyst		Time on Stream (hours)							
			1	2	3	4	5	6	7	8
Reaction temperature at 350 ^{0}C W/F ~ 41 g.h.mol-1 Methanol/Acetonitrile ratio 10/1 Nitrogen carrier gas flow rate ~25 ml/min	CsNaX30	Methanol Conversion	2.5	2.3	2.4	2.4	2.1	2.3	2.2	2.1
		Acetonitrile Conversion	10.9	10.5	10.6	10.1	9.8	9.6	8.9	8.7
		Propionitrile Yield	7.8	7.2	7.5	6.7	6.1	5.6	5.7	5.3
		Acrylonitrile Yield	2.9	3.2	2.8	3.3	3.6	3.8	3.1	3.3
		Others Yield	0.2	0.1	0.3	0.1	0.1	0.2	0.1	0.1
		Selectivity of Propionitrile	71.6	68.6	70.8	66.3	62.2	58.3	64.0	60.9
		Selectivity of Acrylonitrile	26.6	30.5	26.4	32.7	36.7	39.6	34.8	37.9

Table B.12 Conversion of methanol, acetonitrile and yield, selectivity of products from alkylation of acetonitrile with methanol at 375 °C, over CsNaX30

Reaction Condition	Catalyst		Time on Stream (hours)							
			1	2	3	4	5	6	7	8
Reaction temperature at 375 °C W/F ~ 41 g.h.mol-1 Methanol/Acetonitrile ratio 10/1 Nitrogen carrier gas flow rate ~25 ml/min	CsNaX30	Methanol Conversion	4.6	4.4	4.1	4.3	4.2	3.9	3.8	3.9
		Acetonitrile Conversion	14.3	14.5	14.1	13.7	13.5	13.5	13.1	12.8
		Propionitrile Yield	9.8	9.7	9.3	8.8	8.7	8.4	8.6	8.1
		Acrylonitrile Yield	2.4	2.7	2.5	3.0	2.7	3.3	3.0	3.4
		Others Yield	2.1	2.1	2.3	1.9	2.1	1.8	1.5	1.3
		Selectivity of Propionitrile	68.5	66.9	66.0	64.2	64.4	62.2	65.6	63.3
		Selectivity of Acrylonitrile	16.8	18.6	17.7	21.9	20.0	24.4	22.9	26.6

Table B.13 Conversion of methanol, acetonitrile and yield, selectivity of products from alkylation of acetonitrile with methanol at 425 °C, over CsNaX30

Reaction Condition	Catalyst		Time on Stream (hours)							
			1	2	3	4	5	6	7	8
Reaction temperature at 425 °C W/F ~ 41 g.h.mol-1 Methanol/Acetonitrile ratio 10/1 Nitrogen carrier gas flow rate ~25 ml/min	CsNaX30	Methanol Conversion	10.9	11.3	10.8	10.7	10.4	10.6	10.1	9.7
		Acetonitrile Conversion	21.5	21.7	21.2	20.7	20.6	20.3	20.1	19.6
		Propionitrile Yield	16.3	16.4	16.1	15.8	15.9	15.3	15.4	14.6
		Acrylonitrile Yield	0.0	0.0	0.0	0.0	0.0	0.0	0.0	0.0
		Others Yield	5.2	5.3	5.1	4.9	4.7	5.0	4.7	5.0
		Selectivity of Propionitrile	75.8	75.6	75.9	76.3	77.2	75.4	76.6	74.5
		Selectivity of Acrylonitrile	0.0	0.0	0.0	0.0	0.0	0.0	0.0	0.0

Table B.14 Conversion of methanol, acetonitrile and yield, selectivity of products from alkylation of acetonitrile with methanol at 400 °C, W/F ~ 12

Reaction Condition	Catalyst		Time on Stream (hours)							
			1	2	3	4	5	6	7	8
Reaction temperature at 400 °C W/F ~ 12 g.h.mol-1 Methanol/Acetonitrile ratio 10/1 Nitrogen carrier gas flow rate ~25 ml/min	CsNaX30	Methanol Conversion	4.6	4.7	4.5	4.0	4.3	4.2	4.2	4.1
		Acetonitrile Conversion	5.9	6.1	6.0	5.7	5.8	5.6	5.4	5.1
		Propionitrile Yield	2.9	3.1	2.6	2.7	2.0	1.8	1.9	1.4
		Acrylonitrile Yield	2.3	2.4	2.7	2.7	3.6	3.7	3.4	3.7
		Others Yield	0.7	0.6	0.7	0.3	0.2	0.1	0.1	0.0
		Selectivity of Propionitrile	49.2	50.8	43.3	47.4	34.5	32.1	35.2	27.5
		Selectivity of Acrylonitrile	39.0	39.3	45.0	47.4	62.1	66.1	63.7	72.4

Table B.15 Conversion of methanol, acetonitrile and yield, selectivity of products from alkylation of acetonitrile with methanol at 400 °C, W/F~ 21

Reaction Condition	Catalyst		Time on Stream (hours)							
			1	2	3	4	5	6	7	8
Reaction temperature at 400 °C W/F ~ 21 g.h.mol-1 Methanol/Acetonitrile ratio 10/1 Nitrogen carrier gas flow rate ~25 ml/min	CsNaX30	Methanol Conversion	5.1	5.0	5.0	4.9	4.7	4.8	4.6	4.7
		Acetonitrile Conversion	11.0	11.2	11.2	10.9	11.3	10.7	10.2	10.3
		Propionitrile Yield	9.6	5.5	5.2	4.2	4.2	3.3	2.4	2.4
		Acrylonitrile Yield	0.5	4.8	5.4	6.3	6.9	7.3	7.7	7.9
		Others Yield	0.9	0.9	0.6	0.4	0.2	0.1	0.1	0.0
		Selectivity of Propionitrile	87.3	49.1	46.4	38.5	37.2	30.8	23.8	22.9
		Selectivity of Acrylonitrile	4.5	42.9	48.2	57.8	61.1	68.2	75.5	76.7

Table B.16 Conversion of methanol, acetonitrile and yield, selectivity of products from alkylation of acetonitrile with methanol at 400 °C, W/F ~29

Reaction Condition	Catalyst		Time on Stream (hours)							
			1	2	3	4	5	6	7	8
Reaction temperature	CsNaX30	Methanol Conversion	5.4	5.2	5.1	5.3	5.2	4.8	4.9	4.8
at 400 °C		Acetonitrile Conversion	15.7	16.1	16.0	15.7	15.8	15.2	14.7	14.2
W/F ~ 41 g.h.mol-1		Propionitrile Yield	11.4	11.2	10.3	9.4	8.2	7.6	7.1	6.9
Methanol/Acetonitrile		Acrylonitrile Yield	1.5	2.2	3.4	3.8	5.5	6.2	6.3	6.6
ratio 10/1		Others Yield	2.8	2.7	2.3	2.5	2.1	1.4	1.3	0.7
Nitrogen carrier gas		Selectivity of Propionitrile	72.6	69.6	64.4	59.9	51.9	50.0	48.3	48.6
flow rate ~25 ml/min		Selectivity of Acrylonitrile	9.6	13.7	21.3	24.2	34.8	40.8	42.9	46.5

Table B.17 Conversion of methanol, acetonitrile and yield, selectivity of products from alkylation of acetonitrile with methanol at 400 °C, CH_3OH/CH_3CN;10/1

Reaction Condition	Catalyst		Time on Stream (hours)							
			1	2	3	4	5	6	7	8
Reaction temperature	CsNaX15	Methanol Conversion	5.7	5.4	5.6	5.3	5.1	5.3	5.2	5.3
at 400 °C		Acetonitrile Conversion	20.2	19.8	19.4	19.3	18.7	18.4	18.1	17.7
W/F ~ 41 g.h.mol-1		Propionitrile Yield	14.5	13.9	13.5	12.8	12.3	11.9	11.5	10.7
Methanol/Acetonitrile		Acrylonitrile Yield	2.6	3.4	3.8	4.7	4.8	5.1	5.1	5.8
ratio 15/1		Others Yield	3.1	2.5	2.1	1.8	1.6	1.4	1.5	1.2
Nitrogen carrier gas		Selectivity of Propionitrile	71.8	70.2	69.6	66.3	65.8	64.7	63.5	60.5
flow rate ~25 ml/min		Selectivity of Acrylonitrile	12.9	17.2	19.6	24.4	25.7	27.7	28.2	32.8

Table B.18 Conversion of Acrylonitrile and yield, selectivity of products from hydrogenation of Acrylonitrile at 400 °C under hydrogen flow

Reaction Condition	Catalyst		Time on Stream (hour)							
			1	2	3	4	5	6	7	8
Weight of catalyst 1 g.	CsNaX30	Acrylonitrile Conversion	6.1	4.5	2.3	0.9	0.5	0.3	0.1	0.1
W/F ~ 5		Acetonitrile Yield	3.2	2.12	1.05	0.43	0.28	0.1	0.03	0.03
Acrylonitrile as feed		Propionitrile Yield	2.9	2.38	1.25	0.47	0.32	0.2	0.07	0.07
Hydrogen carrier gas		Selectivity of Acetonitrile	52.5	47.1	45.7	47.8	56.0	33.3	30.0	30.0
flow rate ~ 25 ml/min		Selectivity of Propionitrile	47.5	52.9	54.3	52.2	64.0	66.7	70.0	70.0

Table B.19 Conversion of substances and yield, selectivity of products from hydrogenation of acrylonitrile with methanol at 400 °C, over CsNaX30

Reaction Condition	Catalyst		Time on Stream (hour)							
			1	2	3	4	5	6	7	8
Weight of catalyst 1 g.	CsNaX30	Methanol Conversion	4.2	4.4	4.3	4.1	4.2	4.2	4.1	4
W/F ~ 200		Acrylonitrile Conversion	100	100	100	86.5	61.2	39.4	23.8	22.4
Methanol/Acrylonitrile		Acetonitrile Yield	79.8	79.5	78.5	65.4	41.5	23.4	12.1	11.3
ratio 50/1		Propionitrile Yield	18.4	18.9	19.4	19.5	17.4	15.1	11.2	10.7
Nitrogen carrier gas		Selectivity of Acetonitrile	79.8	79.5	78.5	75.6	67.8	59.4	50.8	50.4
flow rate ~25 ml/min		Selectivity of Propionitrile	18.4	18.9	19.4	22.5	28.4	38.3	47.1	47.8

Table B.20 Conversion of substances and yield, selectivity of products from hydrogenation of acrylonitrile with methanol at 400 ^{0}C, over CsNaX10

Reaction Condition	Catalyst		Time on Stream (hour)							
			1	2	3	4	5	6	7	8
Weight of catalyst 1 g.	CsNaX10	Methanol Conversion	4.4	4.1	4.3	4.4	4.3	4.2	4.2	4.1
W/F ~ 200		Acrylonitrile Conversion	35.8	34.9	36.1	34.2	31.3	27.4	24.3	23.1
Methanol/Acrylonitrile		Acetonitrile Yield	25.7	24.3	25.2	23.5	21.2	17.1	14.7	13.7
ratio 50/1		Propionitrile Yield	10.1	10.6	10.9	10.7	10.1	10.3	9.6	9.4
Nitrogen carrier gas		Selectivity of Acetonitrile	71.8	69.6	69.8	68.7	67.7	62.4	60.5	59.3
flow rate ~25 ml/min		Selectivity of Propionitrile	28.2	30.4	30.2	31.3	32.3	37.6	39.5	40.7

Table B.21 Conversion of substance and yield of product from hydrogenolysis of propionitrile with at 400 °C, over CsNaX10

Reaction Condition	Catalyst		Time on Stream (hour)							
			1	2	3	4	5	6	7	8
W/F ~ 200 g.h.mol^{-1}	CsNaX10	Methanol Conversion	4.4	4.2	4.1	4.1	3.9	4.2	4	4
Methanol/Propionitrile ratio 50/1		Propionitrile Conversion	23.5	21.8	20.6	18.9	16.6	16.2	15.5	15.2
Nitrogen carrier gas flow rate ~ 25 ml/min		Acetonitrile Yield	23.2	21.5	20.3	18.6	16.4	16.1	15.4	15

Table B.22 Conversion of substance and yield of product from hydrogenolysis of propionitrile with at 400 °C, over CsNaX30

Reaction Condition	Catalyst		Time on Stream (hour)							
			1	2	3	4	5	6	7	8
W/F ~ 200 g.h.mol^{-1}	CsNaX30	Methanol Conversion	4.2	4.3	4.1	4.4	4.2	4.1	4	4.1
Methanol/Propionitrile ratio 50/1		Propionitrile Conversion	76.5	54.3	43.2	32.5	26.2	24.3	23.1	22.4
Nitrogen carrier gas flow rate ~ 25 ml/min		Acetonitrile Yield	74.3	53.2	42.9	32.1	25.9	24.1	23.0	22.3

APPENDIX C

GAS CHROMATOGRAM/MASS SPECTRUM

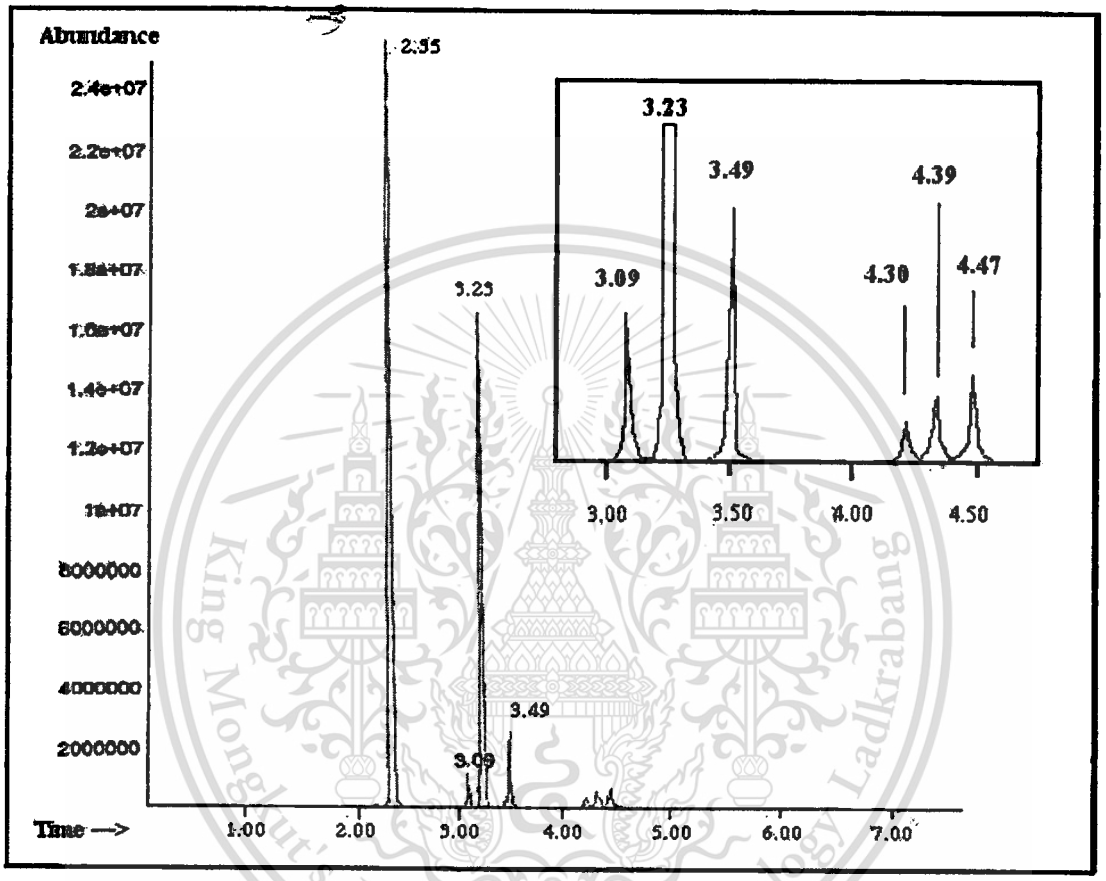

Figure C.1 Chromatogram of methanol, acetonitrile, acrylonitrile, propionitrile, butanedinitrile, butanenitrile and 2-butenenitrile.

```
Library Searched : C:\Database\wiley7n.l
Quality          : 2
ID               : Methanol (CAS) $$ Carbinol $$ Methylol $$ Wood alcohol $$ Mathyl alcohol $$ Met
                   hyl hydroxide $$ Monohydroxymethane $$ Methanol-water mixture $$ CH3OH $$ Colon
                   ial spirit $$ Columbian spirit $$ Hydroxymethane $$ Wood naphtha $$ Alcool meth
                   ylique $$ Alcool m
```

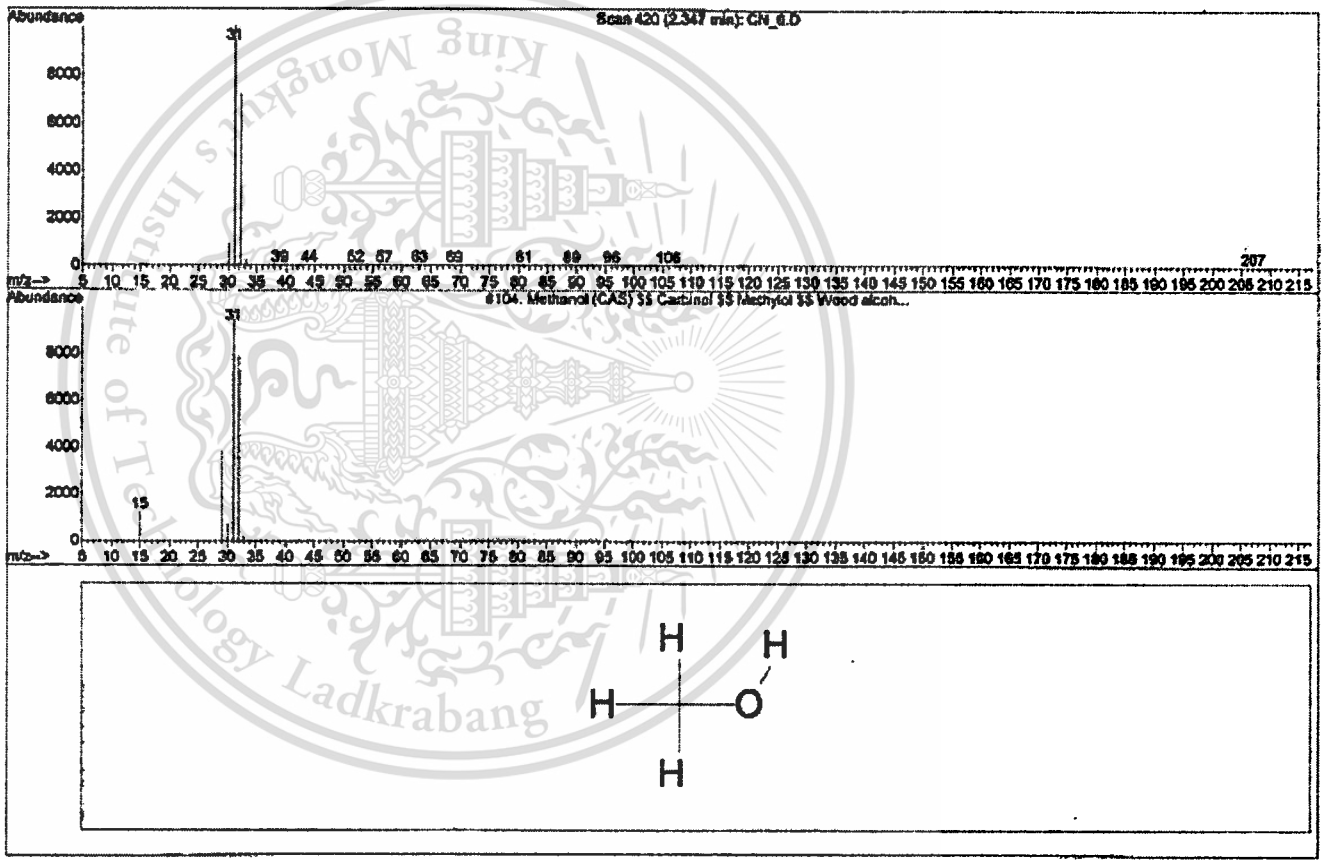

Figure C.2 Mass spectrum of methanol

```
Library Searched : C:\Database\wiley7n.l
Quality          : 90
ID               : 2-Propenenitrile $$ Acrylon $$ Acrylonitrile $$ Carbacryl $$ Cyanoethylene $$ F
                   umigrain $$ Propenenitrile $$ Ventox $$ Vinyl cyanide $$ VCN $$ CH2CHCN $$ Acri
                   tet $$ Acrylnitril $$ Acrylonitrile monomer $$ Akrylonitryl $$ Cianuro di vinil
                   e $$ Cyanure de vi
```

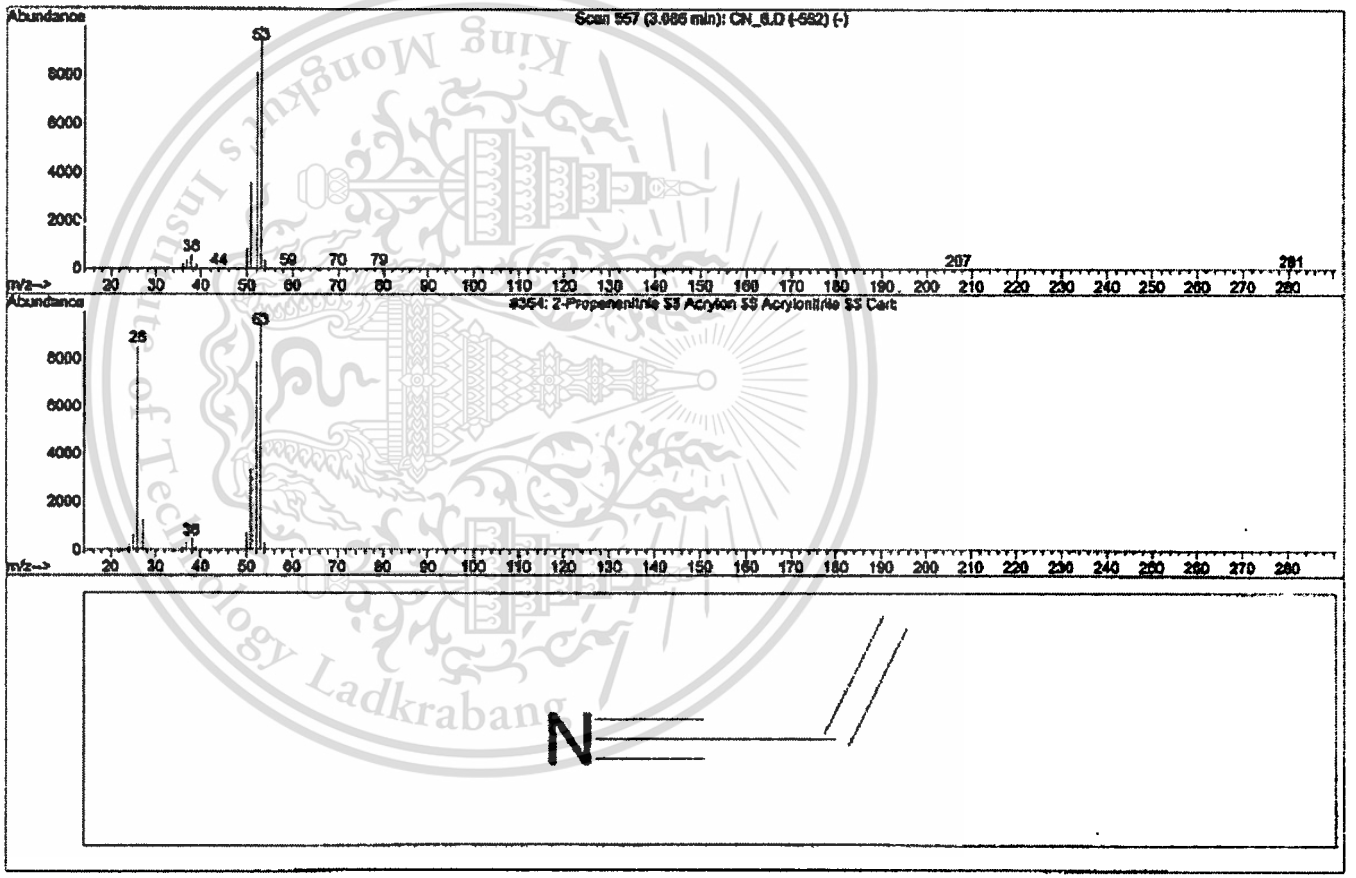

Figure C. 4 Mass spectrum of acrylonitrile

```
Library Searched : C:\Database\wiley7n.l
Quality          : 42
ID               : Acetonitrile (CAS) $$ Methyl cyanide $$ Cyanomethane $$ Ethanenitrile $$ Ethyl
                   nitrile $$ Methane, cyano- $$ Methanecarbonitrile
```

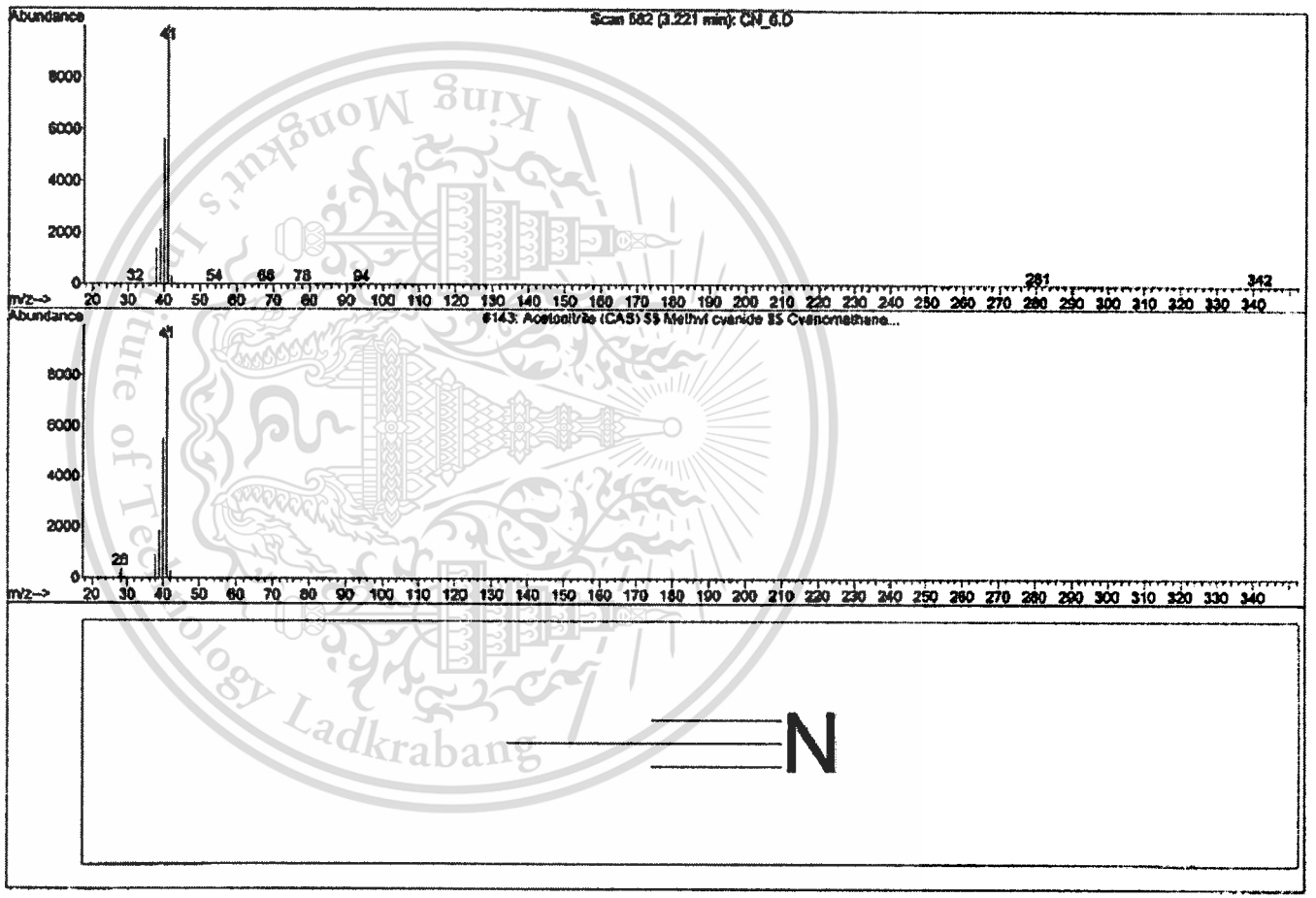

Figure C.3 Mass spectrum of acetonitrile

Library Searched : C:\Database\wiley7n.1
Quality : 64
ID : Propanenitrile

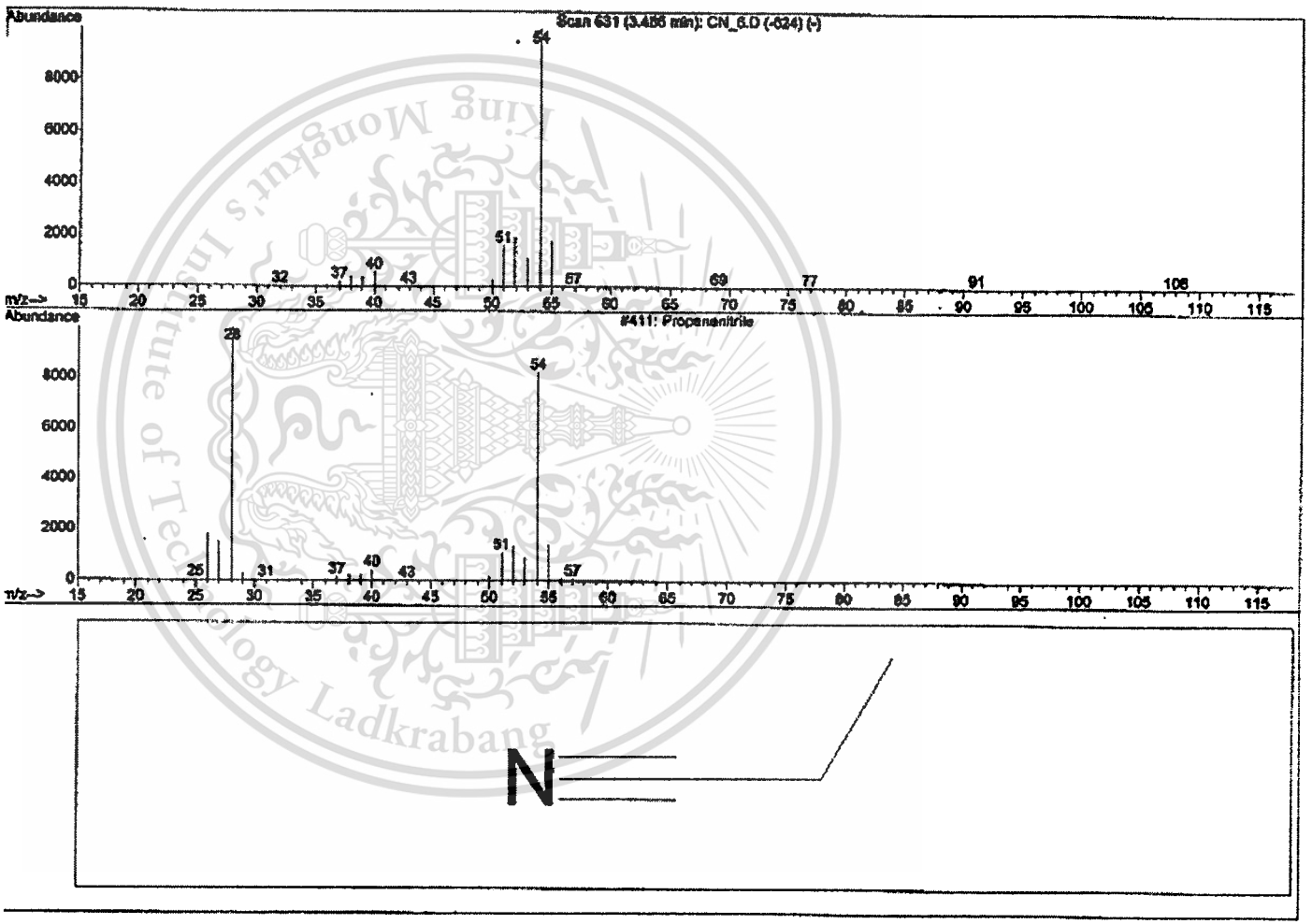

Figure C.5 Mass spectrum of propionitrile

Library Searched : C:\Database\wiley7n.l
Quality : 64
ID : Butanedinitrile, 2,3-dimethyl- (CAS) $$ .ALPHA.,.BETA.-DIMETHYL-SUCCINONITRILE
$$ Succinonitrile, 2,3-dimethyl- $$ 2,3-Dimethylsuccinonitrile

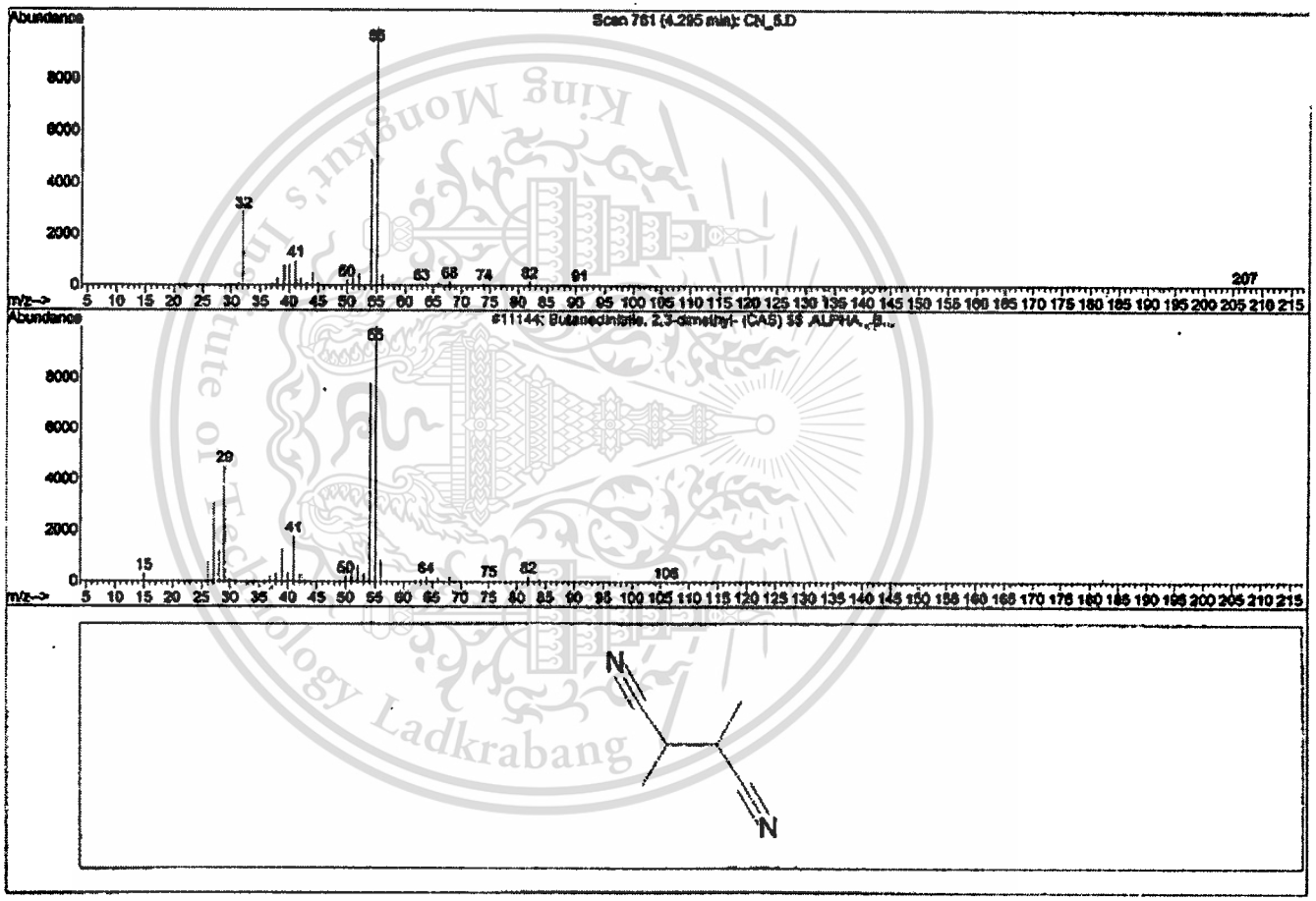

Figure C.6 Mass spectrum of butanedinitrile

Library Searched : C:\Database\wiley7n.l
Quality : 72
ID : Butanenitrile (CAS) $$ n-Butyronitrile $$ Butyronitrile $$ Propyl cyanide $$ 1-Cyanopropane $$ Butyrylonitrile $$ n-Butanenitrile $$ N-PROPYL CYANIDE $$ n-C3H 7CN $$ n-Butanitrile $$ Butyric acid nitrile $$ Propylkyanid $$ UN 2411

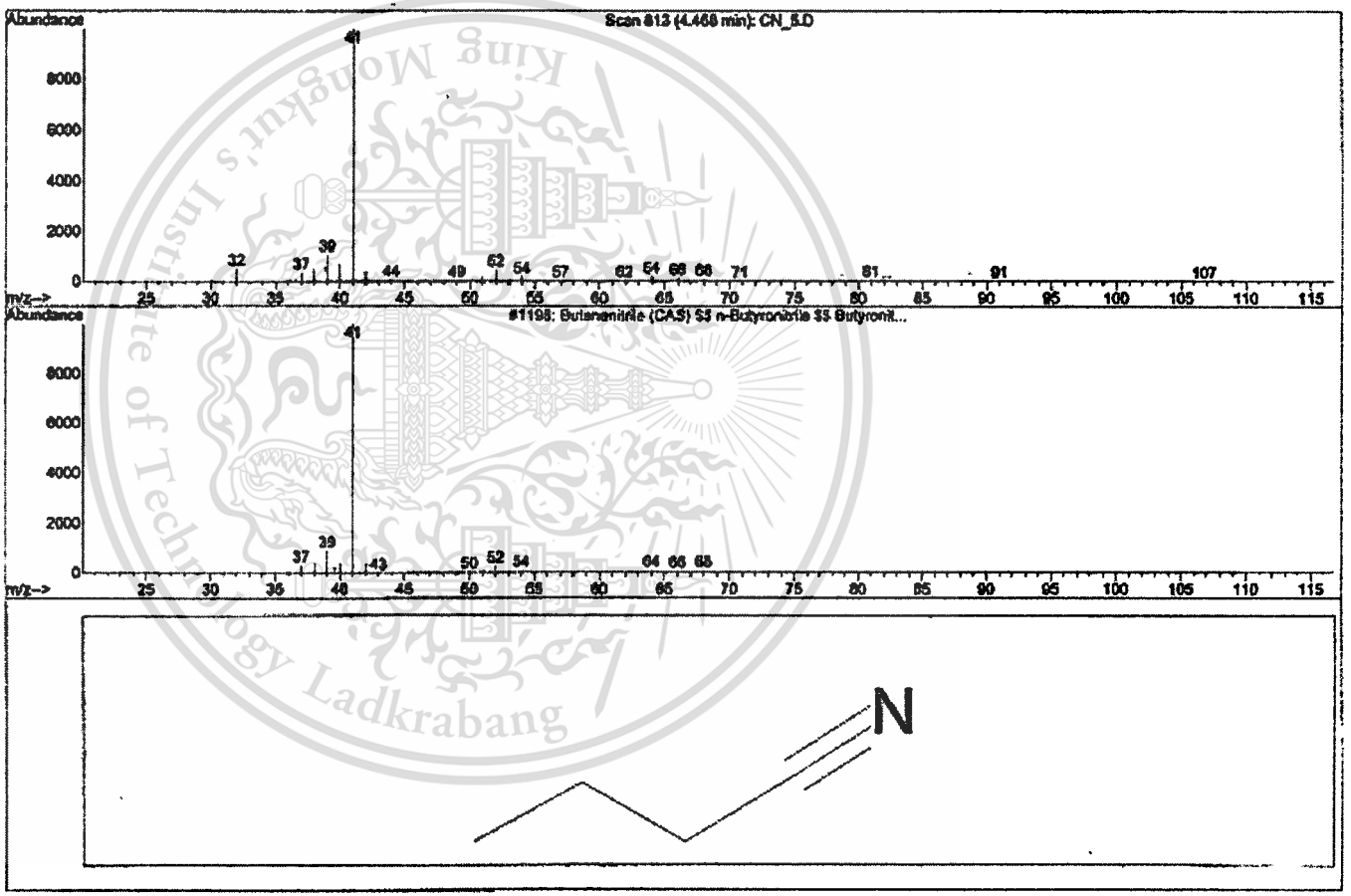

Figure C.7 Mass spectrum of butanenitrile

```
Library Searched : C:\Database\wiley7n.l
Quality          : 96
ID               : 2-Butenenitrile (CAS) $$ Crotonitrile $$ Crotonnitrile $$ Crotononitrile $$ 1-C
                   yanopropene $$ Crotonic nitrile $$ 1-Propenyl cyanide $$ trans-Crotonitrile $$
                   trans-Crotononitrile $$ trans-But-2-enonitrile $$ trans-1-Cyanoprop-1-ene $$ 1-
                   Cyano-1-propylene
```

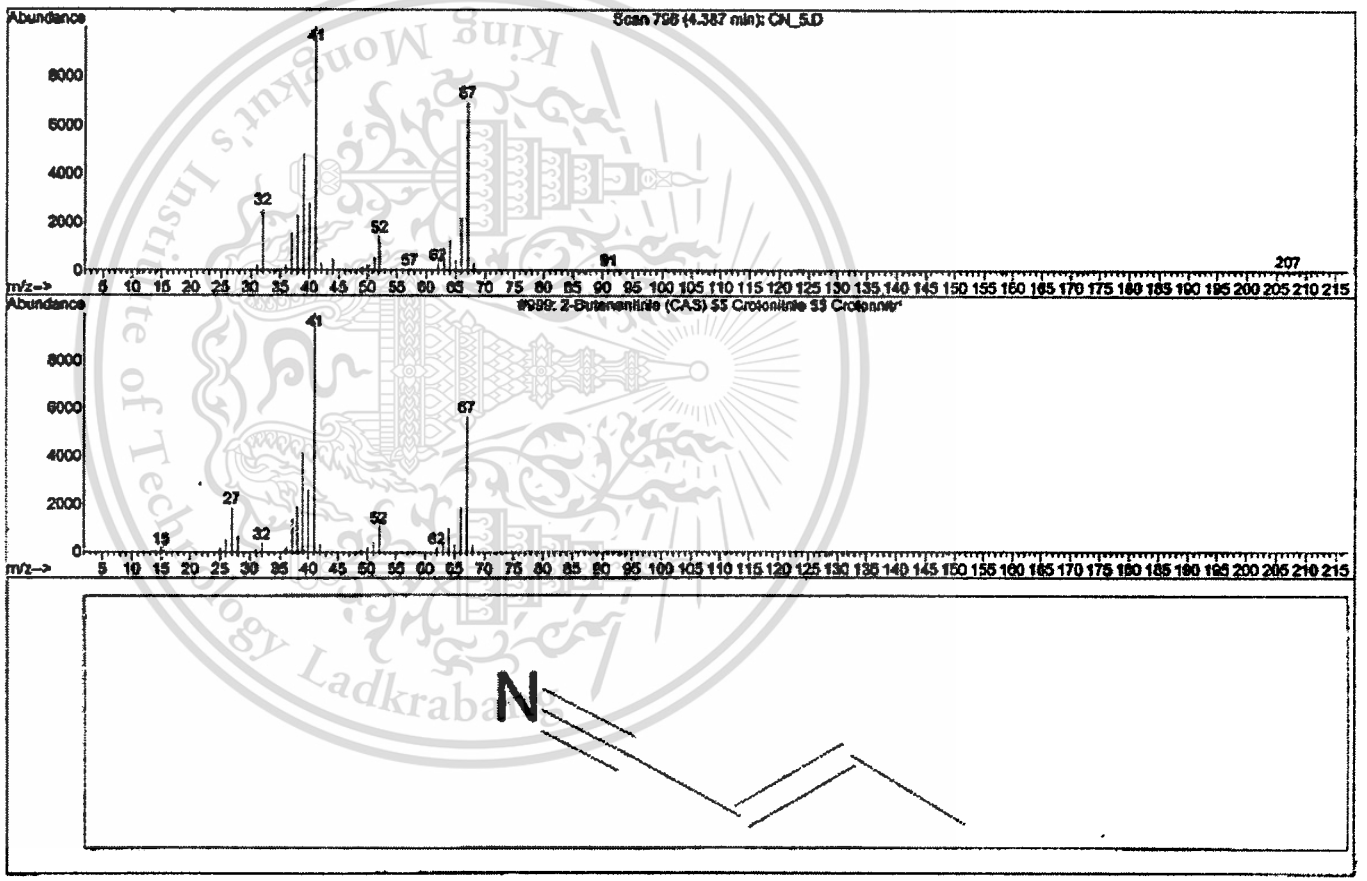

Figure C.8 Mass spectrum of 2-butenitrile

APPENDIX D

LANGMUIR ADSORPTION ISOTHERM

Table D.1 Langmuir adsorption Isotherm data

0.010044	0.06719	76.1337	0.010032	0.07777	152.91
0.011042	0.07242	77.6521	0.011019	0.0841	155.3062
0.012025	0.07759	79.0607	0.012024	0.09065	157.2372
0.013049	0.08284	80.2294	0.013009	0.09694	159.0655
0.014048	0.08788	81.4152	0.014011	0.1032	160.9734
0.01505	0.09278	82.6128	0.01501	0.1093	162.7593
0.01605	0.09767	83.6929	0.016011	0.1152	164.7531
0.01705	0.1025	84.745	0.017011	0.121	166.5788
0.01805	0.1072	85.7739	0.017994	0.1263	168.8841
0.019051	0.1119	86.7114	0.019025	0.1325	170.1407
0.020049	0.1166	87.5664	0.020026	0.1383	171.5982
0.021053	0.1212	84.4995	0.021027	0.1442	172.8212
0.022051	0.1257	89.3735	0.02203	0.15	174.0912
0.023051	0.1301	90.237	0.023034	0.1557	175.3779
0.024052	0.1345	91.9015	0.024037	0.1612	176.746
0.02504	0.1382	92.2611	0.025054	0.1645	180.5566
0.026044	0.142	93.3768	0.026063	0.1712	180.4283
0.027011	0.1462	94.0839	0.026997	0.1759	181.9761
0.028044	0.1505	94.9232	0.028008	0.1812	183.254
0.029041	0.1544	95.7919	0.029016	0.1864	184.5035
0.030054	0.1584	96.5626	0.03006	0.1915	185.7796

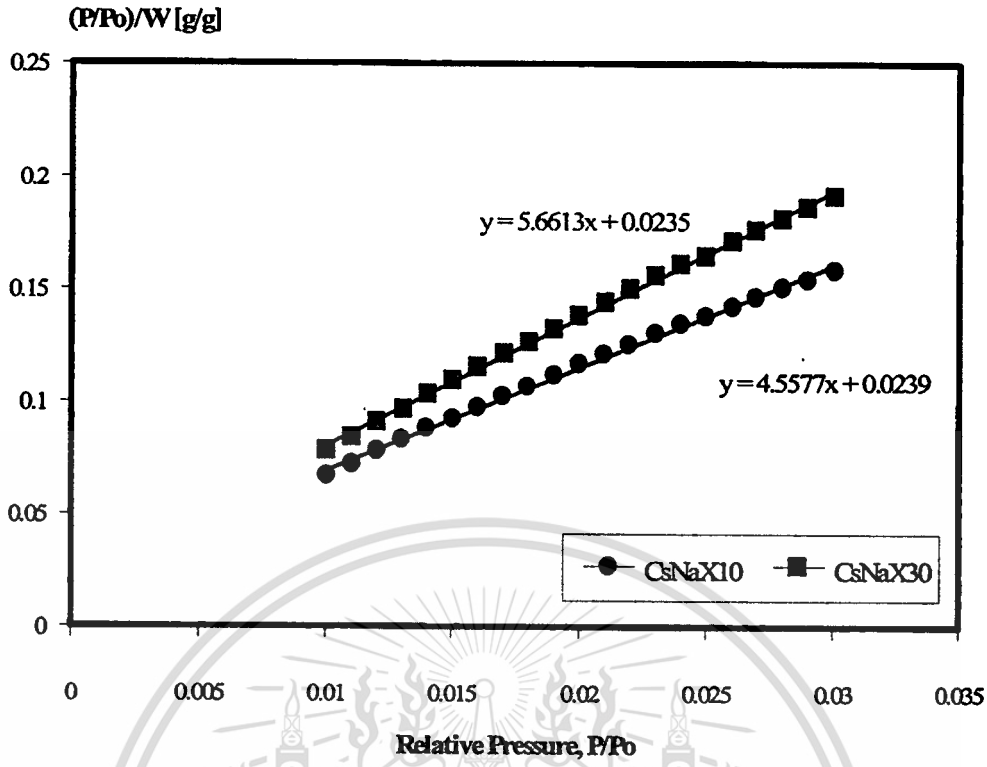

Figure D.1 Langmuir plot of CsNaX10 and CsNaX30

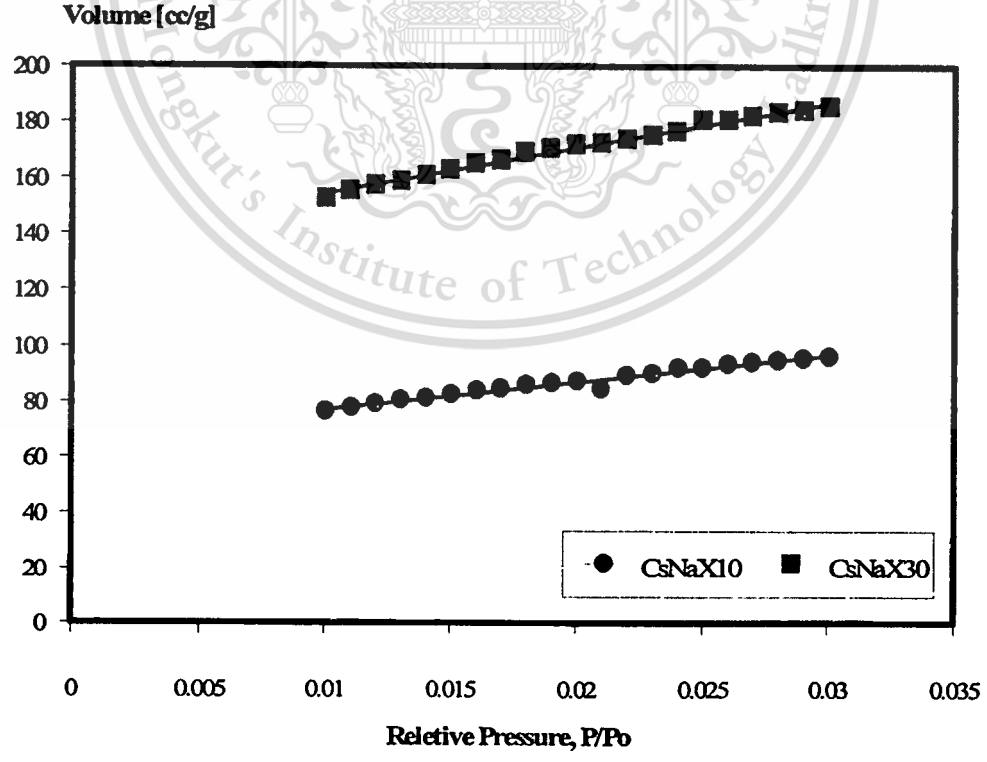

Figure D.2 Isotherm plot of CsNaX10 and CsNaX30

APPENDIX E

X-RAY DIFFRACTION OF STANDARD FAU

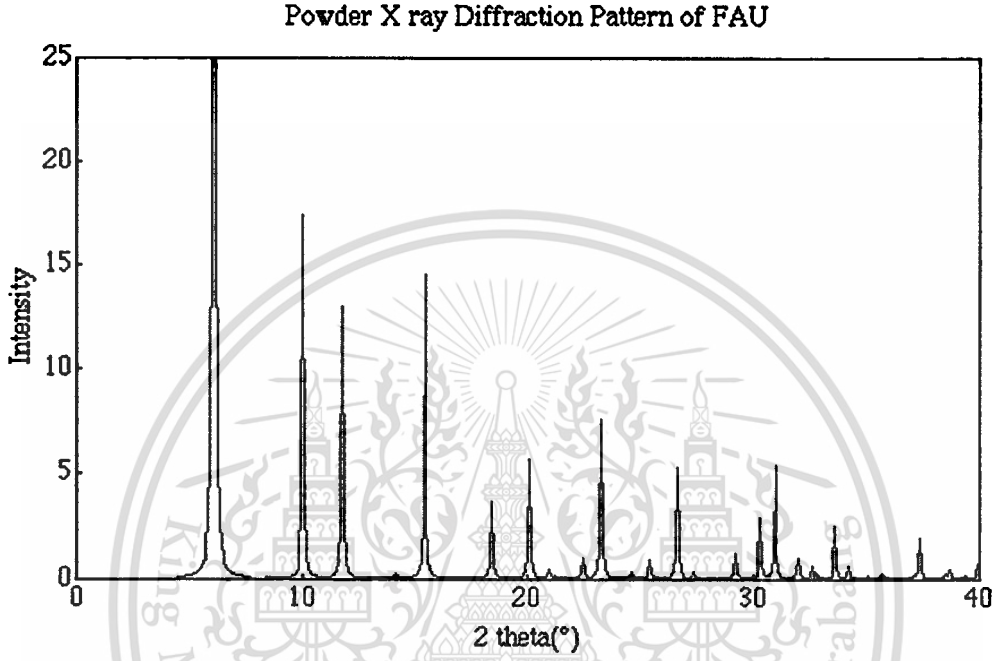

Figure E.1 X-Ray diffraction pattern of standard faujasite typed zeolite [48]

AUTHOR BIOGRPHY

Mr. Prachya Thuensukon was born on June 15, 1978 in Kanchanaburi. He recived a Bachelor degree in Industrial Chemistry from Department of Chemistry, Faculty of Applied Science, King Mongkut's Institute of Technology North Bangkok in 2001. He has been graduated student of the Program of Petrochemicals and Hydrocarbon Chemistry, Graduate School, King Mongkut's Institute of Technology Ladkrabang, science2001